Feeding Mechanisms in Phagotrophic Nanoflagellates

Predation in the Low Reynolds Number World

Suzuki-Tellier, Sei

Publication date:
2023

Document Version
Publisher's PDF, also known as Version of record

Ph.D. Thesis
Doctor in Philosophy

DTU Aqua
National Institute of Aquatic Resources

FEEDING MECHANISMS IN PHAGOTROPHIC NANOFLAGELLATES

Predation in the Low Reynolds Number World

Sei Suzuki-Tellier

Supervisor:
Thomas Kiørboe

Co-supervisor:
Anders Andersen

Kongens Lyngby, 2023

DTU

DTU Aqua
National Institute of Aquatic Resources
Technical University of Denmark

Kemitorvet
Building 202
2800 Kgs. Lyngby
www.dtu.dk/english

To my kids, Taio and Sango,
always full of love and joy
(and snot).

SUMMARY

Exploring small-scale predation

Pelagic waters are nutritionally poor, with food distributed in heterogeneous patches that rapidly dissipate into the diluted environment. Yet, these temporary nutrient-rich regions become hotspots of life. A drop of seawater can contain around a million bacteria cells, which have rapid growth rates and are efficient consumers of dissolved organic matter. Surprisingly, bacterioplankton populations remain mostly constant. This is primarily due to the top-down pressure of small abundant predators known as phagotrophic nanoflagellates. These single-cell organisms (protists), equipped with one or more flagella and ranging from 2 – 20 μm in size, play a key role in the 'microbial loop', i.e. an alternative energy pathway to the classic marine trophic chain (phytoplankton – copepod – small fish). As the main consumers of bacteria and picophytoplankton, phagotrophic nanoflagellates are essential to the marine carbon cycles and global biogeochemical processes.

To survive, flagellates need to clear a million times their own volume of water per day. However, the microscale world is physically counterintuitive: water becomes viscous and particle-particle contacts are constrained. So how do flagellates thrive in 'sticky', nutrient-poor waters? They generate feeding currents by beating the flagellum to draw prey toward them for subsequent captures and ingestions. Phagotrophic nanoflagellates display a variety of flagellar arrangements and feeding behaviors. Moreover, they are functionally and phylogenetically diverse. Despite their ecological significance, their feeding processes remain largely unexplored.

This thesis aims to mechanistically understand the diversity of predation strategies in phagotrophic nanoflagellates. It comprises three collaborative papers, each addressing specific aspects. First, we investigate the feeding behaviors of four species of stramenopiles that generate flow with a hairy flagellum. Second, we describe the predation modes of 'typical excavates' that feed through a ventral groove associated with a vaned flagellum. Lastly, we report, for the first time, the activity of the 'wave' in the ventral groove of excavates and study their prey size range. Feeding behaviors were recorded through high-speed video microscopy, and theoretical models and computational fluid dynamic simulations were used to study the flow-generating forces of the beating flagellum. This thesis provides a mechanistic insight into the functional morphology and functional responses of two taxonomic groups and opens up new avenues for understanding the ecological significance of their feeding processes. By shedding light on these processes, we can gain a deeper understanding of the role of phagotrophic nanoflagellates in aquatic ecosystems.

En undersøgelse af predation på en lille skala

Pelagiske farvande er ernæringsmæssigt fattige. Her er føden fordelt i heterogene pletter, der hurtigt fordeles i det fortyndede miljø. Alligevel bliver disse midlertidigt næringsrige områder vigtige område for liv. En dråbe havvand kan indeholde omkring en million bakterieceller, som har hurtige vækstrater og er effektive forbrugere af opløst organisk materiale. Overraskende nok forbliver populationer af bakterieplankton for det meste konstante. Dette skyldes primært et 'top-down-tryk' (eller 'predationspres') fra talrige små rovdyr, kendt som fagotrofe nanoflagellater. Disse encellede organismer (protister), er udstyret med en eller flere flageller og har en størrelse på 2 - 20 μm. De spiller en nøglerolle i det 'mikrobielle loop', som udgøret alternativ til den klassiske marine fødekæde (phytoplankton - copepod - små fisk). Som de primære forbrugere af bakterier og picophytoplankton er fagotrofe nanoflagellater afgørende for marine kulstofkredsløb og globale biogeokemiske processer.

For at overleve skal flagellater dagligt filtrere et vandvolumen svarende til en million gange deres eget volumen. Dog er den mikroskopiske verden fysisk modsigende: vand bliver viskøst, og partikel-partikler kommer sjældent i kontakt med hinanden. Så hvordan trives flagellater i de 'klæbrige', næringsfattige farvande? De genererer fødestrømme ved at slå deres flagel for at tiltrække bytte til dem for efterfølgende at fange og indtage det. Fagotrofe nanoflagellater udviser en bred vifte af af flagellære arrangementer og typer af predationsadfærd. Desuden er de funktionelt og fylogenetisk forskellige. På trods af deres økologiske betydning forbliver deres fødeprocesser stort set uudforskede.

Formålet med denne afhandling er at opnå en mekanistisk forståelse af de mangfoldige predationsstrategier hos fagotrofe nanoflagellater. Afhandlingen består af tre artikler, der hver især adresserer specifikke aspekter. Først undersøger vi predationsadfærd hos fire arter af 'stramenopiler', der genererer et flow med en behåret flagel. Dernæst beskriver vi predationstilstandene hos 'excavater', der fodrer gennem en ventral rille forbundet med en 'fjerbelagt' flagel. Slutteligt rapporterer vi for første gang aktiviteten af 'bølgen' i den ventrale rille af excavater og studerer deres byttestørrelsesinterval. Fødeadfærd blev optaget gennem højhastigheds-videooptagelse, og teoretiske modeller og væskedynamiske simuleringer blev brugt til at studere kraften, der genererer strømmen fra den slående flagel. Denne afhandling giver en mekanisk indsigt i den funktionelle morfologi og funktionelle respons af to taksonomiske grupper og åbner nye muligheder for at forstå den økologiske betydning af deres predationsprocesser. Ved at kaste lys over disse processer kan vi få en dybere forståelse af de fagotrofe nanoflagellaters rolle i akvatiske økosystemer.

PREFACE

Planktonic organisms are known as the 'oceanic drifters' (from the Greek word *planktos*, meaning 'wanderer' or 'drifter') because they are incapable of swimming against the big currents. When first studying marine ecology, the concept of 'drifting' was personally misleading. It planted an image of a jellyfish simply 'going with the flow', passive and randomly. Eventually, I learned about the fascinating diel vertical migrations of copepods and realized that, from the beginning, my perception of planktonic populations had been way-off. This moment was eye-opening and sparked my passion for marine microbiology. Since, I began an academic journey with the aim to learn more about the captivating aquatic life that is invisible to the naked eye. Now, I am proud to present this work that sets a milestone in my devotion; a devotion that has grown specifically towards phagotrophic flagellates.

This Ph.D. thesis was prepared at the National Institute of Aquatic Resources at the Technical University of Denmark, in fulfillment of the requirements for acquiring a Doctor degree in Philosophy. The research was carried out from September 2018 until July 2023 at the Centre for Ocean Life, a Villum Foundation Centre of Excellence in Kongens Lyngby, Denmark. During this period I was supervised by Thomas Kiørboe and Anders P. Andersen. Four weeks in November 2019 were spent as an external research stay working at the Department of Marine Biology and Oceanography at the ICM-CSIC in Barcelona, Spain. This Ph.D. was funded by the Carlsberg Foundation and by the Centre for Ocean Life, a Villum Kahn Rasmmussen Centre for Excellence funded by the Villum Foundation. Additional support for conference participation was received from the Otto Mønsted Foundation.

Kongens Lyngby, 5th of August 2023

Sei Suzuki-Tellier

ACKNOWLEDGMENTS

Looking back to when I started, I'm in disbelief at what I have achieved and gained from this whole experience. Thomas, your valuable mentorship has been the pillar of this work. You have always been there, one door knock away, to listen to my worries and guide me toward progress. You have taught me so much: thank you. Thank you to Anders, too. I am grateful for your patience and for being such a great teacher. I will always appreciate you sharing your passion for physics with me. I am grateful that you always found time to help me when needed.

I would not be here without the great opportunity I was given by Stuart Humphries and his group. To Òscar Guadayol, Fouad El Baidouri, and Rudi Schuech. I was a newbie. You welcomed me and I learned so much from you! I hope to keep 'bumping into' you, in the future.

I want to also acknowledge three women that have inspired me from the beginning. Sandra Varga, Catrin Günther, and Mariona Segura. You have been my role models as strong, caring, and professional scientists. Thank you.

I have had the privilege to meet many people throughout my (extended) time as a Ph.D. student. Colleagues with whom I have shared a lot of laughs and conversations. People whom I hold close to my heart. The Centre for Ocean Life has been a marvelous workplace, professionally and socially. Thank you all. A special mention goes to my office mates: Camila, Mridul, Emily, Federica, Amalia, Trine, and Louise. And Fredrik! It has been a blast. Fruitful meetings at the ping pong table, silly pranks, and lots of laughs. But you have also been a great support, especially this last year. I am so grateful. And to Josephine, Kristian, and Mads, with whom I also started this journey. I have always valued being able to talk to you and I have never felt alone.

To Rocío and Nico. You both were important parts of our arrival in Denmark. I am so happy we have shared so many moments, together. May our 'Dansk Family' spirit overcome the long distances between us.

To my family. Particularly to you, Josh. It has been a roller-coaster ride ever since we arrived. But look at us now. Thank you for believing in me and standing by my side. This would have not been possible without you.

And thank you, Magnus, for lending me your Danish knowledge and doing a better translation job than Chat GPT.

I am sure I am leaving out many important people because it is late and I have not had much sleep. This list could go on, and on, and on…

LIST OF PUBLICATIONS

This Ph.D. thesis is based on the following publications:

I. Suzuki-Tellier, S., Andersen, A., and Kiørboe, T. 2022. Mechanisms and fluid dynamics of foraging in heterotrophic nanoflagellates. *Limnology and Oceanography*, *67*(6), 1287–1298. doi: 10.1002/lno.12077

II. Suzuki-Tellier, S., Miano, F., Asadzadeh, S.S., Simpson, A.G.B., Kiørboe, T. Functional Morphology and Fluid Dynamics of Foraging in 'Typical Excavates'; a Key Assemblage for Understanding Deep Eukaryote Evolution (in preparation).

III. Suzuki-Tellier, S., Kiørboe, T., Simpson, A.G.B. New Insights in Flagellate Predation: the Significance and Function of the Feeding Groove of 'Typical Excavates' (in preparation).

CONTENTS

CHAPTER 1

Introduction

Phagotrophic nanoflagellates are crucial to one of the main biological processes in the ocean: the 'microbial loop' (Azam et al., 1983; Worden et al., 2015). As primary consumers of bacteria and picophytoplankton, phagotrophic nanoflagellates are an alternative energy pathway for higher trophic levels and have a significant impact on global biogeochemical cycles. Thus, the predatory activity by these flagellated protists has important repercussions on the structure and functions of microbial communities. However, many of these feeding processes remain fundamentally unclear or unexplored.

Early work on phagotrophic nanoflagellates was based on the study of microbial population dynamics through field observations or incubation experiments (e.g. Davis & Sieburth, 1984; Rassoulzadegan & Sheldon, 1986; Dryden & Wright, 1987), which often relied on epifluorescent microscope counts with morphological identifications at a high taxonomical level. Consequently, phagotrophic nanoflagellates have been traditionally assessed inside a 'black box' as a single functional group, jointly with other heterotrophic (e.g., dinoflagellates or ciliates) and mixotrophic (e.g., haptophytes) microorganisms. Although the 'black-box' approach has contributed to our understanding of the ecological significance of phagotrophic nanoflagellates, it has inevitably masked the phylogenetic, physiological, and functional diversity of this group. The work by Fenchel (1982a, 1982b, 1982c, 1982d) kick-started and significantly advanced our understanding of the functional ecology of phagotrophic protists. More than a decade later, researchers expanded upon this knowledge and investigated the microbial predator-prey interactions through direct observations (Ishigaki & Terazaki, 1998; Boenigk & Arndt, 2000b, 2000a; Christensen-Dalsgaard & Fenchel, 2003). However, the number of studies of this nature has decreased in more recent years. Phagotrophic nanoflagellates are found in all the major branches across the Eukaryotic Tree of Life (Burki et al., 2020; Tikhonenkov, 2020), but research in predation behavior has focused on just a few species from a few groups. Despite the increasing number of newly isolated predators, many lack detailed insights into their feeding modes. In addition, a good fraction remains uncultured (Massana et al., 2009; Logares et al., 2012).

Protists live in the low Reynolds number regime, which is dominated by viscous forces whilst inertia is virtually null. The 'sticky' waters impede particle-particle contacts, and objects become motionless as soon as the propelling force ceases. Moreover, phagotrophic flagellates typically

inhabit nutritionally scarce and non-homogeneous environments, and it is estimated that, to survive, they need to clear a million times their own volume of water in search of prey (Kiørboe, 2011; Kiørboe & Hirst, 2014). How do phagotrophic nanoflagellates overcome these adverse physical and nutritional conditions? The low Reynolds number world is characterized by a laminar flow pattern that consists of smooth streamlines that are adjacent to each other, and by increasing the proximity of the streamlines to the predator's body, prey encounter efficiency is enhanced (Fig 1.1). Phagotrophic nanoflagellates optimize encounter probabilities by generating feeding currents: the beating flagellum converges close-by streamlines and increases the volume of water that the predator can scan through over time (i.e., the clearance rate). Different flagellate species produce feeding flows with flagella of different lengths, arrangements, and beat patterns (Nielsen & Kiørboe, 2021). Yet, the specific fluid dynamics involved in feeding have rarely been resolved, as biophysicists traditionally have examined the flow patterns of swimming microorganisms, with limited interest in their ecology and biology. Moreover, the feeding rates estimated with simple fluid dynamic arguments can be orders of magnitude lower than the rates needed to survive (Langlois et al., 2009).

Phagotrophic nanoflagellates are abundant, ubiquitous, diverse, and ecologically significant – yet, they are a severely understudied group. Overall, we lack fundamental knowledge of the mechanisms and fluid dynamics involved in their predation modes. It is important to mechanistically pinpoint their feeding strategies to better understand the different predator-prey interactions that structure the microbial food webs, which are the fuel to marine life. By opening the 'black box', we can identify the different ecological functions of phagotrophic flagellates that have a great impact on microbial diversity. Finally, improving our understanding of the complex interactions within microbial communities will contribute to the development of more realistic theoretical models of marine life systems.

This thesis studies the predation modes of free-living, suspension-feeding phagotrophic nanoflagellates. I will begin by introducing their ecology, fluid dynamics, and different feeding strategies and behaviors (Chapters 2 – 4). Then, I will provide a concise summary of my findings (Chapter 5), before presenting the three papers that make up the core of this thesis (Chapters 6 – 8). Finally, I will conclude by discussing some speculations and proposing future research avenues.

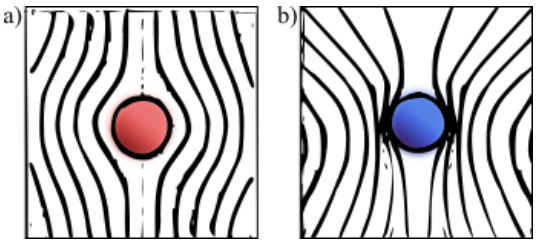

Figure 1.1. Streamlines in a laminar flow at the low Reynolds number regime. Adjacent streamlines surrounding a spherical body (a flagellate) when: a) there is no acting force, and b) there is an acting force, produced by a beating flagellum, that converges the streamlines closer to the body.

References

Azam, F., Fenchel, T., Field, J. G., Gray, J. S., Meyer-Reil, L. A., & Thingstad, F. (1983). The Ecological Role of Water-Column Microbes in the Sea. *Marine Ecology Progress Series*. https://doi.org/10.3354/meps010257

Boenigk, J., & Arndt, H. (2000a). Comparative studies on the feeding behavior of two heterotrophic nanoflagellates: The filter-feeding choanoflagellate Monosiga ovata and the raptorial-feeding kinetoplastid Rhynchomonas nasuta. *Aquatic Microbial Ecology*, *22*(3), 243–249. https://doi.org/10.3354/ame022243

Boenigk, J., & Arndt, H. (2000b). Particle Handling during Interception Feeding by Four Species of Heterotrophic Nanoflagellates. *Journal of Eukaryotic Microbiology*, *47*(4), 350–358. https://doi.org/10.1111/j.1550-7408.2000.tb00060.x

Burki, F., Roger, A. J., Brown, M. W., & Simpson, A. G. B. (2020). The New Tree of Eukaryotes. *Trends in Ecology & Evolution*, *35*(1), 43–55. https://doi.org/10.1016/j.tree.2019.08.008

Christensen-Dalsgaard, K. K., & Fenchel, T. (2003). Increased filtration efficiency of attached compared to free-swimming flagellates. *Aquatic Microbial Ecology*, *33*(1), 77–86. https://doi.org/10.3354/ame033077

Davis, P., & Sieburth, Jm. (1984). Estuarine and oceanic microflagellate predation of actively growing bacteria estimation by frequency of dividing-divided bacteria. *Marine Ecology Progress Series*, *19*, 237–246. https://doi.org/10.3354/meps019237

Dryden, R. C., & Wright, S. J. L. (1987). Predation of cyanobacteria by protozoa. *Canadian Journal of Microbiology*, *33*(6), 471–482. https://doi.org/10.1139/m87-080

Fenchel, T. (1982a). Ecology of Heterotrophic Microflagellates. I. Some Important Forms and Their Functional Morphology. *Marine Ecology Progress Series*, *8*(3), 211–223.

Fenchel, T. (1982b). Ecology of Heterotrophic Microflagellates. II. Bioenergetics and Growth. *Marine Ecology Progress Series*, *8*(3), 225–231.

Fenchel, T. (1982c). Ecology of Heterotrophic Microflagellates. III. Adaptations to Heterogeneous Environments. *Marine Ecology Progress Series*, *9*(1), 25–33.

Fenchel, T. (1982d). Ecology of Heterotrophic Microflagellates. IV. Quantitative Occurrence and Importance as Bacterial Consumers. *Marine Ecology Progress Series*, *9*(1), 35–42.

Ishigaki, T., & Terazaki, M. (1998). Grazing Behavior of Heterotrophic NanoFlagellates Observed with a High Speed VTR System. *Journal of Eukaryotic Microbiology*, *45*(5), 484–487. https://doi.org/10.1111/j.1550-7408.1998.tb05104.x

Kiørboe, T. (2011). How zooplankton feed: Mechanisms, traits and trade-offs. *Biological Reviews*, *86*(2), 311–339. https://doi.org/10.1111/j.1469-185X.2010.00148.x

Kiørboe, T., & Hirst, A. G. (2014). Shifts in Mass Scaling of Respiration, Feeding, and Growth Rates across Life-Form Transitions in Marine Pelagic Organisms. *The American Naturalist*, *183*(4), E118–E130. https://doi.org/10.1086/675241

Langlois, V. J., Andersen, A., Bohr, T., Visser, A. W., & Kiørboe, T. (2009). Significance of swimming and feeding currents for nutrient uptake in osmotrophic and interception-feeding flagellates. *Aquatic Microbial Ecology*, *54*(1), 35–44. https://doi.org/10.3354/ame01253

Logares, R., Audic, S., Santini, S., Pernice, M. C., de Vargas, C., & Massana, R. (2012). Diversity patterns and activity of uncultured marine heterotrophic flagellates unveiled with pyrosequencing. *The ISME Journal*, *6*(10), Article 10. https://doi.org/10.1038/ismej.2012.36

Massana, R., Unrein, F., Rodríguez-Martínez, R., Forn, I., Lefort, T., Pinhassi, J., & Not, F. (2009). Grazing rates and functional diversity of uncultured heterotrophic flagellates. *The ISME Journal*, *3*(5), Article 5. https://doi.org/10.1038/ismej.2008.130

Nielsen, L. T., & Kiørboe, T. (2021). Foraging trade-offs, flagellar arrangements, and flow architecture of planktonic protists. *Proceedings of the National Academy of Sciences*, *118*(3), e2009930118. https://doi.org/10.1073/pnas.2009930118

Rassoulzadegan, F., & Sheldon, R. W. (1986). Predator-prey interactions of nanozooplankton and bacteria in an oligotrophic marine environment1. *Limnology and Oceanography*, *31*(5), 1010–1029. https://doi.org/10.4319/lo.1986.31.5.1010

Tikhonenkov, D. V. (2020). Predatory flagellates – the new recently discovered deep branches of the eukaryotic tree and their evolutionary and ecological significance. *Protistology*, *14*(1). https://doi.org/10.21685/1680-0826-2020-14-1-2

Worden, A. Z., Follows, M. J., Giovannoni, S. J., Wilken, S., Zimmerman, A. E., & Keeling, P. J. (2015). Rethinking the marine carbon cycle: Factoring in the multifarious lifestyles of microbes. *Science*, *347*(6223), 1257594. https://doi.org/10.1126/science.1257594

CHAPTER 2

Ecology of Flagellates

2.1 The complexity of microbial food webs

Microbial food webs are crucial for supporting life in aquatic systems across all scales. The feeding activity of micron-size plankton will ultimately determine the survival and population dynamics of meter-long sharks and tuna. Contrary to the traditional view of a linear bottom-up carbon transfer, trophic interactions occur in multiple directions among microorganisms with diverse diets, feeding associations (symbiotic or not), and nutritional needs that change with life stages (Fig. 2.1). These trophic levels, comprising primary producers and consumers, exhibit immense phylogenetic, morphological, and ecophysiological diversity. As a result, microbial food webs form intricate and dynamic networks of biotic interactions, driven by the flexible and non-discrete feeding behaviors of water-dwelling microorganisms. Mapping microbial food webs is challenging yet essential for understanding the functions of microscale populations within the entire ecosystem.

Free-living flagellates, i.e. single-cell eukaryotes (protists) equipped with one or more flagella, play a key role in microbial food webs. For example, pico-prasinophyte *Micromonas* are abundant primary producers (Bolaños et al., 2020), while stramenopiles, choanoflagellates, and colorless dinoflagellates are important heterotrophic consumers (Pernthaler, 2005; Sherr & Sherr, 2007). Heterotrophic flagellates exhibit diverse feeding strategies, including phagocytosis (engulfing other organisms), osmotrophy (absorbing dissolved nutrients) (Clay, 2015; Soukal et al., 2021), myzocytosis (extracting prey cell contents) (Sam-Yellowe et al., 2022), and saprotrophy (decomposing) (Raghukumar, 2002). In addition, flagellates can also ingest viruses as small sources of carbon (Deng et al., 2014). Lastly, many flagellates like haptophytes, chlorophytes, and most pigmented dinoflagellates exhibit mixotrophy (Stoecker, 1999; Anderson et al., 2018), combining phagocytosis and photosynthesis. Flagellates are found across all plankton size-based groups, ranging from microflagellates (> 20 μm) to nanoflagellates (2 – 20 μm) and picoflagellates (< 3 μm). Overall, their varied diets and sizes significantly contribute to energetic pathways at different trophic levels. Thus, ‘flagellates’ is a broad term with heavy weight on the global carbon cycles.

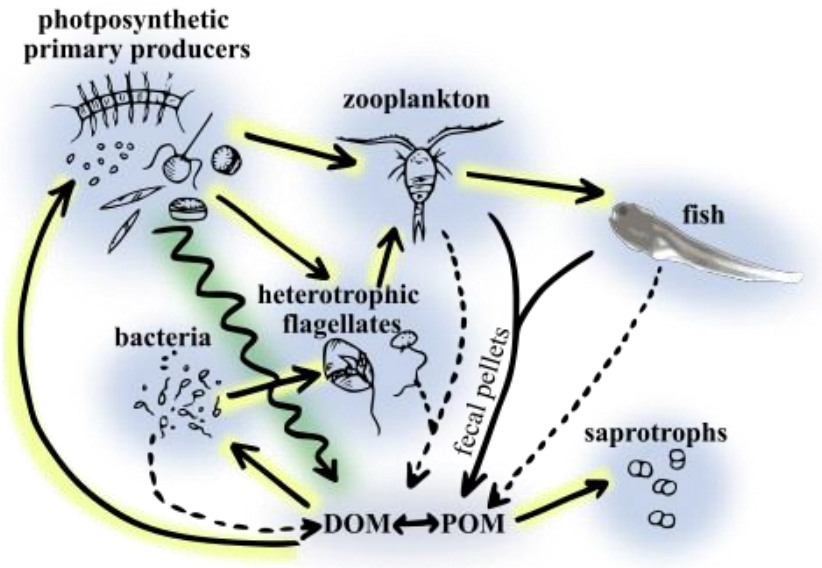

Figure 2.1. Simplified schematic representation of a microbial food web. Exudates and lysates of phytoplankton (cyanobacteria, mixotrophs, and exclusively photosynthetic eukaryotes) are a big source (green curvy arrow) of dissolved organic matter (DOM), which is consumed by bacteria and phytoplankton. Heterotrophic protists, mainly flagellates, consume the small primary producers. Larger zooplankton prey upon protists and phytoplankton, which in turn are eaten by small fish, and the carbon flow is transferred to higher trophic levels in the food chain. All organisms are subject to viral or parasitical infections that can cause death (dashed arrows) and, subsequently, the formation of particulate organic matter (POM) or DOM. Saprotrophs decomposed the POM and DOM. Information from Worden et. al. (2015).

2.2 The ecological significance of phagotrophic nanoflagellates

Forty years ago, phagotrophic nanoflagellates were put in the spotlight of marine food webs (Azam et al., 1983). Previously, primary production and carbon cycling were mainly attributed to larger phytoplankton, such as diatoms and dinoflagellates, while bacteria were considered primarily as remineralizers, recycling organic matter into inorganic nutrients. In the late 70s, technical advances highly improved the methods used to count cells and measure the metabolic activity of bacteria in the ocean (Fuhrman & Azam, 1982), providing researchers with more accurate estimates of their biomass and productivity. Surprisingly, despite their rapid growth rate, bacterial cell counts in nature were found to be high but relatively constant, around a million cells per milliliter. This consistency was controlled by the grazing pressure of heterotrophic nanoflagellates: scientists reported the effective predation activity and observed coupled oscillations in bacterial and flagellate population sizes, with prey peak counts declining when flagellate numbers increased (Fenchel, 1982a, 1982b, 1982c, 1982d; Newell, 1984). Furthermore,

it became apparent that bacteria are not only remineralisers, but also have an important role in cycling dissolved organic matter lost from primary production back into higher trophic levels when grazed upon. The intricate interactions between phytoplankton (DOM producers and nutrient consumers), bacteria (DOM and nutrient consumers), and nano-predators (phytoplankton and bacteria consumers) result in an essential ecological process of relatively fast nutrient cycling. Hence, the revision of past data plus the collaborative studies at the time unveiled an alternative trophic pathway for primary production that was coined as the 'microbial loop' (Azam et al., 1983) (Fig. 2.1). In the microbial loop, the high productivity of bacteria and the subsequent grazing of nanoflagellates have a relevant impact of on the overall productivity of aquatic ecosystems.

Over time, the network of interactions in the microbial loop has gained complexity with the inclusion of new actors (Fenchel, 2008; Worden et al., 2015). For instance, minute photosynthetic prokaryotes, like *Synnechococcus* and *Prochlorococcus*, have been recognized as important primary producers in oligotrophic waters (Campbell & Vaulot, 1993); mixotrophy has credited double trophic pathways for microorganisms capable of both phagocytosis and photosynthesis (Hartmann et al., 2012); and viruses have been established as a new functional group, responsible for a large fraction of bacterial mortality (Middelboe & Jørgensen, 2006) while also consumed by flagellates (Deng et al., 2014). The growing complexity of microbial food webs is challenging to current carbon cycle and biogeochemical cycle models, which are often built with broad functional groups and fail to reflect the flexible ecophysiology and feeding behavior of many organisms (Worden et al., 2015). Many of these mathematical models are important tools for climate sensitivity studies. Therefore, it is essential to better understand these trophic interactions, where phagotrophic nanoflagellates play a key role.

2.3 Fitted in a 'black box'

It is a struggle to count flagellates in a fixed natural assemblage under the microscope, due to the laborious task of spotting them amongst a sea of similar-sized 'dots'. For most, the flagellum is the only identifying morphology to differentiate them from other protists, yeast, or big bacteria; yet, it can be lost during the fixation process or appear practically invisible. Additionally, some cells prepared for epifluorescence observation may experience significant volume shrinkage (Choi & Stoecker, 1989). Hence quantitative data derived from microscope counts of fixed samples can be misleading. On the other hand, counting live samples is more accurate, especially in specimen identification, but demanding and time-constraining. Species of heterotrophic flagellates that are rare or particularly small are usually underestimated or neglected during ecological assessments. Species that constitute a small fraction of the total community biomass can be easily overlooked when, as a common practice, < 10% of the cells in an original sample are studied (due to counting small portions of a filter or serial dilutions). Conversely, specimens

might be abundant but hard to see. Minute heterotrophic flagellates (picoflagellates, < 3 μm) are highly present in marine and freshwater systems (Massana et al., 2002; Lefèvre et al., 2005), but were not properly recognized until specific genetic tools were developed. Despite molecular advances, many significant species of heterotrophic flagellates are classed as 'uncultured' (del Campo et al., 2013) and, thus, remain largely unexplored. Microbial predator-prey interactions have been commonly studied through incubation experiments with natural assemblages or using laboratory monocultures. This approach monitors the abundancies of different populations for a period of time, to calculate the removal (or not) of prey and determine the population dynamics. Nonetheless, these types of assessments mask a pool of biotic relations from the individual level.

The diversity of heterotrophic flagellates has been (and still is) hard to grasp. In the past, low sampling efforts have limited the findings of new species, and microscope techniques have challenged cell counts and identifications. Furthermore, studies of functional responses exclusively based on incubation experiments went without an understanding of the underlying mechanisms and behaviors. Hence, in many ways, heterotrophic flagellates have been traditionally placed inside a 'black box' as a single functional group with a few 'example species'. With improved molecular and microscope methods, the true phylogenetic and functional diversity of flagellates is progressively unveiled. For instance, high-speed video microscopy has allowed researchers to capture events that happen in a split of a second, and fluorescent in situ hybridization (FISH) has obtained grazing rates of uncultured heterotrophic flagellates (Massana et al., 2009).

2.4 Functions, diversity, and distribution

An ecological function is the role or impact of a natural group or population of organisms on the properties of the ecosystem that it inhabits. Ecological functions are driven by functional traits (Kiørboe et al., 2018). Commonly, functional traits are defined by the patterns of resource use of a species (Naeem & Wright, 2003), mainly diet and trophic position, which are closely correlated with the phylogeny and morphology of an organism. Phagotrophic nanoflagellates are phylogenetically diverse, spreading across the eukaryotic Tree of Life (eToL) with species in every major branch (Adl et al., 2019; Burki et al., 2020) (Fig. 2.2).

In addition, they present a vast variety of cell morphologies and flagellar configurations that highly influence their ability to feed and evade predation mortality (Kiørboe, 2023; Nielsen & Kiørboe, 2021; Sleigh, 1981) (Fig. 2.3). Moreover, phagotrophic modes span from herbivory, bacteriovory, and eukaryovory, to omnivory, and with a broad prey-size spectrum (see review Boenigk & Arndt, 2002). Lastly, phagotrophic nanoflagellates are abundant (around $10^2 – 10^4$ cells / mL in pelagic waters; Sanders et al., 1992) and ubiquitous, living in pelagic waters, lakes and streams, the marine and limnetic benthos, brackish marshal sediments, wastewater treatment plants, and more. Hence, it is evident that phagotrophic nanoflagellates are functionally diverse.

Due to technical constraints for specimen identification (mentioned in section 2.3), early studies of microbial community composition, and in particular the distribution of pico- and nanoflagellates species, were challenging and, consequently, used broad functional groups (e.g., Patterson & Larsen, 1991). With the arrival of advanced molecular methods, surveys of small protists have brought to light the high taxonomic diversity in heterotrophic flagellate populations from different habitats and aquatic systems (e.g., Díez et al., 2001; Moon-van der Staay et al., 2001; Mukherjee et al., 2015; Park & Simpson, 2015; and see review Adl et al., 2019). A recent global assessment of pelagic environments has recorded a 'core community' in surface waters composed primarily of uncultured taxa (MAST clades, i.e., unidentified lineages of marine stramenopiles, Picozoa and Chrysophyceae) followed by the patchy presence of Chrysophyceae and Bicosoecida groups (Obiol et al., 2021). The authors also found that the diversity from surface waters substantially decreased with depth and was only dominated by Chrysophyceae and Bicosoecida, Diplonemea, and to a less extent by Kinetoplastida; however, the survey failed to detect euglenozoans that have been shown to be dominant in many deep-sea and benthic habitats (see review Arndt et al., 2000). Despite this discrepancy due to a methodological default, the new

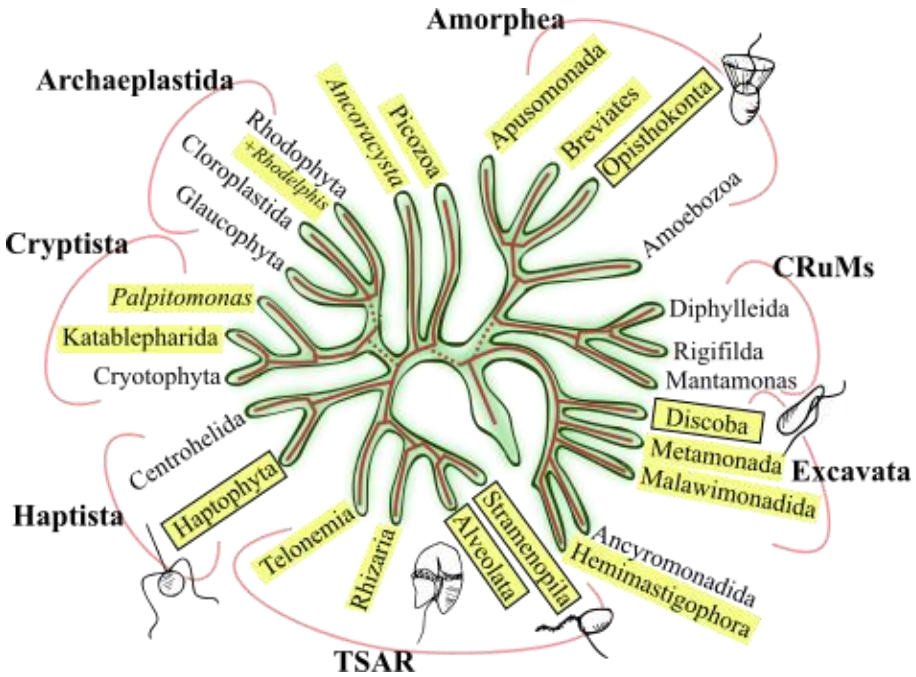

Figure 2.2. The eukaryotic Tree of Life (eToL). Phagotrophic flagellates are widespread across the supergroups of the eToL (taxa highlighted in yellow). Few studies have investigated the feeding mechanisms of phagotrophic flagellates, and are mostly restricted to just a few taxa (boxed names with representative species drawing). Information extracted from Burki et. al. (2020).

Coincidently, another recent study, using scanning and transmission electron microscopy, has revealed the morphotypes of omnipresent biflagellated stramenopiles and choanoflagellates at a relative abundance ratio of around 10:1 in marine oligotrophic waters (Kamennaya et al., 2022). findings of Obiol et al. (2021) largely match with early non-molecular studies of community composition (again from review Arndt et al., 2000), which attributed the main heterotrophic nanoflagellate biomass (20 – 50%) in pelagic and limnetic waters to stramenopile taxa (mostly Chrysophyceae and Bicosoecida, and interestingly a significant presence of incertae sedis groups, i.e. of uncertain taxonomic placement), and secondly to choanoflagellates (5 – 40%). Furthermore, Kamennaya et al. (2022) hypothesized the feeding and swimming functions of the dominant morphotypes through theoretical models of propulsion and prey interception and suggest a morphological underpinning for the dominance of stramenopiles. To date, most ecophysiological studies have been restricted to a small handful of available cultured species, when in reality most of the dominant species in natural environments remain uncultured (del Campo et al., 2013). And genomic evidence supports the hypothesis that these uncultured species are functionally diverse (Seeleuthner et al., 2018). Overall, there seems to be a consensus from experts to prioritize efforts in culturing the 'non-available', yet significant, species for further ecological assessments that will improve our understanding of the natural microbial systems.

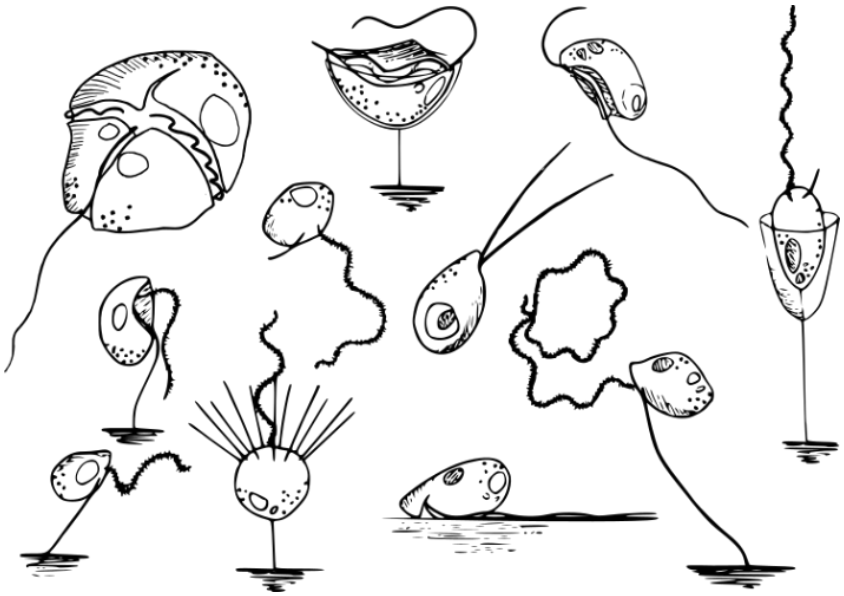

Figure 2.3. Morphological diversity of phagotrophic flagellates with different flagellar types (hairy, vaned, naked) and configurations. From top to bottom and left to right: dinoflagellate, *Developayella* sp., *Cafeteria* sp., *Reclinomonas* sp., *Paraphysomonas* sp., *Pteridomonas* sp., '*Malawimonas californiensis'*, *Telonema* sp., *Rhynchomonas nasuta*, *Pseudobodo* sp., *Biocosoeca* sp.

Modern environmental molecular methods of high throughput have unveiled the omnipresence and biodiversity of flagellates. However, molecular analysis using cultures from 'traditional' single-cell isolations have identified an impressive number of new protist lineages, most unnoticed by the environmental surveys. These new lineages, often composed of one or two heterotrophic nanoflagellate species, could be key to understanding the profound relationships of the eukaryotic Tree of Life (eToL) (Burki et al., 2020). Moreover, a few of the 'new' flagellates are eukaryotrophs (e.g. *Rhodelphis*, *Colponema*, *Ancoracysta*, *Acavomonas*, *Telonema*), that is, they prey upon other small predatory flagellates, acting as a top-down control to their populations (Tikhonenkov, 2020). Nonetheless, the ecological functions of eukaryotrophic nanoflagellates remain poorly understood. Along with the discovery of new deep-branching taxa, for the past 15 years, the eToL has been remarkably remodeled (Burki et al., 2020). This has complicated the long-standing goal to find the position of the rooting last eukaryotic common ancestor (LECA). Some phylogenomic studies have suggested a root in proximity to an excavate (Derelle et al., 2015). The supergroup Excavata is currently composed of three groups: Discoba, Metamonada, and Malawimonadida. The phylogenetic relationship among excavates is unclear, however, current evidence primarily supports the homology of their cell morphology (Simpson, 2003). Therefore, it is plausible that LECA resembled a 'typical excavate': presenting a feeding ventral groove associated with a flagellum that bears a vane. Thus, studying the forms of predation of a 'typical excavate' would give a theoretical insight into LECA's primitive forms of feeding and the roles it fulfilled in the ancestral ecosystems of around 1 billion years ago.

References

Adl, S. M., Bass, D., Lane, C. E., Lukeš, J., Schoch, C. L., Smirnov, A., Agatha, S., Berney, C., Brown, M. W., Burki, F., Cárdenas, P., Čepička, I., Chistyakova, L., del Campo, J., Dunthorn, M., Edvardsen, B., Eglit, Y., Guillou, L., Hampl, V., … Zhang, Q. (2019). Revisions to the Classification, Nomenclature, and Diversity of Eukaryotes. *Journal of Eukaryotic Microbiology*, *66*(1), 4–119. https://doi.org/10.1111/jeu.12691

Anderson, R., Charvet, S., & Hansen, P. J. (2018). Mixotrophy in Chlorophytes and Haptophytes—Effect of Irradiance, Macronutrient, Micronutrient and Vitamin Limitation. *Frontiers in Microbiology*, *9*. https://www.frontiersin.org/articles/10.3389/fmicb.2018.01704

Arndt, H., Dietrich, D., Auer, B., Cleven, E.-J., Gräfenhan, T., Weitere, M., & Mylnikov, A. P. (2000). Functional diversity of heterotrophic flagellates in aquatic ecosystems. In B. S. C. Leadbeater & J. C. Green (Eds.), *Flagellates* (0 ed., pp. 252–280). CRC Press. https://doi.org/10.1201/9781482268225-18

Azam, F., Fenchel, T., Field, J. G., Gray, J. S., Meyer-Reil, L. A., & Thingstad, F. (1983). The Ecological Role of Water-Column Microbes in the Sea. *Marine Ecology Progress Series*. https://doi.org/10.3354/meps010257

Boenigk, J., & Arndt, H. (2002). Bacterivory by heterotrophic flagellates: Community structure and feeding strategies. *Antonie van Leeuwenhoek*, *81*(1), 465–480. https://doi.org/10.1023/A:1020509305868

Bolaños, L. M., Karp-Boss, L., Choi, C. J., Worden, A. Z., Graff, J. R., Haëntjens, N., Chase, A. P., Della Penna, A., Gaube, P., Morison, F., Menden-Deuer, S., Westberry, T. K., O'Malley, R. T., Boss, E., Behrenfeld, M. J., & Giovannoni, S. J. (2020). Small phytoplankton dominate western North Atlantic biomass. *The ISME Journal*, *14*(7), Article 7. https://doi.org/10.1038/s41396-020-0636-0

Burki, F., Roger, A. J., Brown, M. W., & Simpson, A. G. B. (2020). The New Tree of Eukaryotes. *Trends in Ecology & Evolution*, *35*(1), 43–55. https://doi.org/10.1016/j.tree.2019.08.008

Campbell, L., & Vaulot, D. (1993). Photosynthetic picoplankton community structure in the subtropical North Pacific Ocean near Hawaii (station ALOHA). *Deep Sea Research Part I: Oceanographic Research Papers*, *40*(10), 2043–2060. https://doi.org/10.1016/0967-0637(93)90044-4

Choi, J. W., & Stoecker, D. K. (1989). Effects of Fixation on Cell Volume of Marine Planktonic Protozoa. *Applied and Environmental Microbiology*, *55*(7), 1761–1765.

Clay, B. L. (2015). Cryptomonads. In *Freshwater Algae of North America* (pp. 809–850). Elsevier. https://doi.org/10.1016/B978-0-12-385876-4.00018-9

del Campo, J., Balagué, V., Forn, I., Lekunberri, I., & Massana, R. (2013). Culturing Bias in Marine Heterotrophic Flagellates Analyzed Through Seawater Enrichment Incubations. *Microbial Ecology*, *66*(3), 489–499. https://doi.org/10.1007/s00248-013-0251-y

Deng, L., Krauss, S., Feichtmayer, J., Hofmann, R., Arndt, H., & Griebler, C. (2014). Grazing of heterotrophic flagellates on viruses is driven by feeding behaviour. *Environmental Microbiology Reports*, *6*(4), 325–330. https://doi.org/10.1111/1758-2229.12119

Derelle, R., Torruella, G., Klimeš, V., Brinkmann, H., Kim, E., Vlček, Č., Lang, B. F., & Eliáš, M. (2015). Bacterial proteins pinpoint a single eukaryotic root. *Proceedings of the National Academy of Sciences*, *112*(7), E693–E699. https://doi.org/10.1073/pnas.1420657112

Díez, B., Pedrós-Alió, C., & Massana, R. (2001). Study of Genetic Diversity of Eukaryotic Picoplankton in Different Oceanic Regions by Small-Subunit rRNA Gene Cloning and Sequencing. *Applied and Environmental Microbiology*, *67*(7), 2932–2941. https://doi.org/10.1128/AEM.67.7.2932-2941.2001

Fenchel, T. (1982a). Ecology of Heterotrophic Microflagellates. I. Some Important Forms and Their Functional Morphology. *Marine Ecology Progress Series*, *8*(3), 211–223.

Fenchel, T. (1982b). Ecology of Heterotrophic Microflagellates. II. Bioenergetics and Growth. *Marine Ecology Progress Series*, *8*(3), 225–231.

Fenchel, T. (1982c). Ecology of Heterotrophic Microflagellates. III. Adaptations to Heterogeneous Environments. *Marine Ecology Progress Series*, *9*(1), 25–33.

Fenchel, T. (1982d). Ecology of Heterotrophic Microflagellates. IV. Quantitative Occurrence and Importance as Bacterial Consumers. *Marine Ecology Progress Series*, *9*(1), 35–42.

Fenchel, T. (2008). The microbial loop – 25 years later. *Journal of Experimental Marine Biology and Ecology*, *366*(1), 99–103. https://doi.org/10.1016/j.jembe.2008.07.013

Fuhrman, J. A., & Azam, F. (1982). Thymidine incorporation as a measure of heterotrophic bacterioplankton production in marine surface waters: Evaluation and field results. *Marine Biology*, *66*(2), 109–120. https://doi.org/10.1007/BF00397184

Hartmann, M., Grob, C., Tarran, G. A., Martin, A. P., Burkill, P. H., Scanlan, D. J., & Zubkov, M. V. (2012). Mixotrophic basis of Atlantic oligotrophic ecosystems. *Proceedings of the National Academy of Sciences*, *109*(15), 5756–5760. https://doi.org/10.1073/pnas.1118179109

Kamennaya, N. A., Kennaway, G., Sleigh, M. A., & Zubkov, M. V. (2022). Notable predominant morphology of the smallest most abundant protozoa of the open ocean revealed by electron microscopy. *Journal of Plankton Research*, *44*(4), 542–558. https://doi.org/10.1093/plankt/fbac031

Kiørboe, T. (2023). Predation in a Microbial World: Mechanisms and Trade-Offs of Flagellate Foraging. *Annual Review of Marine Science*, *16*(1), null. https://doi.org/10.1146/annurev-marine-020123-102001

Kiørboe, T., Visser, A., & Andersen, K. H. (2018). A trait-based approach to ocean ecology. *ICES Journal of Marine Science*, *75*(6), 1849–1863. https://doi.org/10.1093/icesjms/fsy090

Lefèvre, E., Carrias, J.-F., Bardot, C., Sime-Ngando, T., & Amblard, C. (2005). A Preliminary Study of Heterotrophic Picoflagellates Using Oligonucleotidic Probes in Lake Pavin. *Hydrobiologia*, *551*(1), 61–67. https://doi.org/10.1007/s10750-005-4450-5

Massana, R., Guillou, L., Díez, B., & Pedrós-Alió, C. (2002). Unveiling the Organisms behind Novel Eukaryotic Ribosomal DNA Sequences from the Ocean. *Applied and Environmental Microbiology*, *68*(9), 4554–4558. https://doi.org/10.1128/AEM.68.9.4554-4558.2002

Massana, R., Unrein, F., Rodríguez-Martínez, R., Forn, I., Lefort, T., Pinhassi, J., & Not, F. (2009). Grazing rates and functional diversity of uncultured heterotrophic flagellates. *The ISME Journal*, *3*(5), Article 5. https://doi.org/10.1038/ismej.2008.130

Middelboe, M., & Jørgensen, N. O. G. (2006). Viral lysis of bacteria: An important source of dissolved amino acids and cell wall compounds. *Journal of the Marine Biological Association of the United Kingdom*, *86*(3), 605–612. https://doi.org/10.1017/S0025315406013518

Moon-van der Staay, S. Y., De Wachter, R., & Vaulot, D. (2001). Oceanic 18S rDNA sequences from picoplankton reveal unsuspected eukaryotic diversity. *Nature*, *409*(6820), Article 6820. https://doi.org/10.1038/35054541

Mukherjee, I., Hodoki, Y., & Nakano, S. (2015). Kinetoplastid flagellates overlooked by universal primers dominate in the oxygenated hypolimnion of Lake Biwa, Japan. *FEMS Microbiology Ecology*, *91*(8), fiv083. https://doi.org/10.1093/femsec/fiv083

Naeem, S., & Wright, J. P. (2003). Disentangling biodiversity effects on ecosystem functioning: Deriving solutions to a seemingly insurmountable problem. *Ecology Letters*, *6*(6), 567–579. https://doi.org/10.1046/j.1461-0248.2003.00471.x

Newell, R. C. (1984). The Biological Role of Detritus in the Marine Environment. In M. J. R. Fasham (Ed.), *Flows of Energy and Materials in Marine Ecosystems: Theory and Practice* (pp. 317–343). Springer US. https://doi.org/10.1007/978-1-4757-0387-0_13

Nielsen, L. T., & Kiørboe, T. (2021). Foraging trade-offs, flagellar arrangements, and flow architecture of planktonic protists. *Proceedings of the National Academy of Sciences*, *118*(3), e2009930118. https://doi.org/10.1073/pnas.2009930118

Obiol, A., Muhovic, I., & Massana, R. (2021). Oceanic heterotrophic flagellates are dominated by a few widespread taxa. *Limnology and Oceanography*, *66*(12), 4240–4253. https://doi.org/10.1002/lno.11956

Park, J. S., & Simpson, A. G. B. (2015). Diversity of Heterotrophic Protists from Extremely Hypersaline Habitats. *Protist*, *166*(4), 422–437. https://doi.org/10.1016/j.protis.2015.06.001

Patterson, D. J., & Larsen, J. (1991). *The Biology of free-living heterotrophic flagellates*. Published for the Systematics Association by Clarendon Press ; Oxford University Press. http://catdir.loc.gov/catdir/enhancements/fy0635/91019780-d.html

Pernthaler, J. (2005). Predation on prokaryotes in the water column and its ecological implications. *Nature Reviews Microbiology*, *3*(7), Article 7. https://doi.org/10.1038/nrmicro1180

Raghukumar, S. (2002). Ecology of the marine protists, the Labyrinthulomycetes (Thraustochytrids and Labyrinthulids). *European Journal of Protistology*, *38*(2), 127–145. https://doi.org/10.1078/0932-4739-00832

Sam-Yellowe, T. Y., Fujioka, H., & Peterson, J. W. (2022). Ultrastructure of Myzocytosis and Cyst Formation, and the Role of Actin in Tubular Tether Formation in Colpodella sp. (ATCC 50594). *Pathogens*, *11*(4), 455. https://doi.org/10.3390/pathogens11040455

Sanders, R., Caron, D., & Berninger U, G. (1992). Relationships between bacteria and heterotrophic nanoplankton in marine and fresh waters: An inter-ecosystem comparison. *Marine Ecology Progress Series*, *86*, 1–14. https://doi.org/10.3354/meps086001

Seeleuthner, Y., Mondy, S., Lombard, V., Carradec, Q., Pelletier, E., Wessner, M., Leconte, J., Mangot, J.-F., Poulain, J., Labadie, K., Logares, R., Sunagawa, S., de Berardinis, V., Salanoubat, M., Dimier, C., Kandels-Lewis, S., Picheral, M., Searson, S., Pesant, S., … Wincker, P. (2018). Single-cell genomics of multiple uncultured stramenopiles reveals underestimated functional diversity across oceans. *Nature Communications*, *9*(1), Article 1. https://doi.org/10.1038/s41467-017-02235-3

Sherr, E. B., & Sherr, B. F. (2007). Heterotrophic dinoflagellates: A significant component of microzooplankton biomass and major grazers of diatoms in the sea. *Marine Ecology Progress Series*, *352*, 187–197. https://doi.org/10.3354/meps07161

Simpson, A. G. B. (2003). Cytoskeletal organization, phylogenetic affinities and systematics in the contentious taxon Excavata (Eukaryota). *International Journal of Systematic and Evolutionary Microbiology*, *53*(6), 1759–1777. https://doi.org/10.1099/ijs.0.02578-0

Sleigh, M. A. (1981). Flagellar beat patterns and their possible evolution. *Biosystems*, *14*(3), 423–431. https://doi.org/10.1016/0303-2647(81)90047-2

Soukal, P., Hrdá, Š., Karnkowska, A., Milanowski, R., Szabová, J., Hradilová, M., Strnad, H., Vlček, Č., Čepička, I., & Hampl, V. (2021). Heterotrophic euglenid Rhabdomonas costata resembles its phototrophic relatives in many aspects of molecular and cell biology. *Scientific Reports*, *11*(1), Article 1. https://doi.org/10.1038/s41598-021-92174-3

Stoecker, D. K. (1999). Mixotrophy among Dinoflagellates1. *Journal of Eukaryotic Microbiology*, *46*(4), 397–401. https://doi.org/10.1111/j.1550-7408.1999.tb04619.x

Tikhonenkov, D. V. (2020). Predatory flagellates – the new recently discovered deep branches of the eukaryotic tree and their evolutionary and ecological significance. *Protistology*, *14*(1). https://doi.org/10.21685/1680-0826-2020-14-1-2

Worden, A. Z., Follows, M. J., Giovannoni, S. J., Wilken, S., Zimmerman, A. E., & Keeling, P. J. (2015). Rethinking the marine carbon cycle: Factoring in the multifarious lifestyles of microbes. *Science*, *347*(6223), 1257594. https://doi.org/10.1126/science.1257594

CHAPTER 3

Fluid Dynamics of Flagellates

3.1 Living in the low Reynolds number regime

We, humans, live in a turbulent world. The air we exhale forms vortices when it pumps out of our noses and water gets stirred up when we jump into a pool for a swim. We are in close relation to the fluids of our surroundings, and this is true for all living organisms. However, not all life forms experience it in the same way. A good way to measure how a being is interacting with environmental fluids is by using the dimensionless Reynolds number (Re). Considering that organisms live in water, the Reynolds number derives from the governing equations of Navier-Stokes of momentum conservation and continuity for incompressible Newtonian flow:

$$\rho\left(\frac{\partial \boldsymbol{v}}{\partial t} + (\boldsymbol{v}\cdot\boldsymbol{\nabla})\,\boldsymbol{v}\right) = -\boldsymbol{\nabla}p + \mu\nabla^2\boldsymbol{v} + \boldsymbol{F}\,, \tag{1}$$

$$\boldsymbol{\nabla}\cdot\boldsymbol{v} = 0\,, \tag{2}$$

where ρ is the density of the fluid, $\boldsymbol{v}$ is the velocity field, p is the pressure field, μ is the dynamic viscosity, and $\boldsymbol{F}$ is an external body force such as gravity. Both fields, velocity, and pressure, are functions of position ($\boldsymbol{x}$) and time (t) (Rode, 2021). To simplify the non-linear terms of inertia from the Navier-Stokes equation (1), the characteristic scaling of parameters can be considered to evaluate the relation of the terms. By doing so, L becomes the characteristic length, e.g. of an organism, with the magnitude of the gradient $\boldsymbol{\nabla}$ roughly scaled as L^{-1}, and U becomes the characteristic swimming speed that scales the velocity field. The Reynolds number is the ratio of inertia forces to viscous forces that will define the behavior of the fluid and indicate the dominating forces acting on a body in such a fluid flow. We find the advective to viscous ratio in the Navier-Stokes equation and can, thus, define the Reynolds number as

$$Re \approx \frac{|\rho(\boldsymbol{v}\cdot\boldsymbol{\nabla})\boldsymbol{v}|}{|\mu\nabla^2\boldsymbol{v}|} \approx \frac{\rho U^2 L^{-1}}{\mu U L^{-2}} = \frac{\rho U L}{\mu}\,. \tag{3}$$

Let us consider that the density of seawater (ρ) is 10^3 kg · m^{-3}, and the dynamic viscosity (μ) is 10^{-3} Pa · s. As shown in Table 3.1, the Reynolds number of a 10-meter-long whale is Re ≈ 10^8; whereas the number drops down to Re ≈ 10^{-3} and Re ≈ 10^{-5} for a swimming flagellate and bacterium, respectively. Reynolds numbers much greater than unity correspond to a chaotic turbulent flow regime. In contrast, the very small values calculated for the bacterium and flagellate mean that they inhabit a laminar flow regime that is strongly governed by viscosity (Dusenbery, 2009). Thus, inertia is practically null. A way that helps visualize the alien low Reynolds number world in which these microorganisms live is to imagine oneself trying to swim in a pool filled with molasses (Purcell, 1977).

	L (m)	*U* (m · s^{-1})	Re
Bacterium	10^{-6}	10^{-5}	10^{-5}
Flagellate	10^{-5}	10^{-4}	10^{-3}
Copepod	10^{-3}	10^{-1}	10^{2}
Human	1	1	10^{6}
Whale	10	10	10^{8}

Table 3.1. Examples of Reynolds numbers (Re) for swimming life forms of different scale and flow regimes. The parameters used to calculate the Reynolds number for each organism are *L*, the characteristic length, and *U*, the characteristic magnitude of the velocity.

Living in a low Reynolds number world has a series of implications. First, high viscosity impedes particle-to-particle contact. The 'sticky' water layers close to a body in motion are dragged along, pushing away other bodies in the vicinity. Second, whilst a whale can coast ahead several body lengths with a single tail flap, a swimming microorganism virtually stops immediately as soon as the propulsion force ceases. Lastly, a microbe will go nowhere by swimming with a reciprocal motion (i.e., a movement from one position to the next, which subsequently reverses back, with the same pattern, to the initial position). As explained with the 'Scallop Theorem', the slow opening of the shells of a scallop, followed by a quick closing results in a net displacement. Yet, for the same pattern in the micron scale, the difference in duration between one swimming phase (slow opening) with the next (fast closing) will not matter. Counterintuitively, '*the pattern of motion is the same, whether slow or fast, whether forward or backward in time*' (Purcell, 1977).

So how is motion achieved by the biggest fraction of life on earth in microhabitats governed by viscosity? The bacteria *Pseudomonas aeruginosa* can 'slingshot' themselves across dense biofilms using some extended grappling hooks (Jin et al., 2011), and the stomach ulcer-causing bacteria *Heliobacter pylori* can swim with its helical cell by reducing the viscoelasticity of the

mucus via urease secretion (Celli et al., 2009). These are examples of adaptations to overcome extreme viscous conditions. Most microbes, however, handle the low Reynolds number conditions with cilia or flagella, i.e., mobile hair-like organelles. The rotating 'corkscrew' motion of the bacterial flagellum (i.e. prokaryotic flagellum), the 'roar-like' moves of cilia, and the undulating beats of the eukaryotic flagellum are non-reciprocal movements specifically adapted to propel the surrounding fluid for swimming or feeding (Berg & Anderson, 1973; Lauga & Powers, 2009) (Fig. 3.1).

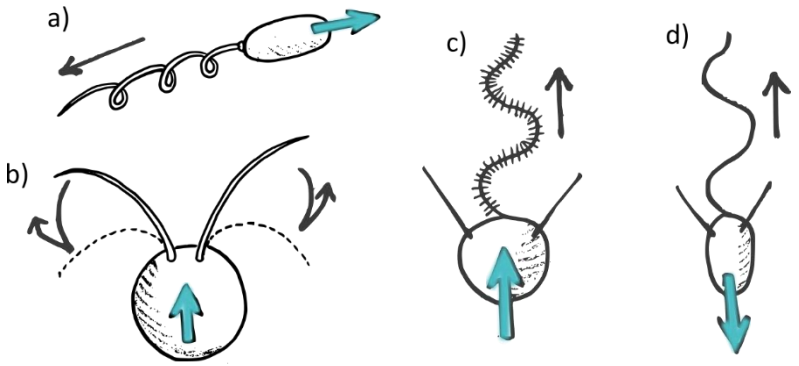

Figure 3.1. Motion in the low Reynolds number regime. Cilia and flagella exhibiting different kinematics for propulsion: a) corkscrew flagellum of a bacterium, b) synchronized cilia of *Chlamydomonas*, c) hairy flagellum of *Pteridomonas* sp., and d) naked flagellum of a choanoflagellate. Arrows indicate the direction of cell displacement (blue) and wave propagation (black). Note that the black arrows of *Chlamydomonas* represent the effective stroke (reaching the dashed line position) and the recovery stroke (returning to the initial position). Figure inspired by Sleigh (1981).

3.2 The flagellum

Flagella are versatile organelles. The transversal cross-section view of a eukaryotic flagellum reveals the renowned 9+2 configuration of the axoneme: a pair of central singlet microtubules surrounded by nine outer doublet microtubules (Fig. 3.2). Motility is achieved with the ATP-driven sliding of an outer doublet microtubule that is constrained by the connections with other outer doublet microtubules, resulting in an applied force that causes the flagellum to bend (Murray, 1994). The universal cytoskeletal organization of the eukaryotic flagellum is the machinery for many living functions: swimming, surface attachment, feeding, sensory perception, and more (Moran et al., 2014). The multifunctional hair-like structure can serve more than one purpose for the same individual, hence, it is no surprise to find flagella (or cilia) in most animal cells, and in the most abundant group of planktonic protists: flagellates.

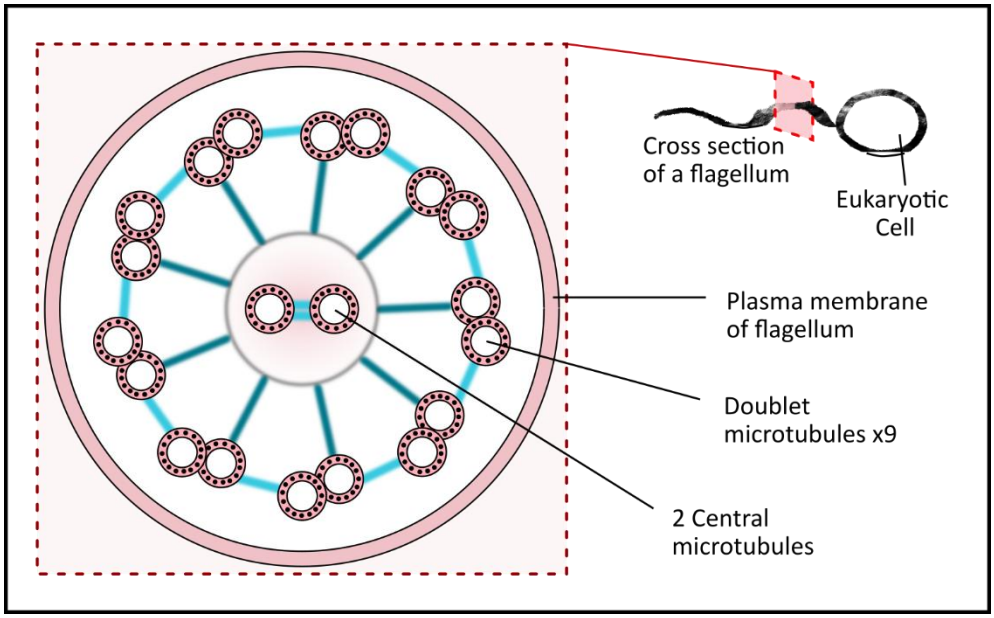

Figure 3.2. Axoneme. The cross-sectional view of a eukaryotic flagellum's ultrastructure shows the universal composition of two central singlet microtubules surrounded by nine doublet microtubules (9+2 configuration).

The propagating wave of a flagellum displaces the surrounding fluids through a drag-based thrust mechanism (Fig. 3.3). In simple terms, the segment of a filament that is moving obliquely at low Reynolds number will experience a larger sideways drag (derived from the perpendicular velocity component) than a lengthwise drag (derived from the parallel velocity component), which will result in a net propelling force perpendicular to the oblique motion, when the time-periodic flagellar motion is non-reciprocal (Lauga & Powers, 2009; Gilpin et al., 2020). For a tethered cell, the flagellar thrust results in a flow that follows a direction from the base to the tip of the flagellum, as observed in choanoflagellates (Mah et al., 2014); for a non-tethered cell it translates into forward locomotion with the flagellum 'pushing' from behind, as found in sea urchin spermatozoa (Gray & Hancock, 1955). Interestingly, the direction of thrust reverses in the presence of mastigonemes. Mastigonemes are fine, often rigid, tubular protrusions arranged in one or two rows along the length of the flagellum of some organisms. The 'hairy flagellum' is typical in stramenopiles and is used to generate feeding currents by phagotrophic species. How do these hairs cause a flagellum to work so differently? Thrust reversal was attributed to the 'roughness' of the hairs that acted like rows at the crest of a propagating wave, obtaining an increased net lengthwise drag relative to the sideways drag (contrary to a naked flagellum) (Holwill & Sleigh, 1967; Jahn et al., 1964). In addition, calculations on single hairs concluded that to reverse the flow direction, mastigonemes should be nearly rigid (Brennen, 1975).

However, the mentioned studies neglected the expected hydrodynamic interactions between mastigonemes. In fact, three-dimensional simulations of a planar-beat hispid flagellum proved that these interactions are essential to generating the thrust and reversing the direction, with longer hairs increasing the overall fluid dynamical effects; moreover, theoretical modeling showed that the flagellar curvature at the crest of the wave has a strong influence on the magnitude of the thrust (Asadzadeh et al., 2022). Hence, Asadzadeh et al. (2022) proposed that a long flagellum bearing long mastigonemes and beating in short wavelengths (curvy) optimizes thrust generation and, thus, is more efficient for swimming and feeding. However, long hairs might interfere with each other during a beat cycle, and the authors suggested that flagellates have solved this problem with hairs protruding at a small angle relative to the beat plane, more than one hair emerging from the same point (bundling), or a three-dimensional flagellar beat pattern.

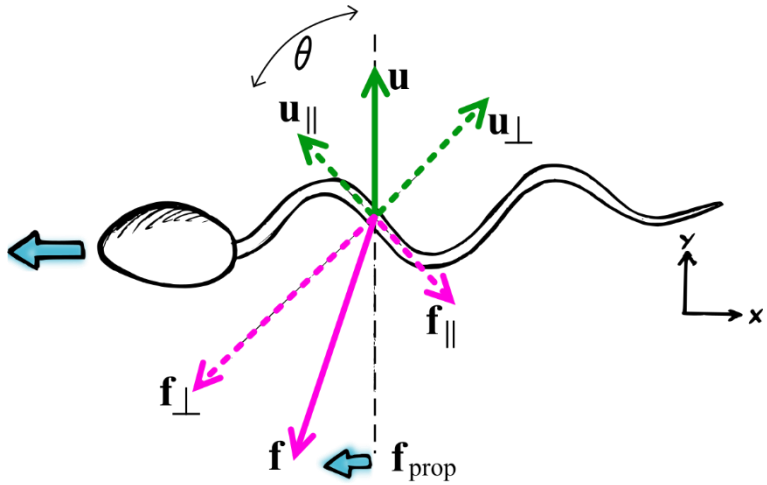

Figure 3.3. **Drag-based thrust.** A short segment of the flagellum (considered to be straight) moves obliquely with a velocity $\boldsymbol{u}$ at an angle θ with the local tangent. The velocity $\boldsymbol{u}$ resolves into a parallel, $u_{\parallel}$, and a perpendicular, $u_{\perp}$, component, which result in corresponding drag force components of opposite direction ($f_{\parallel}$ and $f_{\perp}$). When the perpendicular drag is larger than the parallel component, an additional local drag force $\boldsymbol{f}_{prop}$ is generated, acting perpendicular to the velocity $\boldsymbol{u}$. For a net motion (blue arrow) of the organism, the time-periodic movement of the flagellum has to be non-reciprocal. This figure has been adapted from Lauga & Powers (2009).

Indeed, most flagellar beat patterns are of a complex three-dimensional architecture. Suspension-feeding flagellates present a great diversity of flagellar configurations to intercept prey (Fenchel, 1986; Kiørboe, 2023; Sleigh, 1981). Far from the planar beating flagella of choanoflagellates and the pedinellid *Actinomonas* sp. (Sleigh, 1964), which are smooth and hairy respectively, one can find the curios motions of the bent flagellum of *Paraphysomonas danica* (Chrysophyta)

(Christensen-Dalsgaard & Fenchel, 2004), the comical 'twisted spirally' flagellum of *Pseudobodo tremulans* (Bicosoeca) (Fenchel, 1982), or the 'ballet step' beating of *Developayella elegans* (Heterokont) (Tong, 1995). Furthermore, flagellar beating patterns can undergo sudden changes of behavior as a reaction to external biotic or abiotic stimuli: like the sudden coiling flagellum of the loricated *Bicosoeca maris* (Moestrup & Thomsen, 1976) or the prey capturing flagellar dynamics of some stramenopiles (Boenigk & Arndt, 2000). The combination of diverse arrangements, beat patterns, and behaviors will result in an array of flow architectures with different contrasts of predation efficiencies and risks (Nielsen & Kiørboe, 2021). Nonetheless, the complex configurations have challenged the achievement of fully resolved studies of the flagellar activity in most specimens.

3.3 Measuring the action of a flagella

To study the flow generated by the flagella of microorganisms in the low Reynolds number regime of an incompressible fluid, the Navier-Stokes equation (1) and (2) can be simplified into a linearized time-dependent equation

$$-\boldsymbol{\nabla} p + \mu \nabla^2 \boldsymbol{v} + \boldsymbol{F} = 0\,, \tag{4}$$

$$\boldsymbol{\nabla} \cdot \boldsymbol{v} = 0\,. \tag{5}$$

The fundamental solution of the Stokes equations (4) and (5) is the Stokeslet solution. In the case of a beating flagellum, the Stokeslet is introduced considering that the active flagellum produces a force that induces a fluid velocity. Given a Stokeslet placed at the origin point with an acting force $\boldsymbol{F}$ = (0, 0, -*F*), the derived velocity field becomes

$$v_x(\boldsymbol{x}) = -\frac{F}{8\pi\mu}\,\frac{x\,z}{|\boldsymbol{x}|^3}\,, \tag{6}$$

$$v_y(\boldsymbol{x}) = -\frac{F}{8\pi\mu}\,\frac{y\,z}{|\boldsymbol{x}|^3}\,, \tag{7}$$

$$v_z(\boldsymbol{x}) = -\frac{F}{8\pi\mu}\left(\frac{1}{|\boldsymbol{x}|} + \frac{z^2}{|\boldsymbol{x}|^3}\right). \tag{8}$$

Here, the velocity field of a feeding flagellate can be solved, considering that the flow field decays as one over the distance. Building upon the model of a flow induced by a point force, the observed

clearance rate of a flagellate (i.e., the rate of processed volume of water in search for prey) can be matched with the current described by the model, and the magnitude of the force produced by the flagellum can be estimated.

The flow-generating force of a flagellate is produced along the active flagellum that can beat in elaborate ways while hydrodynamically interacting with the cell body or other cellular structures, and possible alien surfaces. Without full knowledge of the morphology and beat pattern of the flagellum, and its interactions with other bodies, you cannot determine the force production, computationally or analytically. Instead, the force production can be inferred from an observed feeding flow, relying on information from a theoretical model to connect the observed flow with the estimated force of the flagellum. Following this method, the force produced by the ciliate *Vorticella* was estimated by excluding the complex near-field and performing a least-squares regression fitting in the far field (Pepper et al., 2021). The fitted background flow field was subtracted from the fitted experimental flow of *Vorticella* to acquire the flux generated by the ciliate alone, and subsequently, a point force model was fitted to the data. Likewise, another study computed the force of an attached choanoflagellate (*Salpingoeca rosetta*) by considering the feeding flow as a constant point force and then matching the modeled values with parameters from the observed far-field (Roper et al., 2013). On the other hand, Christensen-Dalsgaard and Fenchel (2003) measured the speed of *Paraphysomonas vestita* (crysophyte) swimming while towing a latex sphere to estimate the flagellum force from the Stokes drag equation.

The methods by Roper et al. (2013) and Pepper et al. (2021) required flow measurements to compute the flagellar force estimates. Flow fields can be described experimentally using tracer micro-particles with neutral buoyancy that are seeded into the fluid. The micro-particles follow the streamlines of a flow produced by an organism, and the drawn paths are then recorded with video microscopy. Particle tracking velocimetry (PTV) is done by time-solving the translation of individual particles captured from one frame to the next. Thus, tracer particle velocities can be measured, which can then lead to flow rate estimates. Particle tracking can be done manually (Boenigk & Arndt, 2000) or automatically (Rode et al., 2022). Alternatively, particle image velocimetry (PIV) (Raffel et al., 2007) uses specialized software to capture the translations of particles within an interrogation window, i.e., a small finite area of the field of view, between consecutive frames. Then, interrogation windows are cross-correlated to compute velocity vectors at certain points in the flow.

Many biophysical studies have investigated the flow generation and force production of flagella and cilia (Lauga, 2020). However, the majority have focused on the function of motility while repeatedly using ‘model organisms’ such as sea-urchin sperm cells, biflagellate algae *Chlamydomonas*, and bacteria *Escherichia coli*. These organisms often present different flagellar architectures and kinematics from the ones found in phagotrophic nanoflagellates. Hence, the knowledge of the fluid dynamics involved in the feeding by flagellates is yet in its infancy.

References

Asadzadeh, S. S., Walther, J. H., Andersen, A., & Kiørboe, T. (2022). Hydrodynamic interactions are key in thrust-generation of hairy flagella. *Physical Review Fluids*, *7*(7), 073101. https://doi.org/10.1103/PhysRevFluids.7.073101

Berg, H. C., & Anderson, R. A. (1973). Bacteria Swim by Rotating their Flagellar Filaments. *Nature*, *245*(5425), Article 5425. https://doi.org/10.1038/245380a0

Boenigk, J., & Arndt, H. (2000). Particle Handling during Interception Feeding by Four Species of Heterotrophic Nanoflagellates. *Journal of Eukaryotic Microbiology*, *47*(4), 350–358. https://doi.org/10.1111/j.1550-7408.2000.tb00060.x

Brennen, C. (1975). Locomotion of Flagellates with Mastigonemes. *Journal of Mechanochemistry and Cell Motility*, *3*(3), Article 3.

Celli, J. P., Turner, B. S., Afdhal, N. H., Keates, S., Ghiran, I., Kelly, C. P., Ewoldt, R. H., McKinley, G. H., So, P., Erramilli, S., & Bansil, R. (2009). Helicobacter pylori moves through mucus by reducing mucin viscoelasticity. *Proceedings of the National Academy of Sciences*, *106*(34), 14321–14326. https://doi.org/10.1073/pnas.0903438106

Christensen-Dalsgaard, K. K., & Fenchel, T. o. m. (2004). Complex Flagellar Motions and Swimming Patterns of the Flagellates Paraphysomonas vestita and Pteridomonas danica. *Protist*, *155*(1), 79–87. https://doi.org/10.1078/1434461000166

Christensen-Dalsgaard, K. K., & Fenchel, T. (2003). Increased filtration efficiency of attached compared to free-swimming flagellates. *Aquatic Microbial Ecology*, *33*(1), 77–86. https://doi.org/10.3354/ame033077

Dusenbery, D. B. (2009). *Living at Micro Scale: The Unexpected Physics of Being Small*. Harvard University Press. https://doi.org/10.2307/j.ctv1pncp4p

Fenchel, T. (1982). Ecology of Heterotrophic Microflagellates. I. Some Important Forms and Their Functional Morphology. *Marine Ecology Progress Series*, *8*(3), 211–223.

Fenchel, T. (1986). The Ecology of Heterotrophic Microflagellates. In K. C. Marshall (Ed.), *Advances in Microbial Ecology* (pp. 57–97). Springer US. https://doi.org/10.1007/978-1-4757-0611-6_2

Gilpin, W., Bull, M. S., & Prakash, M. (2020). The multiscale physics of cilia and flagella. *Nature Reviews Physics*, *2*(2), Article 2. https://doi.org/10.1038/s42254-019-0129-0

Gray, J., & Hancock, G. J. (1955). The Propulsion of Sea-Urchin Spermatozoa. *Journal of Experimental Biology*, *32*(4), 802–814. https://doi.org/10.1242/jeb.32.4.802

Holwill, M. E. J., & Sleigh, M. A. (1967). Propulsion by Hispid Flagella. *Journal of Experimental Biology*, *47*(2), 267–276. https://doi.org/10.1242/jeb.47.2.267

Jahn, T. L., Lanoman, M. D., & Fonseca, J. R. (1964). The Mechanism of Locomotion of Flagellates. II. Function of the Mastigonemes of Ochromonas*. *The Journal of Protozoology*, *11*(3), 291–296. https://doi.org/10.1111/j.1550-7408.1964.tb01756.x

Jin, F., Conrad, J. C., Gibiansky, M. L., & Wong, G. C. L. (2011). Bacteria use type-IV pili to slingshot on surfaces. *Proceedings of the National Academy of Sciences*, *108*(31), 12617–12622. https://doi.org/10.1073/pnas.1105073108

Kiørboe, T. (2023). Predation in a Microbial World: Mechanisms and Trade-Offs of Flagellate Foraging. *Annual Review of Marine Science*, *16*(1), null. https://doi.org/10.1146/annurev-marine-020123-102001

Lauga, E. (2020). *The Fluid Dynamics of Cell Motility*. Cambridge University Press. https://doi.org/10.1017/9781316796047

Lauga, E., & Powers, T. R. (2009). The hydrodynamics of swimming microorganisms. *Reports on Progress in Physics*, *72*, 096601. https://doi.org/10.1088/0034-4885/72/9/096601

Mah, J. L., Christensen-Dalsgaard, K. K., & Leys, S. P. (2014). Choanoflagellate and choanocyte collar-flagellar systems and the assumption of homology. *Evolution & Development*, *16*(1), 25–37. https://doi.org/10.1111/ede.12060

Moestrup, Ø., & Thomsen, H. A. (1976). Fine structural studies on the flagellate genus Bicoeca I. - Bicoeca maris with particular emphasis on the flagellar apparatus. Protistologica, 12(1), 101-120.

Moran, J., McKean, P. G., & Ginger, M. L. (2014). Eukaryotic Flagella: Variations in Form, Function, and Composition during Evolution. *BioScience*, *64*(12), 1103–1114. https://doi.org/10.1093/biosci/biu175

Murray, J. M. (1994). Eukaryotic flagella. *Current Opinion in Structural Biology*, *4*(2), 180–186. https://doi.org/10.1016/S0959-440X(94)90306-9

Nielsen, L. T., & Kiørboe, T. (2021). Foraging trade-offs, flagellar arrangements, and flow architecture of planktonic protists. *Proceedings of the National Academy of Sciences*, *118*(3), e2009930118. https://doi.org/10.1073/pnas.2009930118

Pepper, R. E., Riley, E. E., Baron, M., Hurot, T., Nielsen, L. T., Koehl, M. a. R., Kiørboe, T., & Andersen, A. (2021). The effect of external flow on the feeding currents of sessile microorganisms. *Journal of The Royal Society Interface*, *18*(175), 20200953. https://doi.org/10.1098/rsif.2020.0953

Purcell, E. M. (1977). Life at low Reynolds number. *American Journal of Physics*, *45*(1), 3–11. https://doi.org/10.1119/1.10903

Raffel, M., Willert, C. E., Wereley, S., & Kompenhans, J. (2007). *Particle Image Velocimetry: A Practical Guide*. Springer Science & Business Media.

Rode, M. (2021). Physics of microbial feeding: Studies of feeding flows near surfaces, ciliate filtration, and non-intrusive tethering of microswimmers. [Doctoral thesis, DTU Aqua].

Rode, M., Kiørboe, T., & Andersen, A. (2022). Feeding flow and membranelle filtration in ciliates. *Physical Review Fluids*, *7*(2), 023102. https://doi.org/10.1103/PhysRevFluids.7.023102

Roper, M., Dayel, M. J., Pepper, R. E., & Koehl, M. A. R. (2013). Cooperatively Generated Stresslet Flows Supply Fresh Fluid to Multicellular Choanoflagellate Colonies. *Physical Review Letters*, *110*(22), 228104. https://doi.org/10.1103/PhysRevLett.110.228104

Sleigh, M. A. (1964). Flagellar movement of the Sessile Flagellates Actinomonas, Codonosiga, Monas, and Poteriodendron. *Journal of Cell Science*, *s3-105*(72), 405–414. https://doi.org/10.1242/jcs.s3-105.72.405

Sleigh, M. A. (1981). Flagellar beat patterns and their possible evolution. *Biosystems*, *14*(3), 423–431. https://doi.org/10.1016/0303-2647(81)90047-2

Tong, S. M. (1995). Developayella elegans nov. Gen., nov. Spec., a new type of heterotrophic flagellate from marine plankton. *European Journal of Protistology*, *31*(1), 24–31. https://doi.org/10.1016/S0932-4739(11)80352-4

CHAPTER 4

Predation

4.1 Methods of predation studies

The ecological significance of phagotrophic flagellates as prokaryote and pico-phytoplankton predators has motivated many studies to target the understanding of the feeding functional responses. In fact, the attribution of the essential role in the microbial loop originated from scientists observing the decrease of bacterial abundancies followed by an increased presence of small flagellates during ecological surveys of natural environments (e.g., Fenchel, 1982). In addition, microbial predation studies can be carried out with so-called 'incubation experiments'. That is, controlled assemblages of predator and prey populations, from natural samples or laboratory cultures, are maintained under certain conditions for a period of time, and population shifts are recorded for subsequent calculations of prey removal or uptake. The effects on the feeding of variable factors such as temperature (e.g., Vázquez-Domínguez et al., 2012), prey species (e.g., Šimek et al., 2018), light (e.g., Izaguirre et al., 2012), and food quality (e.g., Anderson et al., 2011), among others have been tested. There are many ways to calculate grazing rates, non-molecular (mentioned in Vaqué et al., 1994) and molecular-based (e.g., Massana et al., 2009). Most typically grazing is measured with microscope counts of fluorescently labeled tracer particles inside the predator's gut (i.e., to calculate prey uptake) or that remain in the medium (i.e., to calculate prey removal). Incubation experiments have determined the feeding ecology of phagotrophic nanoflagellates, however, the underlying mechanisms are left 'in the dark' and conflicting results may occur. For example, the prasinophyte *Micromonas* was considered a phagotrophic algae when confocal and epifluorescence microscope imaging revealed engulfed food particles (McKie-Krisberg & Sanders, 2014); but Jimenez et al., (2021) later argued that the supposed observed ingestions were the product of an experimental artifact of viewing particles stuck on cell surfaces, as flow cytometry ingestion measurements showed no evidence of phagotrophy.

High-speed video microscopy has facilitated direct observations of what is eaten and what is not. Studies are down to the individual level and the different feeding processes of phagotrophic nanoflagellates are disclosed. With high-speed imaging, scientists can measure the time budget of feeding phases (see section 4.2), visualize the flow to compute the rate of processed volume of water (i.e. clearance rates), describe the flagellar kinematics, and directly report the ratios of prey

capture to ingestions and rejections (Fenchel, 1986; Boenigk & Arndt, 2000a, 2000b; Christensen-Dalsgaard & Fenchel, 2004, 2003).

4.2 Predation strategies and prey selection

The following overview of predation strategies and prey selectivity has been mostly extracted from the work by Boenigk & Arndt, (2002). The feeding process can be divided into two main stages: prey-searching and prey-handling. The majority of pelagic phagotrophic nanoflagellates are suspension feeders, directly intercepting prey by generating a feeding current with a beating flagellum, and feeding in close association with an organic substrate (e.g., marine snow): loosely or temporarily attached (like chrysomonads and bicosoecids), and more permanently attached (like some choanoflagellates and loricated bicosoecids). Attachment is suggested to be advantageous due to higher concentrations of prey close to surfaces (Andersen & Kiørboe, 2020), in contrast to the nutritionally diluted open waters. Therefore, it is plausible that surface-associated flagellates are more invested in handling times, given that their prey encounter probability is higher, whilst the time budget of free-swimming predators is majorly dedicated to prey-searching. In benthic systems, suspension feeders are the minority, and most will move along the substrate and 'grasp' on bacteria attached to the surface. Specialized feeding structures arise with different strategies, e.g., filtering apparatus of suspension feeding choanoflagellates or grasping proboscis-like extensions of benthic gliders like *Rhynchomonas nasuta*. Thus, flagellates have adapted the time budget of each feeding stage, cell morphology, and predation behavior to the prey availability of their habitat, among other conditions.

Prey handling stages comprise a contact phase, processing phase, ingestion phase, and refractory phase (Boenigk & Arndt, 2000b) (Fig. 4.1). From the moment predator-prey contact is established, the flagellate will respond to retain the food within milliseconds (contact phase) and proceed to manipulate it in preparation for ingestion, which may include transportation of the particle toward the 'mouth' and its reorientation for efficient phagocytosis (processing phase). Then, food is engulfed and contained inside a vacuole (ingestion phase). Finally, the flagellate may experience a transitional behavioral period before resuming the search for new prey (refractory time). Feeding strategies with prevalent prey-handling stages usually involve prey selection. Prey selection can occur through passive or active forces. Passive selections are a product of prey contact rates or morphological constraints of the feeding apparatus. Active selections call for the predator's decision-making of engulfment, given certain physical or chemical cues from the prey. According to the conceptual framework proposed by Montagnes et al., (2008), selectivity can take place in all the different feeding phases, before and after ingestion. Phagotrophic nanoflagellates can discriminate against low nutritional particles (Landry, 1977; Jürgens & DeMott, 1995; Boenigk & Novarino, 2004; Shannon et al., 2007), certain prey species (Boenigk et al., 2001), and prey surface properties (Matz et al., 2002). As mentioned, limitations

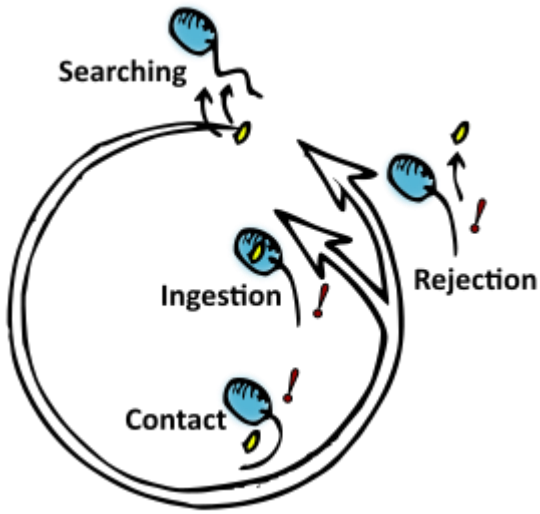

Figure 4.1. Generic feeding series of phagotrophic nanoflagellates. The beating flagellum generates a feeding current to draw prey toward the predator (searching phase). When food is intercepted (contact phase), the flagellate will retain the prey (capture phase) and manipulate it for ingestion or rejection. The time spent interacting with the prey is the handling time (exclamation marks). Finally, the feeding current will resume, if it was ever paused for prey handling.

of the predator's feeding morphology will dictate a passive selection against sub-optimal food particle sizes (Pfandl et al., 2004; Šimek & Chrzanowski, 1992). Moreover, food preferences vary with different food concentrations (Boenigk et al., 2002). In turn, predation pressure by nanoflagellates shapes bacterial communities (Jürgens & Matz, 2002). In response to grazing, bacteria shift in cell size and shape (Grujčić et al., 2015; Hahn et al., 1999), escape by swimming (Matz et al., 2002), exhibit certain surface properties (Matz & Jürgens, 2001), promote colony formation (Boraas et al., 1998; Erken et al., 2012), and more. Predator nanoflagellates are in an arms race with bacterial prey populations, resulting in the diversity of feeding forms and defense mechanisms that contribute to the complexity and dynamicity of microbial trophic interactions.

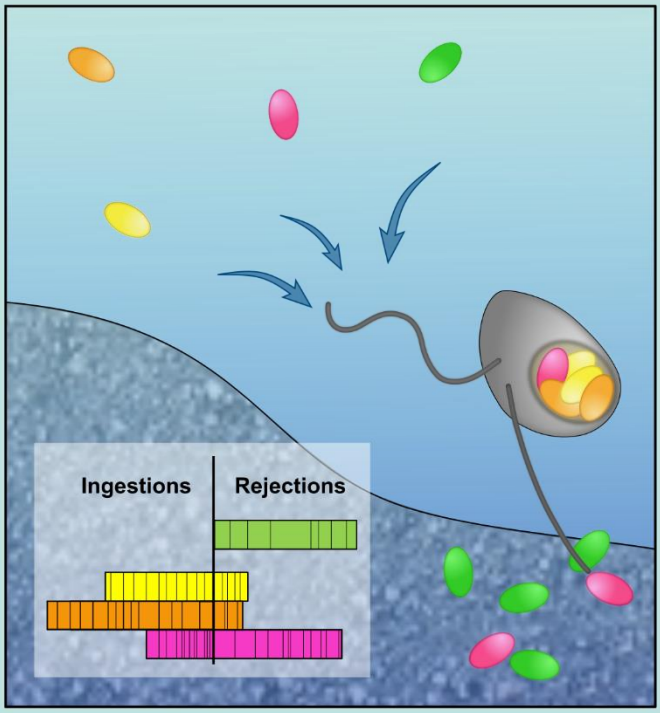

Evidence of prey selection by *Cafeteria roenbergensis* with *Synechococcus* strains (unpublished).

Prey selectivity was evaluated during a pilot experiment, using four strains of *Synechococcus* (EUM Syn10, WH8109, BL_107, and PCC7336). The predator, *C. roenbergensis*, was seeded with one of the cyanobacteria strains at a time inside an observation chamber, and the number of ingestions and rejections was directly observed under the microscope. Between 8 – 14 individual flagellates were observed per treatment, capturing a minimum of 3 cyanobacteria. All the prey cells were round and smaller than the predator (around 2 µm in diameter), except PCC7336 occasionally formed longer cells that were excluded from the data. *Cafeteria roenbergensis* showed a clear preference to ingest strains WH8109 (orange) and BL_107 (yellow) with total ingestion-to-rejection ratios of 66:11 and 43:13, respectively. The majority of the *Synechococcus* strain EUM Syn10 (pink) cells were rejected (27:50 ingestion:rejection) and strain PCC7336 was never ingested. Despite *C. roenbergensis* being often observed handling PCC7336 for a long time and making great attempts for ingestion, the 'almost engulfed' cyanobacteria would eventually be rejected. Given the similar morphology and dimensions of all four strains, it is plausible that the predator is motivated to select against *Synechococcus* EUM Syn10 and PCC7336 due to predation-inhibiting chemical cues or surface properties of the prey. In culture, PCC7336 forms a green biofilm at the bottom of the flask, and EUM Syn10 increases the viscosity of the medium at high cell concentrations. However, it is unknown if these culturing properties are related to the high number of rejections. A similar prey selection pattern was observed with the nanoflagellate species *Pseudobodo* sp. (data not presented).

References

Andersen, A., & Kiørboe, T. (2020). The effect of tethering on the clearance rate of suspension-feeding plankton. *Proceedings of the National Academy of Sciences*, *117*(48), 30101–30103. https://doi.org/10.1073/pnas.2017441117

Anderson, R., Kjelleberg, S., McDougald, D., & Jürgens, K. (2011). Species-specific patterns in the vulnerability of -carbon-starved bacteria to protist grazing. *Aquatic Microbial Ecology*, *64*(2), 105–116. https://doi.org/10.3354/ame01518

Boenigk, J., & Arndt, H. (2000a). Comparative studies on the feeding behavior of two heterotrophic nanoflagellates: The filter-feeding choanoflagellate Monosiga ovata and the raptorial-feeding kinetoplastid Rhynchomonas nasuta. *Aquatic Microbial Ecology*, *22*(3), 243–249. https://doi.org/10.3354/ame022243

Boenigk, J., & Arndt, H. (2000b). Particle Handling during Interception Feeding by Four Species of Heterotrophic Nanoflagellates. *Journal of Eukaryotic Microbiology*, *47*(4), 350–358. https://doi.org/10.1111/j.1550-7408.2000.tb00060.x

Boenigk, J., & Arndt, H. (2002). Bacterivory by heterotrophic flagellates: Community structure and feeding strategies. *Antonie van Leeuwenhoek*, *81*(1), 465–480. https://doi.org/10.1023/A:1020509305868

Boenigk, J., Matz, C., Jürgens, K., & Arndt, H. (2001). The Influence of Preculture Conditions and Food Quality on the Ingestion and Digestion Process of Three Species of Heterotrophic Nanoflagellates. *Microbial Ecology*, *42*(2), 168–176.

Boenigk, J., Matz, C., Jürgens, K., & Arndt, H. (2002). Food concentration-dependent regulation of food selectivity of interception-feeding bacterivorous nanoflagellates. *Aquatic Microbial Ecology*, *27*(2), 195–202. https://doi.org/10.3354/ame027195

Boenigk, J., & Novarino, G. (2004). Effect of suspended clay on the feeding and growth of bacterivorous flagellates and ciliates. *Aquatic Microbial Ecology*, *34*(2), 181–192. https://doi.org/10.3354/ame034181

Boraas, M. E., Seale, D. B., & Boxhorn, J. E. (1998). Phagotrophy by a flagellate selects for colonial prey: A possible origin of multicellularity. *Evolutionary Ecology*, *12*(2), 153–164. https://doi.org/10.1023/A:1006527528063

Christensen-Dalsgaard, K. K., & Fenchel, T. o. m. (2004). Complex Flagellar Motions and Swimming Patterns of the Flagellates Paraphysomonas vestita and Pteridomonas danica. *Protist*, *155*(1), 79–87. https://doi.org/10.1078/1434461000166

Christensen-Dalsgaard, K. K., & Fenchel, T. (2003). Increased filtration efficiency of attached compared to free-swimming flagellates. *Aquatic Microbial Ecology*, *33*(1), 77–86. https://doi.org/10.3354/ame033077

Erken, M., Farrenschon, N., Speckmann, S., Arndt, H., & Weitere, M. (2012). Quantification of Individual Flagellate—Bacteria Interactions within Semi-natural Biofilms. *Protist*, *163*(4), 632–642. https://doi.org/10.1016/j.protis.2011.10.008

Fenchel, T. (1982). Ecology of Heterotrophic Microflagellates. IV. Quantitative Occurrence and Importance as Bacterial Consumers. *Marine Ecology Progress Series*, *9*(1), 35–42.

Fenchel, T. (1986). The Ecology of Heterotrophic Microflagellates. In K. C. Marshall (Ed.), *Advances in Microbial Ecology* (pp. 57–97). Springer US. https://doi.org/10.1007/978-1-4757-0611-6_2

Grujčić, V., Kasalický, V., & Šimek, K. (2015). Prey-Specific Growth Responses of Freshwater Flagellate Communities Induced by Morphologically Distinct Bacteria from the Genus Limnohabitans. *Applied and Environmental Microbiology*, *81*(15), 4993–5002. https://doi.org/10.1128/AEM.00396-15

Hahn, M. W., Moore, E. R. B., & Höfle, M. G. (1999). Bacterial Filament Formation, a Defense Mechanism against Flagellate Grazing, Is Growth Rate Controlled in Bacteria of Different Phyla. *Applied and Environmental Microbiology*, *65*(1), 25–35. https://doi.org/10.1128/AEM.65.1.25-35.1999

Izaguirre, I., Sinistro, R., Schiaffino, M. R., Sánchez, M. L., Unrein, F., & Massana, R. (2012). Grazing rates of protists in wetlands under contrasting light conditions due to floating plants. *Aquatic Microbial Ecology*, *65*(3), 221–232. https://doi.org/10.3354/ame01547

Jimenez, V., Burns, J. A., Le Gall, F., Not, F., & Vaulot, D. (2021). No evidence of Phago-mixotropy in Micromonas polaris (Mamiellophyceae), the Dominant Picophytoplankton Species in the Arctic. *Journal of Phycology*, *57*(2), 435–446. https://doi.org/10.1111/jpy.13125

Jürgens, K., & DeMott, W. R. (1995). Behavioral flexibility in prey selection by bacterivorous nanoflagellates. *Limnology and Oceanography*, *40*(8), 1503–1507. https://doi.org/10.4319/lo.1995.40.8.1503

Jürgens, K., & Matz, C. (2002). Predation as a shaping force for the phenotypic and genotypic composition of planktonic bacteria. *Antonie van Leeuwenhoek*, *81*(1), 413–434. https://doi.org/10.1023/A:1020505204959

Landry, M. R. (1977). A review of important concepts in the trophic organization of pelagic ecosystems. *Helgoländer Wissenschaftliche Meeresuntersuchungen*, *30*(1), 8–17. https://doi.org/10.1007/BF02207821

Massana, R., Unrein, F., Rodríguez-Martínez, R., Forn, I., Lefort, T., Pinhassi, J., & Not, F. (2009). Grazing rates and functional diversity of uncultured heterotrophic flagellates. *The ISME Journal*, *3*(5), Article 5. https://doi.org/10.1038/ismej.2008.130

Matz, C., Boenigk, J., Arndt, H., & Jürgens, K. (2002). Role of bacterial phenotypic traits in selective feeding of the heterotrophic nanoflagellate Spumella sp. *Aquatic Microbial Ecology*, *27*(2), 137–148. https://doi.org/10.3354/ame027137

Matz, C., & Jürgens, K. (2001). Effects of Hydrophobic and Electrostatic Cell Surface Properties of Bacteria on Feeding Rates of Heterotrophic Nanoflagellates. *Applied and Environmental Microbiology*, *67*(2), 814–820. https://doi.org/10.1128/AEM.67.2.814-820.2001

McKie-Krisberg, Z. M., & Sanders, R. W. (2014). Phagotrophy by the picoeukaryotic green alga Micromonas: Implications for Arctic Oceans. *The ISME Journal*, *8*(10), 1953–1961. https://doi.org/10.1038/ismej.2014.16

Montagnes, D. J. S., Barbosa, A. B., Boenigk, J., Davidson, K., Jürgens, K., Macek, M., Parry, J. D., Roberts, E. C., & Simek, K. (2008). Selective feeding behaviour of key free-living protists: Avenues for continued study. *Aquatic Microbial Ecology*, *53*(1), 83–98. https://doi.org/10.3354/ame01229

Pfandl, K., Posch, T., & Boenigk, J. (2004). Unexpected Effects of Prey Dimensions and Morphologies on the Size Selective Feeding by Two Bacterivorous Flagellates (Ochromonas sp. And Spumella sp.). *Journal of Eukaryotic Microbiology*, *51*(6), 626–633. https://doi.org/10.1111/j.1550-7408.2004.tb00596.x

Shannon, S. P., Chrzanowski, T. H., & Grover, J. P. (2007). Prey Food Quality Affects Flagellate Ingestion Rates. *Microbial Ecology*, *53*(1), 66–73. https://doi.org/10.1007/s00248-006-9140-y

Šimek, K., & Chrzanowski, T. H. (1992). Direct and Indirect Evidence of Size-Selective Grazing on Pelagic Bacteria by Freshwater Nanoflagellates. *Applied and Environmental Microbiology*, *58*(11), 3715–3720. https://doi.org/10.1128/aem.58.11.3715-3720.1992

Šimek, K., Grujčić, V., Hahn, M. W., Horňák, K., Jezberová, J., Kasalický, V., Nedoma, J., Salcher, M. M., & Shabarova, T. (2018). Bacterial prey food characteristics modulate community growth response of freshwater bacterivorous flagellates. *Limnology and Oceanography*, *63*(1), 484–502. https://doi.org/10.1002/lno.10759

Vaqué, D., Gasol, J. M., & Marrasé, C. (1994). Grazing rates on bacteria: The significance of methodology and ecological factors. *Marine Ecology Progress Series*, *109*(2/3), 263–274.

Vázquez-Domínguez, E., Vaqué, D., & Gasol, J. M. (2012). Temperature effects on the heterotrophic bacteria, heterotrophic nanoflagellates, and microbial top predators of the NW Mediterranean. *Aquatic Microbial Ecology*, *67*(2), 107–121. https://doi.org/10.3354/ame01583

CHAPTER 5

Objectives and Findings

Phagotrophic nanoflagellates encounter two major challenges when feeding. Firstly, the microscale environment is governed by viscous forces that hinder predator-prey interactions. Secondly, the ocean is often nutritionally diluted, requiring these flagellates to clear a volume a million times their cell size daily in search of prey. Despite their ecological relevance, the feeding mechanisms of phagotrophic nanoflagellates are poorly explored. In this thesis, I performed high-speed video microscopy to fundamentally pinpoint the diverse predation strategies that these micron-size predators carry out to overcome the environmental adversities. With the overarching aim of providing a mechanistic understanding of the functional responses observed in phagotrophic nanoflagellates, I conducted three studies that correspond to chapters 6, 7, and 8. The following section is a synopsis of the main findings from each study.

5.1 Paper I

Mechanisms and Fluid Dynamics of Foraging in Heterotrophic Nanoflagellates (Chapter 6)

All studied predators (*Paraphysomonas foraminifera*, *Pteridomonas danica*, *Cafeteria roenbergensis*, and *Pseudobodo* sp.) generated a feeding current with a hispid flagellum while attached to a substrate, and prey capture and handling behaviors varied among the different species. The measured prey-handling times of three species limited the maximum ingestion rates from 1000 to 20,000 prey per day. These values largely account for previously reported maximum rates of about 10^4 bacterial prey per day. I performed particle tracking to describe feeding flows and estimate maximum clearance rates. Then I used a point force model to determine the current-generating force from the beating flagellum. Both calculations resulted in clearance rates (10^6 – 10^7 specific cell volumes per day) and flagellar forces (approximately 4 – 13 pN) that aligned closely with previous estimates. Lastly, I attempted to compare the already acquired indirect estimate of the force produced by the flagellum of *Pteridomonas danica* with a direct estimate derived from resistive force theory. Both the indirect and direct measurements yielded similar magnitudes. However, when compared to the performance of a naked flagellum, the resistive force model highlighted the significant role of mastigonemes in increasing force production by an order of magnitude. Building upon previous research, our study presents a mechanistic

understanding of the prey capture and handling processes that provide an underlying basis for the functional responses of phagotrophic nanoflagellates.

5.2 Paper II

Functional Morphology and Fluid Dynamics of Foraging in 'Typical Excavates'; a Key Assemblage for Understanding Deep Eukaryote Evolution (Chapter 7)

I explored the suspension-feeding and swimming behavior of five excavate species (*Jakoba libera, Reclinomonas americana, Kipferlia bialata, Carpediemonas membranifera,* and *Malawimonas californiensis*) from the three principal phylogenetic clades – Discoba, Metamonada, and Malawimonadida. My observations confirm that the 'typical excavate' morphology, i.e., a vaned flagellum beating inside or close to the ventral groove, serves the purpose of feeding rather than swimming. The estimated clearance rates from particle tracking were on the order of 10^6 cell volumes per day, and are similar to estimates for other phagotrophic flagellates of similar sizes. Computational fluid dynamics (CFD) simulations determined that the interactions between the groove and the vaned flagellum are mainly responsible for generating feeding currents and that other species-specific morphological variations are trivial. Additional computations have shown that the increment in clearance rate achieved with a vaned flagellum requires less energy consumption than by increasing the beating frequency. Lastly, the CFD model of a grooveless cell demonstrated that the presence of the ventral furrow results in smoother and more directional feeding currents and, consequently, in higher clearance rates; although, the benefit of a groove is only true with a vaned flagellum. The similarity in functional morphology of the studied excavates supports the theory that the 'typical excavate' cell architecture is homologous across the three clades. Therefore, we conclude that the hypothesis of the Last Common Ancestor (LECA) resembling a 'typical excavate' and, thus, having similar foraging mechanisms is plausible.

5.3 Paper III

New Insights in Flagellate Predation: the Significance and Function of the Feeding Groove of 'Typical Excavates' (Chapter 8)

Here, I further investigated the functional morphology of 'typical excavates'. The four examined species (*Reclinomonas americana, Kipferlia bialata, Malawimonas californiensis,* and *Gefionella okellyi*), drawn from the three main clades of the supergroup Excavata, had a deformation or undulation of the groove's floor that intermittently moved across posteriorly. We termed the moving element 'the wave'. The wave of *K. bialata* was frequent and periodically active, whilst in the other species it showed longer paused periods. We described the wave as a

form of surface motility, distinct to excavates, because it transports captured particles along the cell surface and toward the ingestion region. Moreover, we observed that the passing of the wave was essential for phagocytosis to occur. In addition, we hypothesized that a semi-rigid feeding groove will limit the prey-size range of a predator. By offering different bead sizes as 'food' to the excavates, we found that the species-specific morphology of the groove imposed an upper size limit for prey capture. Thus, capture efficiency was species-specific and prey-size dependent. The ingestion efficiencies of *R. americana* and *M. californiensis* were high for all captured food sizes. Conversely, *K. bialata* performed low ingestion efficiencies with a seemingly 'leaky' groove, and we speculate on an active prey selection. We suggest that the different feeding behaviors (wave activity and ingestion efficiencies) of the studied species are adapted to the availability of prey in their respective natural habitats. Lastly, we argue that the wave is widespread among 'typical excavates', and that it provides further evidence for the homology of the feeding mechanism across the different Exacavata clades.

CHAPTER 6

Paper I

Mechanisms and Fluid Dynamics of Foraging in Heterotrophic Nanoflagellates

Sei Suzuki-Tellier, Anders Andersen, and Thomas Kiørboe

Centre for Ocean Life, National Institute of Aquatic Resources,

Technical University of Denmark, DK-2800 Kgs. Lyngby, Denmark

This paper has been published:

Suzuki-Tellier, S., Andersen, A., and Kiørboe, T. 2022. Mechanisms and fluid dynamics of foraging in heterotrophic nanoflagellates. *Limnology and Oceanography*, *67*(6), 1287–1298. doi: 10.1002/lno.12077

Data is available in the Dryad repository as:

Suzuki-Tellier, Sei; Andersen, Anders Peter; Kiørboe, Thomas (2023), Flagellate grazing morphometrics, particle tracking, prey-handling behavior, clearance rates and forces, Dryad, Dataset, doi:10.5061/dryad.bk3j9kdbs

Abstract

Heterotrophic nanoflagellates are the main consumers of bacteria and picophytoplankton in the ocean. In their microscale world, viscosity impedes predator–prey contact, and the mechanisms that allow flagellates to daily clear a volume of water for prey corresponding to 10^6 times their own volume is unclear. It is also unclear what limits observed maximum ingestion rates of about 10^4 bacterial preys per day. We used high-speed video microscopy to describe feeding flows, flagellum kinematics, and prey searching, capture, and handling in four species with different foraging strategies. In three species, prey handling times limit ingestion rates and account well for their reported maximum values. Similarly, observed feeding flows match reported clearance rates. Simple point force models allowed us to estimate the forces required to generate the feeding flows, between 4 and 13 pN, and consistent with the force produced by the hairy (hispid) flagellum, as estimated using resistive force theory. Hispid flagella can produce a force that is much higher than the force produced by a naked (smooth) flagellum with similar kinematics, and the hairy flagellum is therefore key to foraging in most nanoflagellates. Our findings provide a mechanistic underpinning of observed functional responses of prey ingestion rates in nanoflagellates.

6.1 Introduction

Heterotrophic nanoflagellates play a key role in microbial food webs in the oceans by feeding on phytoplankton and bacteria and by transferring primary production to higher trophic levels when grazed upon. Their top-down control shapes the structure and function of microbial communities and mediate essential biogeochemical cycles in the sea (Fenchel 1982a; Azam et al. 1983; Worden et al. 2015). Despite their importance, the mechanisms of prey capture and the processes limiting their ingestion rates are not fully understood (Boenigk and Arndt 2002; Weisse et al. 2016).

Flagellates live in a low Reynolds number world where viscosity impedes predator–prey contact (Jabbarzadeh and Fu 2018). Yet, nanoflagellates are capable of daily clearing a volume of water for prey that corresponds to about 1 million times their cell volume, which is equivalent to a significant fraction of their cell volume per flagellar beat period (Hansen et al. 1997; Kiørboe and Hirst 2014). In the nutritionally dilute ocean, this is the clearance rate needed to sustain a viable population in the face of predation mortality (Kiørboe 2011). How the flagellates overcome the impeding effect of viscosity is unclear for many forms.

Most flagellates use their flagella to swim, to generate feeding currents, and to capture prey. Many studies have examined the fluid dynamics of flagellates from the perspective of swimming (Lauga 2020), but few have done so from the perspective of feeding on particulate food particles (Christensen-Dalsgaard and Fenchel 2003; Dölger et al. 2017; Nielsen et al. 2017), even though feeding is likely a more fundamental component of the fitness than propulsion per se. In a few cases, the flagellum forces have been estimated indirectly from swimming speeds (Christensen-Dalsgaard and Fenchel 2003) or from quantification of feeding flows (Roper et al. 2013; Nielsen et al. 2017). However, there is large variation in flagellar kinematics and arrangements between species that yields big differences in the strength and architecture of the feeding flows (Nielsen and Kiørboe 2021). In most cases, the forces generated by the flagellum and required to account for the necessary high clearance rates are unknown.

Direct observations of flagellate feeding were pioneered by Sleigh and Fenchel (Sleigh 1964; Fenchel 1982b), and followed by few additional studies (Ishigaki and Terazaki 1998; Boenigk and Arndt 2000a; Pfandl et al. 2004). These studies revealed a variety of prey acquisition and handling strategies. Prey is either intercepted by the cell body, a flagellum, or specialized structures, and then either rejected or transported to the spot on the cell surface where it is phagocytized. During capture and handling of prey, the feeding current may cease, and no further prey can be captured (Ishigaki and Terazaki 1998; Boenigk and Arndt 2000b). Handling time may therefore put an upper limit on prey ingestion rate. The maximum clearance rate governed by the feeding current, and the maximum ingestion rate, potentially governed by the prey handling time, together describe the functional response of the prey ingestion rate as function of prey concentration. This is the key function characterizing predator–prey interactions.

The aims of this study are twofold: (1) to understand what allows heterotrophic nanoflagellates to overcome the impeding effect of viscosity and (2) to provide a mechanistic underpinning of the functional response relations that have been obtained in incubation experiments (Hansen et al. 1997; Kiørboe and Hirst 2014). We build on and expand previous observational work on flagellate foraging, and we describe predator–prey encounters and prey handling in four species with characteristic predation modes. We portray the flagellar dynamics during the different grazing phases and quantify prey handling times to evaluate the potential for prey ingestion. We further quantify the feeding flow, estimate clearance rates from observed flow fields, and use simple fluid dynamic models to compute the forces needed to account for the observed flows as well as the forces that the flagellum produces.

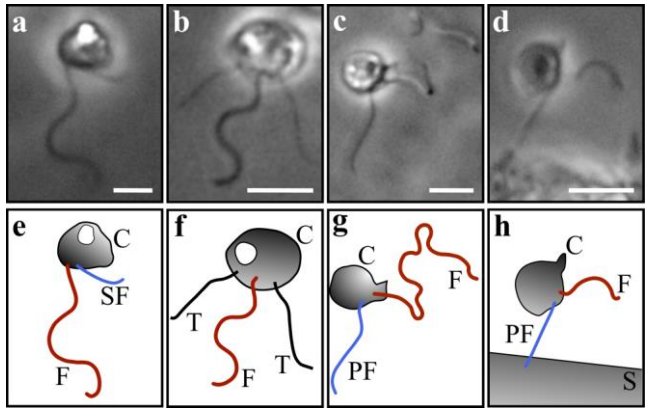

Figure 1. Phase contrast micrographs and drawings of flagellates *Paraphysomonas foraminifera* (a, e), *Pteridomonas danica* (b, f), *Cafeteria roenbergensis* (c, g), and *Pseudobodo* sp. (d, h). Abbreviations in drawings (e, f, g, h): C − cell, F − flagellum, SF − short flagellum, T − tentacles, PF − posterior flagellum, and S − surface. Scale bar = 5 µm.

6.2 Materials and methods

6.2.1 Study organisms, isolation, and culturing

The four selected marine flagellate species *Pteridomonas danica*, *Paraphysomonas foraminifera*, *Cafeteria roenbergensis*, and *Pseudobodo* sp. are direct interception feeders (Fig. 1). They have a hairy (hispid) flagellum that drives the feeding current toward the cell, and in the opposite direction of the propagating flagellum wave. *Cafeteria roenbergensis* has been a key laboratory species, as its different feeding phases are easy to distinguish (Ishigaki and Terazaki 1998; Boenigk and Arndt 2000b). Christensen-Dalsgaard and Fenchel explored the fluid dynamics of *P. danica* and *Paraphysomonas vestita*; the latter sharing the genus with *P. foraminifera* (Fenchel

1982b; Christensen-Dalsgaard and Fenchel 2003). The feeding behavior of a close relative of *P. danica*, *Actinomonas* sp. has been studied (Sleigh 1964; Fenchel 1982b; Ishigaki and Terazaki 1998), and the predation mode of *Pseudobodo* sp. has been described briefly (Fenchel 1982b). Additionally, we made a few observations of *Ochromonas moestrupii* and *Chrysophyacea* sp.

All species were isolated from shallow (30 m) coastal waters (Øresund and Isefjord, Denmark). Cultures were maintained in the dark at 18°C in filtered and pasteurized North Sea water (salinity 30‰), using rice grains to feed the naturally occurring bacteria that served as prey. Species identification was verified using 18s rDNA molecular analysis except for *Pseudobodo* sp., which was morphologically matched with the description of *Pseudobodo tremulans* (Fenchel 1982b).

6.2.2 Microscopy and image analysis

A glass ring (16 mm inner diameter and 3 mm height) was fixed on a glass slide using stopcock grease, filled with 600 µL of the culture, and covered with a glass coverslip. The sample was observed 5 min later to allow the flagellates to attach to the coverslip. The heating effects of light were reduced by having short periods of exposure (< 5 min) at moderate intensities during recordings. Room temperature was 16–20°C, and experiments did not last more than 1.5 h. Food particles consisted of naturally occurring bacteria and particulate organic matter. For cultures with low bacterial abundance, polystyrene microbeads (0.5 µm in diameter and treated with Bovine Serum Albumine to avoid aggregation) were added (10^{-5}%) to increase the rate of particle encounters.

Observations were carried out with an inverted microscope Olympus IX71, using an Olympus UPlanSApo oil immersion objective ×100/1.40 or an Olympus UPLanFL N oil immersion ×100/1.30 objective for phase contrast imaging. Recordings were carried out with a high-speed camera (Phantom Miro LAB 320). Prey captures were recorded at 500 frames per second (fps), and particle tracking was performed at 250 fps. Videos had a minimum resolution of 512 × 512 pixels. The image analysis software ImageJ (Fiji) was used for detailed predator–prey interaction observations, morphometric measurements, and manual particle tracking (Schindelin et al. 2012; Rueden et al. 2017).

6.2.3 Predation behavior and time budget analysis

Predation was divided into five stages, largely following Montagnes et al. (2008): searching, contact, capture, and ingestion or rejection. A rejection was defined as an active release of the prey, in contrast to a loss of prey. The handling time was defined as the duration of the period where the flagellum does not produce a feeding current and another prey cannot be encountered. Handling time does not necessarily commence upon prey contact, and it can end before or after the particle is fully ingested. Prey processing had three possible outcomes: ingestion, rejection,

or loss. In total, 40 prey handling durations (20 ingestions and 20 rejections) were recorded for each species. In addition, 20 “lash rejections” by *Pseudobodo* sp. were analyzed (Supplementary Table S2).

6.2.4 Particle tracking and clearance rates

Flow fields were mapped by particle tracking. A particle was followed from a minimum distance of one cell length from the body, until it was either captured or it had gone well past the flagellate. We recorded 11–15 tracks per individual, studying two individuals per species. Most flagellates slightly shift their orientation while foraging (Supplementary Table S3), and the particle tracks are therefore shown relative to the observed flagellum coordinates. An imaginary, circular filtering area (clearance disc) for prey capture was assumed in front of the cell and perpendicular to the feeding flow. The size of the disc was defined by the tracks of particles that were captured or strongly interacted with the flagellate. A least-squares five-point, centered finite difference scheme was applied to calculate the particle velocities from the measured particle positions. The average velocity component perpendicular to the clearance disc was used to calculate the clearance rate.

6.2.5 Model of the feeding flow

To describe the flow fields and estimate the flow-generating forces from the observed feeding currents we used a point force model (Blake 1971; Fenchel 1986; Rode et al. 2020). The low-Reynolds-number model describes the flow due to a point force above a plane no-slip surface. We examined two situations in which the force direction is either perpendicular (*P. danica*, *P. foraminifera*) or parallel to the surface (*Pseudobodo* sp., *C. roenbergensis*). In both cases, we use F to denote the magnitude of the force and h its height above the surface. In the perpendicular case, the flow has rotational symmetry, and the streamlines are the contour lines of the Stokes stream function:

$$\Psi(s,z) = \frac{F\,s^2}{8\,\pi\,\mu}\left(\frac{1}{\sqrt{s^2+(z-h)^2}} - \frac{1}{\sqrt{s^2+(z+h)^2}} - \frac{2\,h\,z}{(s^2+(z+h)^2)^{3/2}}\right), \qquad (1)$$

where μ denotes the dynamic viscosity, s the radial distance from the axis of symmetry, and z the height above the surface (Aderogba and Blake 1978; Blake and Otto 1996). Using the stream function, we can derive the clearance rate, Q, through a circular clearance disc centered on the axis of symmetry and oriented perpendicular to it:

$$Q = \frac{F\,a^2}{4\,\mu}\left(\frac{1}{\sqrt{a^2+(d-h)^2}} - \frac{1}{\sqrt{a^2+(d+h)^2}} - \frac{2\,h\,d}{(a^2+(d+h)^2)^{3/2}}\right), \quad (2)$$

where a denotes the radius of the clearance disc and d its height above the surface (Rode et al. 2020). The equation allows us to estimate the magnitude of the point force, F, using our clearance rate estimate obtained with particle tracking. In the parallel case, the flow does not have rotational symmetry and a Stokes stream function does not exist. We therefore integrate the velocity field numerically to obtain streamlines (Blake and Chwang 1974; Rode et al. 2020). To estimate the clearance rate through a circular clearance disc that is perpendicular to the direction of the point force and positioned the distance h above the surface in the symmetry plane of the flow, we assume that $a \ll h$ and approximate the effect of the image system that ensures that the no-slip boundary condition is satisfied (Rode et al. 2020). We find the approximation:

$$Q \approx \frac{F\,a^2}{4\,\mu}\left(\frac{1}{\sqrt{a^2+l^2}} - \frac{l^2}{(4\,h^2+l^2)^{3/2}} - \frac{12\,h^4}{(4\,h^2+l^2)^{5/2}}\right), \quad (3)$$

where l denotes the distance between the position of the point force and the center of the clearance disc.

6.2.6 The force created by a hairy flagellum

To estimate the flow-generating force of *P. danica* directly from the observed motion of the flagellum, we used resistive force theory (Brennen 1976; Lauga and Powers 2009; Rodenborn et al. 2013). We assume that the flagellate is tethered, and that the motion of the flagellum is a traveling sine wave with wavelength λ and frequency f that is propagating in the positive z-direction:

$$x_f(z,t) = A\,\sin(k\,z - \omega\,t)\,, \quad (4)$$

where x_f denotes the transversal deflection of the flagellum, A the amplitude, $k=2\,\pi/\lambda$ the wave number, and $\omega=2\pi f$ the angular frequency. Using resistive force theory, we obtain the component of the force in the z-direction:

$$F_z = -\mu \left(\xi_\perp - \xi_{||}\right) \left(1 - \frac{1}{\sqrt{1 + k^2 A^2}}\right) \frac{L\,\omega}{k}\,, \tag{5}$$

where L denotes the length of the flagellum, and $\xi_\perp$ and $\xi_{||}$ the perpendicular and the parallel force coefficient, respectively (Gray and Hancock 1955; Brennen 1976). For a naked flagellum we use the dimensionless force coefficients:

$$\xi_\perp^f = \frac{4\,\pi}{\ln(2\,\lambda/b) + 1/2}\,, \qquad \xi_{||}^f = \frac{2\,\pi}{\ln(2\,\lambda/b) - 1/2}\,, \tag{6}$$

where b denotes the radius of the flagellum (Gray and Hancock 1955; Rodenborn et al. 2013). For a flagellum with two rows of stiff hairs that are in the beat plane and remain perpendicular to the flagellum during the beat, we use the dimensionless force coefficients:

$$\xi_\perp^h = \frac{4\,\pi}{\ln(2\,\lambda/b) + 1/2} + \frac{2\,\pi\,\alpha/\chi}{\ln(\alpha/\beta) - 1/2}\,, \tag{7}$$

where α denotes the total length of a pair of hairs, β their radius, and χ the distance between neighboring pairs of hairs (Holwill and Sleigh 1967; Brennen 1976).

6.3 Results

6.3.1 Prey capture and handling

Supplementary Movies 1– 4 illustrate the different behaviors described below; and morphometric data and flagellum properties can be found in Supplementary Table S1.

Paraphysomonas foraminifera attaches to the surface by a filamentous structure from the posterior end of the cell. Cells are located directly on the surface or at a distance. On the anterior side there are two flagella, with their base near the ingestion site. When searching for prey, the long flagellum continuously beats in a curved fashion (46 ± 6 [mean $\pm$ SD] Hz) and creates a feeding current toward the cell, while the second shorter flagellum is inactive. When a food particle enters the feeding current, it is pulled toward the flagellate (Fig. 2a). The flagellate responds to the prey before it establishes an observable contact with the flagellum (Fig. 2b). Most likely the first contact is with the invisible flagellar hairs. As also observed by Christensen-

Dalsgaard and Fenchel, the presence of prey is followed by a series of changes in flagellar behavior (Christensen-Dalsgaard and Fenchel 2004). The end of the long flagellum hooks over into a fixed position while the wave amplitude and the beating frequency increases (67 ± 8 Hz) and the short flagellum starts beating rapidly (104 ± 15 Hz). The particle is transported longitudinally until it is confined between the two flagella (Fig. 2c). Finally, the prey is positioned between the short flagellum and the body, ready for phagocytosis (Fig. 2d). During ingestion, three possible scenarios were observed. In the first case, the long flagellum returns to its original position and beating frequency; thus, a feeding current is generated immediately (Fig. 2e). Alternatively, the long flagellum returns to the searching position but with a reduced beating frequency (28 ± 7 Hz after 2 s); therefore, the flow rate is not restored until after more than 2 s. A third scenario involves an immobilized, stiff, and wavy long flagellum while the short flagellum continued beating until finally pausing. The flagellate remained inactive for a long period, which usually exceeded the recording capacity. Unrecorded observations confirmed that after these long breaks, *P. foraminifera* starts beating again to search for more prey. To reject a captured particle, the flagellate releases the prey by returning the long flagellum to the original beating pattern and position (Fig. 2f), and then continues creating a feeding current (Fig. 2g).

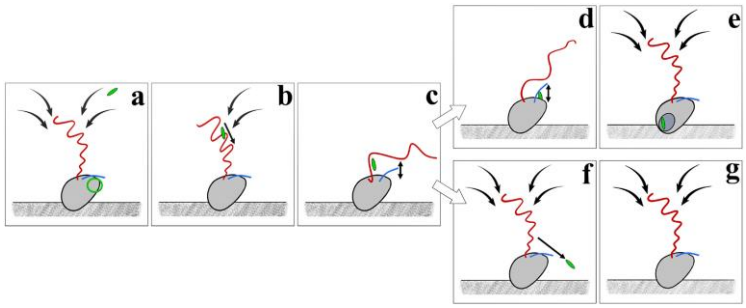

Figure 2. Schematic representation of foraging by *Paraphysomonas foraminifera*. Prey handling steps: searching and capture (a - c); prey ingestion (d - e); and rejection (f - g). Figure objects: long and curved flagellum (solid line, red), short flagellum (solid line, blue), ingestion site (circle, green), feeding current (solid curved arrows), and object in motion (solid straight arrows).

Ochromonas moestrupii and *Chrysophyacea* sp. have a similar feeding behavior as *P. foraminifera*. The prevailing difference is their straight, long, beating flagellum (52 ± 9 and 50 ± 5 Hz, respectively) in contrast to the curved flagellum that characterizes *P. foraminifera*. All three species attach posteriorly in the same manner, and contact and handle the prey with comparable flagellar behaviors for ingestions and rejections.

The handling time of *P. foraminifera* starts when the prey establishes contact with the flagellum. Rejected prey is handled more quickly than ingested prey (Fig. 3; Supplementary Table S2).

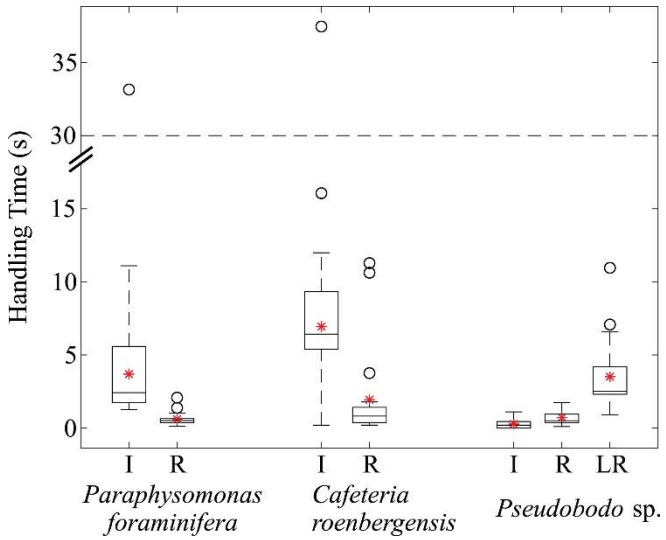

Figure 3. Handling times by *P. foraminifera, *C. roenbergensis*, and *Pseudobodo* sp.** Boxplots for the durations of ingestions (I), rejections (R), and lash rejections (LR); from prey capture to resuming the feeding current (median: dividing black line in the boxplot; mean: asterisk; error bars: dashed lines; outliers: empty circles). A one-way ANOVA test revealed that the three species of flagellates have statistically significant different mean handling times for ingestions ($F_{2,49}$ = [52.58], p = 6.4 x 10^{-13}) and rejections ($F_{2,52}$ = [17.44], p = 1.6 x 10^{-6}). The lash rejection of Pseudobodo sp. was excluded from this analysis. * Not including the ingestion cases of P. foraminifera that were limited by the recording time.

Handling times were independent of prey size over the range of encountered prey sizes (Supporting Information Fig. S1). When the flagellate stopped during an ingestion, the handling time ended when the flagellum reactivated, and the feeding current was restored. This frozen flagellum behavior was reported in 6 out of the 20 ingestions, with 5 exceeding the remaining recording time of 9 – 45 s.

Pteridomonas danica is attached to the surface with a posterior stalk (Fig. 4). Its flagellum beats in a plane with constant frequency, creating a current toward the cell and perpendicular to the attachment surface as also described by Christensen-Dalsgaard and Fenchel (2004). Prey arriving in the flow is intercepted by the tentacle "crown." When food is captured by the tentacles, it is slowly transported toward the cell for phagocytosis. Some particles move outward and

accumulate at the tentacle tips before drifting away. The beating pattern of the flagellate remains uniform throughout all prey encounters, behaving purely like a filtering predator. More than one food particle can be captured or handled simultaneously, and the handling time for *P. danica* is therefore zero.

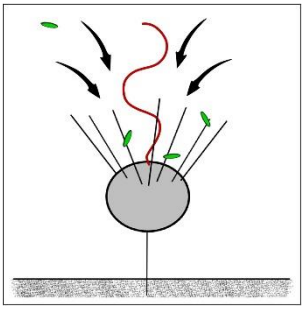

Figure 4. Schematic representation of foraging by *Pteridomonas danica*. A single flagellum creates a feeding current and particles are captured on the crown of tentacles, and subsequently handled for ingestion or rejection.

When sessile, *C. roenbergensis* attaches to the surface with the tip of the posterior flagellum that flexes at irregular intervals. The anterior flagellum beats with constant frequency in a three-dimensional pattern with separate power and recovery phases to create a slightly erratic feeding current parallel to the attachment surface (Fig. 5a). As previously observed (Boenigk and Arndt 2000b), prey particles are intercepted by the cell, not the flagellum (Fig. 5b). Upon prey contact on the sensitive frontal side of the predator, the anterior flagellum stops beating and rapidly arches fully extended against the prey. Thus, food is physically retained between the flagellum and the cell, close to where phagocytosis takes place (Fig. 5c). If the prey establishes first contact elsewhere on the cell, the flagellum continues beating while the food is transported along the cell surface, upstream toward the frontal area. When the prey gets near the ingestion site, the flagellum stops beating to capture the prey and initiate phagocytosis (Fig. 5d). The anterior flagellum resumes its initial beating behavior while or after the prey is phagocytized (Fig. 5e). The flagellate can reject captured prey by returning the flagellum to its original position and releasing the food (Fig. 5f, g). Handling times for *C. roenbergensis* are shorter for rejected than for ingested prey (Fig. 3), and durations were uncorrelated with the prey size (Supporting Information Fig. S1).

When free-swimming, *Pseudobodo* sp. is pulled forward by the extended, beating anterior flagellum while the posterior flagellum inactively trails behind. *Pseudobodo* sp. attach to surfaces while feeding with the long anterior flagellum resembling a lasso loop (Fig. 6a). The flagellum

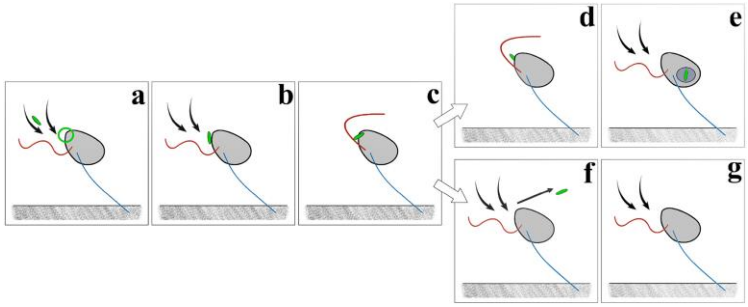

Figure 5. Schematic representation of foraging by *Cafeteria roenbergensis*. Prey handling steps: searching and capture (a - c); prey ingestion (d - e); and rejection (f - g). Figure objects: frontal flagellum (solid line, red), posterior flagellum (solid line, blue), ingestion site (circle, green), feeding current (solid curved arrows), and object in motion (solid straight arrows).

beats (36 ± 10 Hz) and creates a feeding flow through the loop as briefly described previously (Fenchel 1982b). The flow direction can vary from parallel to perpendicular to the surface. The distance between loop and cell (5.7 ± 2.8 μm) is variable during the searching mode. Food particles are intercepted by the anterior flagellum (Fig. 6b). Prey contact triggers an increase in beating frequency (63 ± 15 Hz) at a reduced wave amplitude and a shorter helical pitch. The prey is retained between the cell and the flagellum and transported toward the body (Fig. 6c), either for ingestion (Fig. 6d, e) or rejection. *Pseudobodo* sp. has two ways to actively reject a particle: (1) the quick release and (2) the lash rejection. While the particle is captured between the flagellum and the body, it can be quickly released by reducing the beating frequency and returning the flagellum to its original position (Fig. 6f). Then, the feeding flow is rapidly restored (Fig. 6g). In the lash rejection, the flagellum stops beating for an instant before starting to "uncoil" from base to end, sometimes finalizing fully extended and straight (Fig. 6h). Then, it slowly starts beating (6 ± 3 Hz) with a higher wavelength and amplitude (2.2 ± 0.4 μm). In this rejection mode, the prey is physically pushed away by the flagellate after being captured. Once the prey is released, the flagellum slowly coils back and recovers the initial "loop" beating pattern (Fig. 6i). *Pseudobodo* sp. rejected particles with diameter smaller than 3 μm with a quick release or a lash rejection, in contrast to particles with diameter larger than 5 μm that were only discriminated with the latter strategy (Supporting Information Fig. S1). The handling times of captured particles in *Pseudobodo* sp. were rather short and of similar duration for particles ingested or released quickly, while the lash rejections were of much longer duration (Fig. 3). For almost half of the ingested particles (8/20), the flagellate intercepted and processed the prey without modifying the flagellar beat, thus the handling time was zero. Similar to the other species, handling times were independent of prey size (Supporting Information Fig. S1).

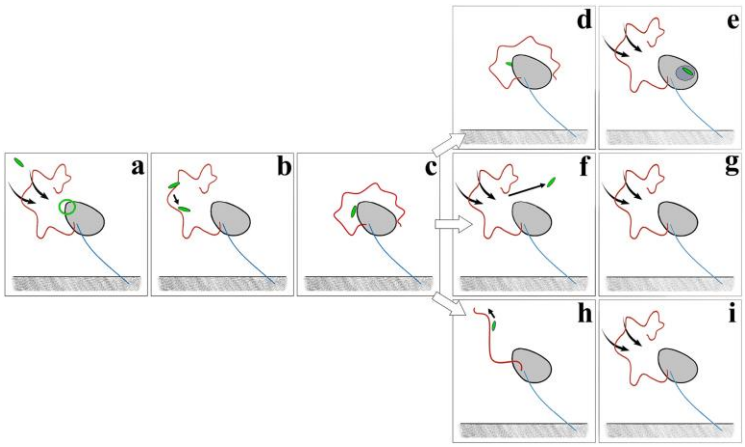

Figure 6. Schematic representation of foraging by *Pseudobodo* sp. Prey handling steps: searching and capture (a - c); prey ingestion (d - e); rejection (f - g); and 'lash' rejection (h - i). Figure objects: 'lasso' flagellum (solid line, red), posterior flagellum (solid line, blue), ingestion site (circle, green), feeding current (solid curved arrows), and object in motion (solid straight arrows).

6.3.2 Particle tracks and clearance rates

For all species, the particles followed hourglass-shaped paths, and only particles nearest the center line of the flow were captured by the cell (Fig. 7; Supporting Information Fig. S2). The sensitivity to the choice of clearance disc was found to be insignificant for clearance discs positioned sufficiently upstream of the beating flagellum (Supplementary Table S4). Estimated maximum clearance rates within species varied by a factor of about 2, and cell volume-specific clearance rates were all of the same order of magnitude and varied from 2 to 18 × 10^6 d^{-1} (Table 1).

6.3.3 Estimation of force magnitudes and theoretical streamlines

The qualitative structures of the feeding flows are captured by the model (Fig. 7). The flow model ignores the cell body and assumes that the force acts at a point, while in reality the force production occurs along the flagellum. This means that the model can describe the flow quantitatively in the clearance disc regions but not in the immediate vicinity of the cell and the beating flagellum. A least-squares fit of the model to the full particle tracks would therefore not provide credible parameter estimation. Two previous studies of flows around sessile choanoflagellates and ciliates have excluded near-field data and made least-squares fits in the far-field (Roper et al. 2013; Pepper et al. 2021), but our information about the far-field is limited compared to the two studies. Instead, we manually positioned and oriented the point forces and applied Eqs. 2 and 3 directly using the detailed information contained in our particle tracks about

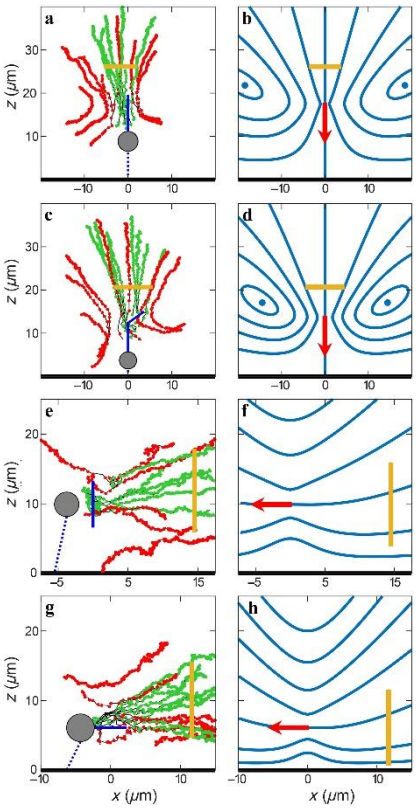

Figure 7. Observed feeding currents by particle tracking and theoretical flow fields generated with the point force model of the individuals Pteridomonas I (a and b), Paraphysomonas I (c and d), Pseudobodo I (e and f) and Cafeteria I (g and h). Clearance discs are in front of the flagellate, represented as a yellow solid line. Left-side panels: the cell body (gray circle) of the flagellate attaches (blue dotted line) to the surface (thick black line), and the beating flagellum (solid blue line) generates a feeding current. Green tracks are for captured particles, and red tracks are for uncaptured prey. Right-side panels: the point force (red arrow) dictates the direction of the feeding current described by the theoretical streamlines (blue solid lines).

the clearance rates and the clearance discs. The point force is positioned at the narrowest point of the hourglass-shaped track pattern where the particle speeds are highest. For *P. danica*, we used a point force located on the flagellum at ¾ of its length from the cell body (Fig. 7a, b; Supporting Information Fig. S2a, b). For *P. foraminifera*, all particle tracks converged toward the curved distal segment of the flagellum (Fig. 7c, d; Supporting Information Fig. S2c, d), and therefore the point force was located in the middle of this section. Due to the complex and variable geometry of *Pseudobodo* sp., the point force was positioned in the middle of the "loop" halfway between the body and the tip of the helical flagellum (Fig. 7e, f; Supporting Information Fig. S2e, f). The point force in the cases of *C. roenbergensis* was set to be at half the projection length of the flagellum, approximately where tracked particles reached maximum velocities (Fig. 7g, h; Supporting Information Fig. S2g, h). The resulting force estimates using Eqs. 2 and 3 were 3.7–12.5 pN with flows perpendicular to the surface (*P. danica* and *P. foraminifera*), requiring a slightly stronger force than the cases of parallel feeding currents (*Pseudobodo* sp. and *C. roenbergensis*; Table 1).

Table 1. Morphological and kinematic parameters, and clearance rate and force estimates for four species of flagellates (*Paraphysomonas foraminifera*, *Pteridomonas danica*, *Pseudobodo* sp. and *Cafeteria roenbergensis*). Particle tracking was performed for two individuals (I and II) of each species to estimate the clearance rate and the force required to drive the flow.

	P. foraminifera		***P. danica***		***Pseudobodo sp***		***C. roenbergensis***	
	I	**II**	**I**	**II**	**I**	**II**	**I**	**II**
Cell diameter (µm)	3.9	3.5	4.6	4.4	3.5	5.5	4.0	3.9
Cell height (µm)	1.7	13.7	6.6	6.2	8.1	15.4	4.1	4.8
Flagellum projection length (µm)	14.0	10.8	8.4	6.7	–	–	4.6	5.2
Flagellum beat frequency f (Hz)	52	44	30	33	21	33	38	47
Clearance disc radius a (µm)	4.5	5.3	3.7	5.7	6.0	5.6	5.4	5.5
Clearance disc height d (µm)	20.7	31.2	26.1	25.1	–	–	–	–
Point force to disc distance l (µm)	–	–	–	–	14.5	15.0	11.7	8.9
Average flow velocity U (µm s^{-1})	78	52	44	30	19	18	17	16
Volume-specific clearance rate Q_v (10^6 cell volume day^{-1})	13	18	3.3	6.2	8.1	1.7	4.2	4.1
Clearance rate Q (10^3 µm^3 s^{-1})	4.9	4.6	1.9	3.2	2.1	1.8	1.6	1.5
Point force height h (µm)	13.7	21.7	17.5	15.6	9.9	18.2	6.1	6.8
Force F (pN)	12.5	10.2	7.7	7.0	6.5	4.9	5.7	3.7

The force required to drive the observed flow can be compared with estimates of the force generated by the flagellum. *P. danica* beats its flagellum in a plane with a roughly sinusoidal beat pattern, allowing us to apply the resistive force theory expression in Eq. 5 to directly estimate the force produced by the flagellum. We have our observed parameters L = 11.5 µm, $2A$ = 2.9 µm, λ = 5.3 µm, and f = 33 Hz (Supplementary Table S1) and the parameters from the literature: b = 0.15 µm (Moestrup 1982), α = 3 µm, β = 0.01 µm (Fenchel 1982b; Patterson and Fenchel 1985), and χ = 0.15 µm (Holwill and Sleigh 1967). With the parameters we would estimate $F_z = -1.0$ pN using Eq. 6 if the flagellum were without hairs, that is, in opposite direction, and we find F_z = 15 pN using the force coefficients in Eq. 7 for the flagellum with hairs. Similar estimates are not possible for the other species that have more complex three-dimensional beat patterns.

6.4 Discussion

6.4.1 Attached vs. free-swimming

Our study complements earlier descriptions of the foraging behavior of heterotrophic nanoflagellates (Sleigh 1964; Fenchel 1982b; Boenigk and Arndt 2000b). We describe feeding only in flagellates attached to surfaces. Attached feeding appears to dominate for small forms, while larger forms, such as dinoflagellates, feed predominantly when freely swimming (Boenigk and Arndt 2002; Nielsen and Kiørboe 2015). We observed *P. danica* capture prey while swimming, and *Spumella* sp., *O. moestrupii*, and loricated choanoflagellates are known to feed while swimming (Boenigk and Arndt 2000b; Pfandl et al. 2004; Nielsen et al. 2017). It has been argued that attachment enhances the feeding current of suspension feeders (Strickler 1982; Tiselius and Jonsson 1990; Christensen-Dalsgaard and Fenchel 2003), but fluid dynamical simulations and models suggest the opposite (Kirkegaard and Goldstein 2016; Andersen and Kiørboe 2020). The reason for attachment in bacterivorous nanoflagellates may therefore rather be favorable food conditions near surfaces, such as marine snow (Alldredge and Silver 1988; Simon et al. 2002). This is consistent with the observation that starving flagellates (*Ochromonas* sp., *P. vestita*, *A. mirabilis*) do not attach, while almost all cells experiencing high prey concentrations attach (Christensen-Dalsgaard and Fenchel 2003; Pfandl et al. 2004). Thus, swimming in heterotrophic nanoflagellates may for many species primarily serve the purpose of finding a nutrient-rich attachment surface. The probing behavior and different configuration of the flagellum of swimming and attached *Pseudobodo* sp. lend further support to this interpretation. Thus, stretching the flagellum in front of the cell allows faster swimming (Langlois et al. 2009). Some choanoflagellates similarly have an attached feeding stage with a short flagellum, and a free-swimming nonfeeding stage with a long flagellum and a smaller more streamlined cell body (Nguyen et al. 2019).

6.4.2 Handling time, clearance rate, and the functional response

Predator–prey interactions are often quantified by the prey ingestion rate as a function of the concentration of prey, typically described by a type II functional response (Holling 1959). This equation has two parameters, the maximum clearance rate, that is, the volume of water cleared for particles per unit time at low prey concentration, and the prey handling time (= 1/maximum ingestion rate). Our behavioral observations allow us to estimate both parameters and to examine to what extent they underpin functional response relations estimated in incubation experiments.

In the species examined here, prey encounter is facilitated by the generation of a feeding current produced by the activity of one hairy flagellum that propels water toward the cell. We identified three different modes of prey encounter: prey particles arriving in the feeding current are perceived and captured by the flagellum, intercepted by the cell body, or by tentacles, and these represent the encounter mechanisms described for nanoflagellates. Prey is then handled by coordinated motions of one or two flagella, or, in the case of *P. danica*, by the tentacles. While the suspension feeding *P. danica* continues to generate a feeding current while handling prey, the feeding current ceases during prey handling in the other species. The prey handling time can be substantial, particularly in P. foraminifera that stops beating the flagellum for up to more than 1 min after the prey has been phagocytized. A similar "refractory period" has been reported for four species of nanoflagellates, including *C. roenbergensis* (Boenigk and Arndt 2000b), leading to handling times between 4 and 95 s per prey, similar to the range reported here. Eventually, ingestion rate may be limited by handling times, and the so estimated maximum ingestion rates vary by more than one order of magnitude between species, from 1000 to 20,000 preys per day. This corresponds largely to the range of species-specific maximum ingestion rates of bacteria in incubation experiments, 600 – 6000 bacteria d−1 (Fenchel 1982c; Boenigk and Arndt 2002). The match becomes better when considering that a varying but sometimes large fraction of captured bacteria may be rejected (Matz et al. 2002; Pfandl et al. 2004). Handling of rejected prey may further reduce time for searching, even though handling time is generally shorter for rejected than ingested prey (Boenigk and Arndt 2002).

Particle tracking allowed us to characterize the flow field generated by the feeding flagellates, to identify the extension of the prey capture zone, and to estimate maximum clearance rates. Our estimates of cell volume-specific maximum clearance rates varied between both individuals and species and ranged between 10^6 and 10^7 d^{-1}. This magnitude is again similar to that obtained in incubation experiments, where estimates vary between species and range between 10^5 and 10^7 d^{-1} (reviewed in Hansen et al. 1997; Kiørboe and Hirst 2014). Overall, functional responses measured in incubation experiments are mechanistically underpinned by behavioral observations.

6.4.3 Flow architecture and fluid dynamics

At the low Reynolds number at which nanoflagellates operate, viscosity impedes predator–prey contact, but the activity of the beating flagellum is obviously sufficient to overcome the effect of viscosity. The impeding effect of viscosity is somewhat relaxed in flagellates that contact prey by the flagellum or tentacles at some distance from the no-slip surface of the cell. However, even in *C. roenbergensis*, where first contact is on the cell surface, the feeding current is sufficiently strong to allow prey encounters.

By applying a point force model that describes the observed flow fields well, we estimated the flow-generating forces to be on the order of 4 – 13 pN for the four species. These estimates ignore the presence of the cell body, and the force produced by the flagellum has to be somewhat larger than the force required to produce the observed flow fields. Christensen-Dalsgaard and Fenchel used an alternative approach and measured the swimming speed of *P. vestita* towing a latex sphere and computed the flagellum force from the Stokes drag to be of similar magnitude, 7 – 13 pN (Christensen-Dalsgaard and Fenchel 2003). This approach neglects hydrodynamic interactions between flagellum, cell, and latex sphere, and the actual force is therefore larger than this estimate as well (Langlois et al. 2009).

How do these indirect estimates compare with direct estimates of the force generated by the beating flagella? The estimate derived for *P. danica* by applying resistive force theory is larger but of similar magnitude as the indirect estimate, 15 and 7 – 8 pN, respectively. The estimate ignores hydrodynamic interactions between adjacent sections of the flagellum (Holwill and Sleigh 1967; Brennen 1976), which is most likely not justified for flagella with closely spaced hairs (Rodenborn et al. 2013) and it is therefore speculative. The estimate suggests that the hairs reverse the direction of the force and increases its magnitude by an order of magnitude compared to a flagellum without hairs. This increase is similar to that estimated by comparing swimming speeds of flagellates with smooth and hispid flagella (Nielsen and Kiørboe 2021).

As noted above, most heterotrophic nanoflagellates have hispid flagella, and this seems to be optimal or even necessary for prey encounter for a number of reasons. First, the presence of hairs significantly increases the force production of the beating flagellum and thereby the clearance rate. Secondly, the presence of hairs makes prey scanning of the flagellum efficient, since prey intercepted by the hairs elicits a capture response. Thirdly, the dominant flow along a flagellum with hairs is outside the envelope of the beating flagellum (Jahn et al. 1964; Sleigh 1981, 1991), presumably allowing efficient prey transport toward the cell. Fourthly, the front-mounted flagellum increases the frequency of prey entrainment (Mathijssen et al. 2018). Finally, the reversal of the flow makes the streamlines come closer to the cell in the up-stream direction from where the prey arrives, and the transport of captured prey toward the cell body is facilitated by the flow.

6.5 Conclusions

Indirect and direct estimates of flagellum forces for one species are of similar magnitudes and consistent with the observed feeding flow, and the estimates of maximum ingestion and clearance rates are similar to those obtained from previous incubation experiments. Thus, our observations and estimates suggest a mechanistic underpinning of functional responses in heterotrophic nanoflagellates. However, experimentally estimated specific clearance rates of flagellates vary by two orders of magnitude (Hansen et al. 1997; Kiørboe and Hirst 2014), and a significant fraction of this variation is accounted for by variation in flagellar arrangement and kinematics and consequent differences in flow architecture and predation risk: species with high clearance rates also disturb a large volume of water, attract flow-sensing predators from a further distance, and experience higher predation risk (Nielsen and Kiørboe 2021). A better mechanistic understanding of this foraging trade-off and the variation in clearance rates requires a better understanding of the fluid dynamics of hairy flagella. This in turn may be facilitated by accurate observations of the often complex three-dimensional beat patterns of the flagella (Christensen-Dalsgaard and Fenchel 2004) and the arrangement of hairs on the flagella in combination with computational fluid dynamics simulations and theoretical modeling.

Acknowledgments

We acknowledge help from Ramon Massana, Vanessa Balagué, Elisabet Laia Sà, Lasse Tor Nielsen, Helge Thomsen, Saeed Asadzadeh, and Mads Rode. We received funding from The Independent Research Fund Denmark (7014-00033B) and the Carlsberg Foundation (CF17-0495), and the Centre for Ocean Life is supported by the Villum Foundation.

References

Aderogba, K., and J. R. Blake. 1978. Action of a force near the planar surface between semi-infinite immiscible liquids at very low Reynolds numbers: *Addendum. Bull. Aust. Math. Soc.* 19: 309–318.

Alldredge, A. L., and M. W. Silver. 1988. Characteristics, dynamics and significance of marine snow. *Prog. Oceanogr*. 20: 41–82. doi:10.1016/0079-6611(88)90053-5

Andersen, A., and T. Kiørboe. 2020. The effect of tethering on the clearance rate of suspension-feeding plankton. *Proc. Natl. Acad. Sci.* 202017441. doi:10.1073/pnas.2017441117

Azam, F., T. Fenchel, J. Field, J. Gray, L. Meyer-Reil, and T. F. Thingstad. 1983. The Ecological Role of Water-Column Microbes in the Sea. *Mar. Ecol. Prog. Ser.* 10: 257–263. doi:10.3354/meps010257

Blake, J. R. 1971. A note on the image system for a stokeslet in a no-slip boundary. *Math. Proc. Cambridge Philos. Soc.* 70: 303–310.

Blake, J. R., and A. T. Chwang. 1974. Fundamental singularities of viscous flow. *J. Eng. Math.* 8: 23–29.

Blake, J. R., and S. R. Otto. 1996. Ciliary propulsion, chaotic filtration and a blinking stokeslet. *J. Eng. Math*. 151–168.

Boenigk, J., and H. Arndt. 2000a. Comparative studies on the feeding behavior of two heterotrophic nanoflagellates: The filter-feeding choanoflagellate Monosiga ovata and the raptorial-feeding kinetoplastid Rhynchomonas nasuta. *Aquat. Microb. Ecol.* 22: 243–249. doi:10.3354/ame022243

Boenigk, J., and H. Arndt. 2000b. Particle handling during interception feeding by four species of heterotrophic nanoflagellates. *J. Eukaryot. Microbiol.* 47: 350–358. doi:10.1111/j.1550-7408.2000.tb00060.x

Boenigk, J., and H. Arndt. 2002. Bacterivory by heterotrophic flagellates: community structure and feeding strategies. *Antonie Van Leeuwenhoek* 81: 465–480.

Brennen, C. 1976. Locomotion of flagellates with mastigonemes. *J. Mechanochemistry Cell Motil.* 3: 207–217.

Christensen-Dalsgaard, K., and T. Fenchel. 2003a. Increased filtration efficiency of attached compared to free-swimming flagellates. *Aquat. Microb. Ecol.* 33: 77–86. doi:10.3354/ame033077

Christensen-Dalsgaard, K. K., and T. Fenchel. 2003b. Increased filtration efficiency of attached compared to free-swimming flagellates. *Aquat. Microb. Ecol.* 33: 77–86. doi:10.3354/ame033077

Christensen-Dalsgaard, K. K., and T. Fenchel. 2004. Complex Flagellar Motions and Swimming Patterns of the Flagellates *Paraphysomonas vestita* and *Pteridomonas danica*. *Protist* 155: 79–87. doi:10.1078/1434461000166

Dölger, J., L. T. Nielsen, T. Kiørboe, and A. Andersen. 2017. Swimming and feeding of mixotrophic biflagellates. *Sci. Rep.* 7: 39892. doi:10.1038/srep39892

Fenchel, T. 1982a. Ecology of Heterotrophic Microflagellates. IV Quantitative Occurrence and Importance as Bacterial Consumers. *Mar. Ecol. Prog. Ser*. 9: 35–42. doi:10.3354/meps009035

Fenchel, T. 1982b. Ecology of Heterotrophic Microflagellates. I. Some Important Forms and Their Functional Morphology. *Mar. Ecol. Prog. Ser.* 8: 211–223.

Fenchel, T. 1982c. Ecology of Heterotrophic Microflagellates. II. Bioenergetics and Growth. *Mar. Ecol. Prog. Ser.* 8: 225–231. doi:10.3354/meps008225

Fenchel, T. 1986. Protozoan filter feeding. *Prog. Protistol.* 1: 65–113.

Gray, J., and G. J. Hancock. 1955. The propulsion of sea-urchin spermatozoa. *J. Exp. Biol*. 32: 802–814.

Hansen, P. J., P. K. Bjørnsen, and B. W. Hansen. 1997. Zooplankton grazing and growth: Scaling within the 2-2,-µm body size range. *Limnol. Oceanogr*. 42: 687–704. doi:10.4319/lo.1997.42.4.0687

Holling, C. S. 1959. Some Characteristics of Simple Types of Predation and Parasitism. *Can. Entomol.* 91: 385–398. doi:10.4039/Ent91385-7

Holwill, M. E., and M. A. Sleigh. 1967. Propulsion by hispid flagella. *J. Exp. Biol*. 47: 267–276.

Ishigaki, T., and M. Terazaki. 1998. Grazing behavior of heterotrophic nanoflagellates observed with a high speed VTR system. *J. Eukaryot. Microbiol*. 45: 484–487. doi:10.1111/j.1550-7408.1998.tb05104.x

Jabbarzadeh, M., and H. C. Fu. 2018. Viscous constraints on microorganism approach and interaction. *J. Fluid Mech*. 851: 715–738. doi:10.1017/jfm.2018.509

Jahn, T. L., M. D. Landman, and J. R. Fonseca. 1964. The Mechanism of Locomotion of Flagellates. II. Function of the Mastigonemes of *Ochromonas*. *J. Protozool*. 3: 291–296.

Kiørboe, T. 2011. How zooplankton feed: Mechanisms, traits and trade-offs. *Biol. Rev.* 86: 311–339. doi:10.1111/j.1469-185X.2010.00148.x

Kiørboe, T., and A. G. Hirst. 2014. Shifts in mass scaling of respiration, feeding, and growth rates across life-form transitions in marine pelagic organisms. *Am. Nat.* 183: E118-30. doi:10.1086/675241

Kirkegaard, J. B., and R. E. Goldstein. 2016. Filter-feeding, near-field flows, and the morphologies of colonial choanoflagellates. *Phys. Rev. E* 94: 052401. doi:10.1103/PhysRevE.94.052401

Langlois, V., A. Andersen, T. Bohr, A. Visser, and T. Kiørboe. 2009. Significance of swimming and feeding currents for nutrient uptake in osmotrophic and interception feeding flagellates. *Aquat. Microb. Ecol*. 54: 35–44. doi:10.3354/ame01253

Lauga, E. 2020. The Fluid Dynamics of Cell Motility, Cambridge University Press.

Lauga, E., and T. R. Powers. 2009. The hydrodynamics of swimming microorganisms. Reports *Prog. Phys*. 72: 096601.

Mathijssen, A. J. T. M., R. Jeanneret, and M. Polin. 2018. Universal entrainment mechanism controls contact times with motile cells. *Phys. Rev. Fluids* 3: 033103. doi:10.1103/PhysRevFluids.3.033103

Matz, C., J. Boenigk, H. Arndt, and K. Jürgens. 2002. Role of bacterial phenotypic traits in selective feeding of the heterotrophic nanoflagellate Spumella sp. *Aquat. Microb. Ecol*. 27: 137–148. doi:10.3354/ame027137

Moestrup, Ø. 1982. Phycological Reviews 7: Flagellar structure in algae: a review, with new observations particularly on the Chrysophyceae, Phaeophyceae (Fucophyceae), Euglenophyceae, and Reckertia. *Phycologia* 21: 427–528. doi:10.2216/i0031-8884-21-4-427.1

Montagnes, D. J. S., A. B. Barbosa, J. Boenigk, and others. 2008. Selective feeding behaviour of key free-living protists: Avenues for continued study. *Aquat. Microb. Ecol.* 53: 83–98. doi:10.3354/ame01229

Nguyen, H., M. A. R. Koehl, C. Oakes, G. Bustamante, and L. Fauci. 2019. Effects of cell morphology and attachment to a surface on the hydrodynamic performance of unicellular choanoflagellates. *J. R. Soc. Interface* 16: 20180736. doi:10.1098/rsif.2018.0736

Nielsen, L. T., S. S. Asadzadeh, J. Dölger, J. H. Walther, T. Kiørboe, and A. Andersen. 2017. Hydrodynamics of microbial filter feeding. *Proc. Natl. Acad. Sci. U. S. A.* 201708873. doi:10.1073/pnas.1708873114

Nielsen, L. T., and T. Kiørboe. 2015. Feeding currents facilitate a mixotrophic way of life. *ISME J.* 9: 2117–2127. doi:10.1038/ismej.2015.27

Nielsen, L. T., and T. Kiørboe. 2021. Foraging trade-offs, flagellar arrangements, and flow architecture of planktonic protists. *Proc. Natl. Acad. Sci*. 118: e2009930118. doi:10.1073/pnas.2009930118

Patterson, D. J., and T. Fenchel. 1985. Insights into the evolution of heliozoa (Protozoa, Sarcodina) as provided by ultrastructural studies on a new species of flagellate from the genus Pteridomonas. *Biol. J. Linn. Soc*. 34: 381–403.

Pepper, R. E., E. E. Riley, M. Baron, T. Hurot, L. T. Nielsen, M. A. R. Koehl, T. Kiørboe, and A. Andersen. 2021. The effect of external flow on the feeding currents of sessile microorganisms. *J. R. Soc. Interface* 18. doi:10.1098/rsif.2020.0953

Pfandl, K., T. Posch, and J. Boenigk. 2004. Unexpected effects of prey dimensions and morphologies on the size selective feeding by two bacterivorous flagellates (*Ochromonas* sp. and *Spumella* sp.). *J. Eukaryot. Microbiol*. 51: 626–633. doi:10.1111/j.1550-7408.2004.tb00596.x

Rode, M., G. Meucci, K. Seegert, T. Kiørboe, and A. Andersen. 2020. Effects of surface proximity and force orientation on the feeding flows of microorganisms on solid surfaces. *Phys. Rev. Fluids* 5: 123104. doi:10.1103/PhysRevFluids.5.123104

Rodenborn, B., C.-H. Chen, H. L. Swinney, B. Liu, and H. P. Zhang. 2013. Propulsion of microorganisms by a helical flagellum. *Proc. Natl. Acad. Sci.* 110: E338–E347. doi:10.1073/pnas.1219831110

Roper, M., M. J. Dayel, R. E. Pepper, and M. A. R. Koehl. 2013. Cooperatively Generated Stresslet Flows Supply Fresh Fluid to Multicellular Choanoflagellate Colonies. *Phys. Rev. Lett.* 110: 228104. doi:10.1103/PhysRevLett.110.228104

Rueden, C. T., J. Schindelin, M. C. Hiner, B. E. DeZonia, A. E. Walter, E. T. Arena, and K. W. Eliceiri. 2017. ImageJ2: ImageJ for the next generation of scientific image data. *BMC Bioinformatics* 18: 1–26. doi:10.1186/s12859-017-1934-z

Schindelin, J., I. Arganda-Carreras, E. Frise, and others. 2012. Fiji: An open-source platform for biological-image analysis. *Nat. Methods* 9: 676–682. doi:10.1038/nmeth.2019

Simon, M., H. P. Grossart, B. Schweitzer, and H. Ploug. 2002. Microbial ecology of organic aggregates in aquatic ecosystems. *Aquat. Microb. Ecol*. 28: 175–211. doi:10.3354/ame028175

Sleigh, M. A. 1964. Flagellar movement of the Sessile Flagellates Actinomonas, Codonosiga, Monas, and Poteriodendron. *J. Cell Sci*. s3-105: 405–414.

Sleigh, M. A. 1991. Mechanisms of flagellar propulsion - A biologist's view of the relation between structure, motion, and fluid mechanics. *Protoplasma* 164: 45–53. doi:10.1007/BF01320814

Sleigh, M. a. 1981. Flagellar beat patterns and their possible evolution. *Biosystems*. 14: 423–431. doi:10.1016/0303-2647(81)90047-2

Strickler, J. R. 1982. Calanoid Copepods , Feeding Currents , and the Role of Gravity. *Science*. 218: 158–160.

Tiselius, P., and P. R. Jonsson. 1990. Foraging behaviour of six calanoid copepods: observations and hydrodynamic analysis. *Mar. Ecol. Prog. Ser.* 66: 23–33. doi:10.3354/meps066023

Weisse, T., R. Anderson, H. Arndt, A. Calbet, P. J. Hansen, and D. J. S. Montagnes. 2016. Functional ecology of aquatic phagotrophic protists – Concepts, limitations, and perspectives. *Eur. J. Protistol*. 55: 50–74. doi:10.1016/j.ejop.2016.03.003

Worden, A. Z., M. J. Follows, S. J. Giovannoni, S. Wilken, A. E. Zimmerman, and P. J. Keeling. 2015. Rethinking the marine carbon cycle: Factoring in the multifarious lifestyles of microbes. *Science*. 347: 1257594–1257594. doi:10.1126/science.1257594

6.6 Appendix Paper I

6.6.1. Handling times and prey size

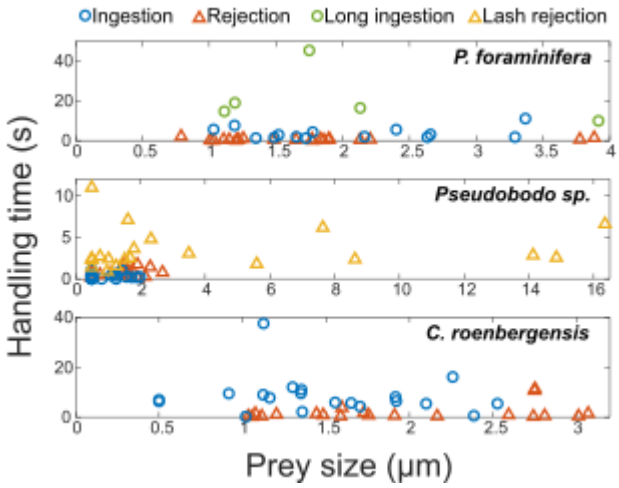

Figure S1. Handling times for different prey sizes (when available) by *Paraphysomonas foraminifera, Pseudobodo* sp., and *Cafeteria roenbergensis*. No correlation was found between the duration of prey handling (for ingestions and rejections) and the prey size in all studied species. For *P. foraminifera*, "Long ingestions" (N = 4) are the minimum handling times that were limited by the recording capacity (i.e., when the flagellum stopped beating).

6.6.2. Feeding currents and point force model

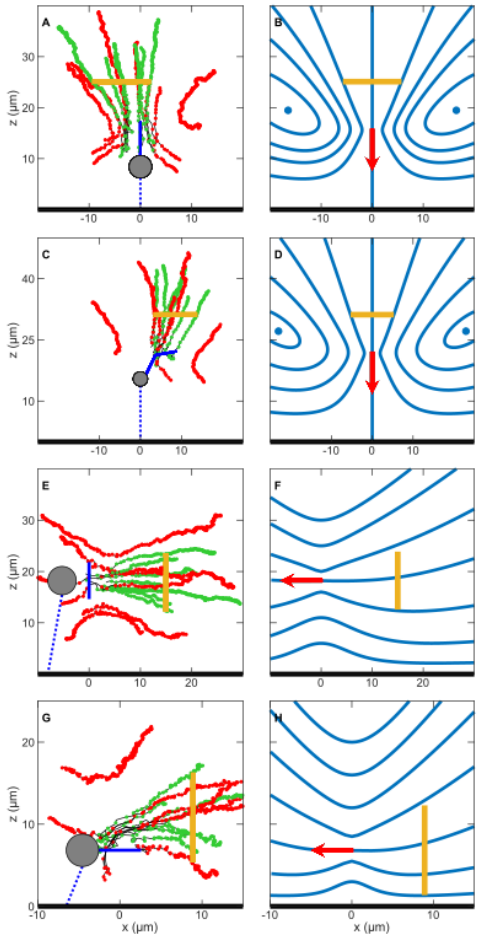

Figure S2. Observed feeding currents by particle tracking and theoretical flow fields generated with the point force model of the individuals Pteridomonas II (a and b), Paraphysomonas II (c and d), Pseudobodo II (e and f) and Cafeteria II (g and h). Clearance discs are represented as a yellow line. Left-side panels: the cell body (gray circle) of the flagellate attaches (blue dotted line) to the surface (thick black line), and the beating flagellum (solid blue line) generates a feeding current. Green tracks are for captured particles, and red tracks are for uncaptured prey. Right-side panels: the point force (red arrow) dictates the direction of the feeding current described by the theoretical streamlines (blue solid lines).

6.6.3. Supplementary tables

Table S1. Morphometric data and flagellum properties.

	CELL		FLAGELLUM				Short flagellum length (µm)	Filtering radius (µm)
Species	**diameter** (µm)	**height** (µm)	**length** (µm)	**peak-to-peak amplitude** (µm)	**Wave length** λ (µm)	**Beating frequency** f (Hz)		
Paraphysomonas foraminifera	4.9 ± 0.9	3.0 ± 2.7	13.4 ± 0.9	–	–	46 ± 6	3.1 ± 0.6	–
n =	35	25	13	–	–	40	25	–
Pteridomonas danica	4.9 ± 1.0	6.9 ± 6.9	11.5 ± 1.7	2.9 ± 0.4	5.3 ± 0.4	33 ± 11	–	2.2 ± 1.1
n =	28	12	21	8	8	28	–	17
Cafeteria roenbergensis	4.9 ± 0.6	–	7.0 ± 0.8	–	–	37 ± 6	–	–
n =	37	–	29	–	–	40	–	–
Pseudobodo sp.	4.5 ± 0.8	10.7 ± 5.1	18.4 ± 9.9	2.5 ± 0.3	–	36 ± 10	–	4.7 ± 1.0
n =	67	7	15	16	–	84	–	71
Ochromonas moestrupii	5.3 ± 0.6	–	12.3 ± 0.3	–	–	52 ± 9	3.1 ± 0.4	–
n =	3	–	3	–	–	4	3	–
Chrysophyacea sp.	4.3 ± 0.5	–	11.5 ± 1.8	–	–	50 ± 5	2.2 ± 0.4	–
n =	13	–	2	–	–	14	9	–

Footnote: cell height is the distance between the substrate and the attached cell. Flagellum features correspond to flagella creating a feeding current, i.e. not interacting with prey. The flagellum amplitude was measured from peak-to-peak of the wave (note that for *Pseudobodo* sp. it is the length of the 2D projection from the 3D beating wave). Short flagellum refers to the second prey-handling flagellum of *P. foraminifera*, *O. moestrupii*, and *Chrysophyacea* sp. The filtering radius is the distance from the tip of a lateral tentacle to the central axis of the body or the radius of the flagellar 'loop' for P. danica and Pseudobodo sp., respectively. The measurements are expressed as the mean ± standard deviation, and n denotes the number of observations per parameter.

Table S2. Handling times during ingestions and rejections.

	Handling Time (s)					
	Ingestion		Rejection		Lash Rejection	
Species	**N**	**mean ± SD**	**N**	**mean ± SD**	**N**	**mean ±SD**
P. danica	0		0		–	
P. foraminifera	15	5.7 ± 7.8*	20	0.6 ± 0.5	–	
Pseudobodo sp.	20	0.3 ± 0.3	20	0.7 ± 0.5	20	3.5 ± 2.4
C. roenbergensis	20	8.5 ± 7.6	20	1.9 ± 3.1	–	
O. moestrupii	1	5.5	2	1.2 ± 0.8	–	
Chrysophyacea sp.	–		12	5.2 ± 6.0	–	

* Not including the cases (N = 5) when *P. foraminifera* stops beating during ingestions that were limited by the recording time.

Table S3. Tilting angle, α, of the force vector generated by the beating flagellum.

Species individual	Average α (°)	SD
Pteridomonas I	7.3	3.9
Pteridomonas II	10.7	3
Paraphysomonas I	14.1	5.3
Paraphysomonas II	8.7	3.9
Pseudobodo I	57.2	9.3
Pseudobodo II	92.5	10.2

Footnote: Minor shifts of orientation while generating feeding currents were observed in *Pteridomonas danica*, *Paraphysomonas foraminifera*, and *Pseudobodo* sp. The angle α is between the force vector and the axis normal to the surface. The force is orthogonal to the surface when $\alpha = 0°$, and parallel when $\alpha = 90°$. The angle was recorded in each track for later averaging.

Table S4. Clearance rates, Q, from each disc of radius a, placed at different distances (distance cell to disc) from the species individual.

		Clearance disc radius *a* (µm)	**Distance cell to disc** (µm)	**Clearance rate** *Q* ($\mu m^3 \cdot s^{-1}$)
Pteridomonas I	Disc 1	2.3	10.0	1374.4
	Disc 2	3.8	15.0	1945.1
	Disc 3	5.5	20.0	2212.6
Pteridomonas II	Disc 1	3.8	10	2672.4
	Disc 2	5.8	14.5	3153.6
	Disc 3	7.5	19	3464.9
Paraphysomonas I	Disc 1	3.0	10.0	4503.8
	Disc 2	4.5	15.0	4928.8
	Disc 3	6.3	20.0	5511.2
Paraphysomonas II	Disc 1	4.2	10.0	5029.2
	Disc 2	5.3	14.0	4626.1
	Disc 3	6.3	18.0	4565.8
Pseudobodo I	Disc 1	5.0	11.5	1836.8
	Disc 2	6.0	16.5	2128.7
Pseudobodo II	Disc 1	4.2	12.5	1909.5
	Disc 2	5.7	17.5	1767.6
Cafeteria I	Disc 1	2.4	5.0	1454.6
	Disc 2	3.9	10.0	1128.4
	Disc 3	5.5	14.0	1578.8
Cafeteria II	Disc 1	2.5	5.5	1473.5
	Disc 2	4.1	8.5	1888.0
	Disc 3	5.5	11.5	1535.3

Footnote: as a method validation, the flow rate through more than one clearance disc per individual was estimated and compared. Variations within each species (*Paraphysomonas foraminifera*, *Pteridomonas danica*, *Pseudobodo* sp., and *Cafeteria roenbergensis*) are by a factor of around two.

CHAPTER 7

Paper II

Functional Morphology and Fluid Dynamics of Foraging in 'Typical Excavates'; a Key Assemblage for Understanding Deep Eukaryote Evolution

Sei Suzuki-Tellier[1]*, Federica Miano[1]*, Seyed Saeed Asadzadeh[1]*, Alastair G.B. Simpson[2], Thomas Kiørboe[1]

[1]Centre for Ocean Life, National Institute of Aquatic Resources, Technical University of Denmark, Kgs Lyngby, Denmark;

[2] Department of Biology, and Centre for Comparative Genomics and Evolutionary Bioinformatics, Dalhousie University, Halifax, NS, Canada.

*Equal authorship

This paper has not yet been submitted to any journal.

Abstract

Phagotrophic flagellates belonging to the group of 'typical excavates' have been hypothesized to be closely related to the Last Eukaryotic Common Ancestor and understanding the functional ecology of excavates may therefore help throw light on early Eukaryotic evolution. Excavates are characterized by a posterior flagellum equipped with a vane that beats in a ventral groove. Here, we combined flow visualization and observations of prey capture in three clades of excavates with computational fluid dynamic modelling to understand the functional significance of this arrangement. Clearance rate magnitudes estimated from flow visualization and modelling are like that of other similarly sized phagotrophic flagellates. The interaction between a vaned flagellum beating in a confinement produces a very efficient feeding current at low energy costs, irrespective of the beat plane and the orientation of the vane and of all other morphological variations. Vaned, constrained flagella are widespread among phagotrophic flagellates. Specifically, a flagellar arrangement very similar and possibly homologous to the excavate arrangement is found in other deep branches of the Eukaryotic tree of life. We suggest that the typical excavate foraging system studied here may have been used by our distant ancestors for more than 1 billion years.

7.1 Introduction

Phagotrophic flagellates are the main consumers of bacteria and pico-phytoplankton in the ocean and, thus, play a key role in regulating pelagic microbial ecosystems. Phagotrophic flagellates are often treated as one functional group in assessments of pelagic ecosystem structure, but this assemblage is phylogenetically very diverse, with representatives in all the major branches of the eukaryotic tree of life. They are also functionally diverse, as the number of flagella, their beat patterns and kinematics, and whether their flagella are naked or equipped with hairs or vanes, all significant for their function, vary between groups (Kiørboe 2016). Many species also can photosynthesize, i.e., they are mixotrophic. This functional diversity may imply great variation in foraging efficiency, as quantified by clearance rates that vary by more than 2 orders of magnitude between flagellates of similar sizes (Edwards et al. 2023b). It may also imply foraging trade-offs, since the more efficient foragers typically also run higher predation risks (Nielsen & Kiørboe 2021) and have lower photosynthetic ability (Edwards et al. 2023a).

The mechanisms of phagotrophic foraging are examined in only a few groups of flagellates. In the small-scale world of flagellates where the Reynolds number (ratio of inertial to viscous forces) is low, viscosity impedes predator-prey contact, and generating sufficient feeding current typically requires forces that are larger than what a single naked flagellum can produce to overcome the impeding effect of viscosity (Kiørboe 2023). Thus, in the groups examined in detail, one finds that the flagellar apparatus has highly specialized adaptations for foraging. Thus, most flagellates in the taxon Stramenopiles have one flagellum equipped with rigid hairs that increases the force production of the beating flagellum by a factor of 5-10 and reverses the direction of the flow to create an efficient feeding current (Asadzadeh et al. 2022; Suzuki-Tellier et al. 2022). Choanoflagellates have their single beating flagellum equipped with a vane that allows it to efficiently pump water through their fine collar filter (Nielsen et al. 2017; Pinskey et al. 2022) and dinoflagellates are equipped with a transverse flagellum running in a groove around the cell circumference and embedded in a ‘sock’ (Berdach 1977) that allows a very powerful feeding current (Schuech et al in prep). These are all groups that are quantitatively very abundant in the water column.

A less appreciated (and phylogenetically less coherent) but locally significant assemblage of phagotrophic flagellates are the ‘typical excavates’. They occur in the water column, mainly attached to marine snow particles, but are often found in sediments as well (Flavin & Nerad 1993; Heiss et al. 2018; Lara et al. 2006; Pánek et al. 2015; Patterson 1990; Simpson & Patterson 1999), and they may dominate in some anoxic marine water masses (Heiss et al. 2018; Stock et al. 2009). They may forage on the elevated concentration of bacteria associated with marine snow and thus play a role in regulating the microbiota of these microbial ‘hot spots’.

Like the other phagotrophic flagellates mentioned above, the typical excavates also have a specialized flagellar apparatus. The best-known forms are biflagellated cells with a naked

anterior flagellum, and a posterior flagellum beating in a ventral groove and bearing 1-3 broad vanes of unclear function (Heiss et al. 2018; Simpson 2003) (Fig. 1a). Bacterial prey are collected and engulfed in the posterior end of the groove, but the prey concentration- and foraging mechanisms are essentially unknown.

In addition to their ecological role in the modern ocean, excavates are of great evolutionary interest because of the possibility that the Last Eukaryotic Common Ancestor (LECA) resembled living typical excavates (Derelle et al. 2015). This is a highly consequential hypothesis for understanding the evolutionary origins and history of modern complex cells. Understanding the mechanisms of swimming and foraging in the excavate flagellates may therefore help us infer how LECA cells used their flagella to feed and swim in the ancient past.

Here we examine the mechanisms and fluid dynamics of foraging in several species of typical excavates belonging to the three major groups: Discoba, Metamonada, and Malawimonadida. We use high-speed video-microscopy to describe the beating of the flagella and capture of prey, particle tracking to visualize the feeding current and estimate clearance rates, and computational fluid dynamics to understand the functional significance of the characteristic morphological features of excavate cells.

7.2 Materials and methods

7.2.1 Culturing

The studied flagellates were laboratory cultures maintained in the Simpson Lab, Dalhousie University (*Carpediemonas membranifera* isolate BICM), or kindly provided by Franz Lang, Université de Montréal (*Reclinomonas americana* isolate ATCC50394, *Jakoba libera* isolate ATCC50422, '*Malawimonas californiensis*' isolate ATCC50740) or Julie Boisard and Courtney Stairs, University of Lund (*Kipferlia bialata* isolate WC1A). Cultures were maintained in the dark at 18°C in highly diluted Miller's LB broth media to feed the naturally occurring bacteria that served as prey. The aerobic freshwater species, *R. americana*, grew with 0.3% LB in Milli-Q® water; the aerobic marine species *J. libera* and *M. californiensis* grew with 0.3% LB in filtered and pasteurized North Sea water (salinity 30‰); and the anaerobic marine species *C. membranifera* and *K. bialata* grew in 3% LB in the sterilized North Sea water, under near-anoxia established by the prokaryotic growth on this richer medium.

7.2.2 Microscope imaging

Phase contrast imaging was performed with an Olympus IX71 inverted microscope equipped with an Olympus UPLanFL N oil immersion x100 / 1.30 objective and an attached high-speed Phantom Camera (Miro LAB 320). Videos had a minimum resolution of 512 x 512 pixels and

were recorded at 300 or 500 frames per second (fps). The effects of light heating were mitigated with short exposure intervals (< 10 minutes) at moderate intensities during recordings. Videos and images were later analyzed using the open-source software ImageJ (Fiji).

Aerobic flagellate species were observed by mounting 100 µL of culture between two glass coverslips (24 x 24 mm) that were spaced by small blobs of Vaseline® in each corner. The observation chamber for anaerobic species consisted of a plastic ring (16 mm inner diameter and 1.5 mm height) fixed with Vaseline® to a coverslip and filled with 300 µL of culture, then sealed on top with a second coverslip, held by surface tension. The latter ring chamber set-up was also used for all species when visualizing their flow fields with tracer particles (see 7.2.4 below)

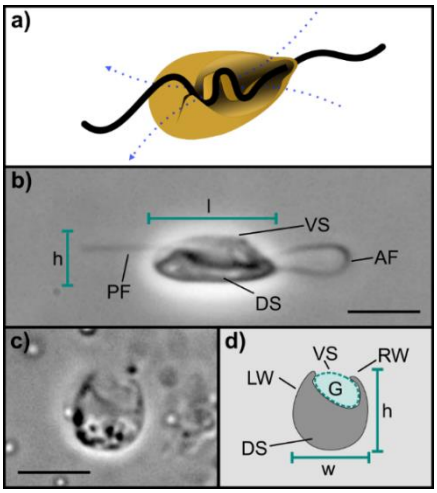

Figure 1. 'Typical excavate' flagellate and morphometric parameters: a) 'typical excavate' flagellate with an anterior flagellum, and a posterior flagellum with a vane that runs in the ventral groove (dashed blue arrows indicate the feeding flow lines); b) Live image of the left longitudinal side of the cell (*Jakoba libera*); c) Live image of the ventral groove transection at mid cell body length (*J. libera*, edited image: horizontal flip); d) schematic drawing of image b. Abbreviations: h = cell height, l = cell length, w = cell width, PF = posterior flagellum, AF = anterior flagellum, VS = ventral side, DS = dorsal side, RW = right-side cell wall, LW = left-side cell wall, and G = groove area (marked with dashed line). Scale = 5 µm.

7.2.3 Flow fields

The ring chamber was filled with a dilute suspension of flagellates, and a single cell was focused on under the microscope. Then, 0.5-µm tracer particles were gently added to the chamber sealed with a coverslip. Videos of each of the four species *(J. libera, R. americana, K. bialata*, and *C. membranifera*) were selected for analyses and particles were tracked at a frequency of 50 or 60 Hz using the Manual Tracking function in ImageJ.

7.2.4 Clearance rates

Clearance rates were estimated on the assumption that particles transported into the ventral groove of an excavate can be considered captured, and hence the clearance rate can be estimated

as the volume flow rate in the groove. We estimate flow velocities in the groove by noting the time and position of particles as they entered the groove and either left the groove or stopped at the rear end of the groove. Here, most particles were eventually discarded, likely because the flagellate could not phagocytize further particles (there is often a full food vacuole). The clearance rate was then estimated as the flow velocity multiplied by the cross-sectional area of the groove.

7.2.5 Computational fluid dynamics

Computational fluid dynamics (CFD) modelling allows one to quantify the flow field generated by a beating flagellum, given known morphology, beat patterns, and beat kinematics, by numerically solving the flow governing Navier-Stokes equations. We developed a CFD model of a simplified generic excavate flagellate (supplementary Fig. S1) with basic morphology parameters (Table 1) and kinematics inspired by *Jakoba libera* (Table 2); that is, a cell with a posterior flagellum beating inside and parallel to the bottom of the ventral groove and equipped with an inward-oriented vane. This basic case could then be modified to have other vane arrangements (outward-oriented, broader vane, two vanes), beat orientation (perpendicular to the bottom of the groove), a higher wall on the right than on the left side of the groove, attachment to a surface positioned on the dorsal or ventral side of the cell, an anterior flagellum beating in a 3-dimensional pattern, and/or a posterior flagellum that is also active outside the ventral groove, as found in the different species described below. We varied one parameter at a time to examine the functional significance of the different morphological features found in excavates and in the different species. Finally, to examine the effect of having the posterior flagellum constrained in a groove, we ran a case without any groove, with the flagellum instead beating above the surface of the cell. As diagnostic output characteristics, we computed flow fields, power consumption, and magnitudes of the clearance rate.

The Navier-Stokes equations were discretized using a finite volume method and solved on a discrete representation of the computational domain composed of polyhedral cells (see supplementary Fig. S2). We utilized the commercial CFD software STAR-CCM+ (version 18.02.008-R8) for the numerical simulations. We used mesh morphing along with the overset method to move the computational mesh for flagellar motion. The morphing method deforms the computational mesh around the flagella in response to their prescribed motion. With the overset method, rather than moving the entire computational mesh, it deforms the mesh only around the flagella, so-called the overset region. A stationary background mesh is overlapped with the deforming mesh, and field data is interpolated between them for a smooth solution (see online supplementary material for a full technical description).

Table 1. Cell body and ventral groove morphometrics of *Jakoba libera, Reclinomonas americana, Kipferlia bialata, Carpediemonas membranifera,* and *Malawimonas californiensis.*

			J. libera	*R. americana*	*K. bialata*	*C. membranifera*	*M. californiensis*
Cell body	**Length (µm)**	**Mean ± SD**	7.8 ± 0.6	7.8 ± 0.7	9.3 ± 0.6	7.2 ± 0.7	5.4 ± 0.4
		n	7	6	5	7	6
	Height (µm)	**Mean ± SD**	3.7 ± 1.0	3.5 ± 0.2	5.4 ± 0.5	4.4 ± 0.7	3.1 ± 0.5
		n	6	2	3	5	3
	Width (µm)	**Mean ± SD**	4.4 ± 0.7	5.5 ± 0.9	5.2 ± 0.0	-	3.1 ± 0.5
		n	3	5	1	-	3
	Depth (μm^2)	**Mean ± SD**	3.3 ± 0.0	4.2 ± 0.5	2.9 ± 0.9	2.0 ± 0.0	2.0 ± 0.0
		n	1	3	4	2	1
	Volume (μm^3)		24	58	102	28	-
Ventral Groove	**Length (µm)**	**Mean ± SD**	6.3 ± 0.0	5.3 ± 0.0	-	5.3 ± 0.0	-
		n	1	1	-	1	-
	Width (µm)	**Mean ± SD**	2.9 ± 0.3	3.7 ± 0.5	3.3 ± 0.0	2.9 ± 0.4	2.3 ± 0.1
		n	3	3	1	6	2
	Depth (µm)	**Mean ± SD**	2.1 ± 0.0	2.8 ± 0.5	1.8 ± 0.0	2.7 ± 0.2	1.4 ± 0.0
		n	1	3	2	2	1
	Area (μm^2)	**Mean ± SD**	5.0 ± 0.0	9.6 ± 1.7	5.6 ± 1.1	3.8 ± 0.0	2.3 ± 0.0
		n	1	3	2	2	1

7.3 Results

7.3.1 Feeding behavior and free-swimming

Prey capture and handling follow a general pattern shared among all the species examined. The ventral groove extends for most of the length of the cell, with its right wall generally being taller and more continuous. A feeding current is generated by the flagella, always involving the posterior vane-bearing flagellum beating with high-amplitude waves. The behavior of the anterior flagellum differs among species; see below. The vane(s) on the posterior flagellum project rigidly more-or-less perpendicularly to the primary plane of beating and show only a small degree of bending at the base or torsion about the axoneme.

The flow drives the prey into the ventral groove, entering roughly in the middle, and draws it towards the posterior end of the cell. Food particles are captured in the groove and handled near the phagocytosis site at the posterior end of the groove. If the prey is rejected, it will exit the groove. The posterior flagellum sometimes actively retains the particle by pushing it against the right wall of the groove when it stops beating. Meanwhile, a moving 'wave' of the cell membrane is observed – often as a transversal slender dark shadow - sweeping posteriorly along the groove and disappearing when the wave reaches the phagocytosis site in the posterior end of the groove (Animations 2 & 3). When the wave reaches the end of the groove, the particle is ingested with the membrane observed to affect the closure of the phagocytic vacuole (observed in *K. bialata* and *R. americana*).

The predation behavior of each species varies over this general pattern, with characteristic differences in flagellar arrangements and beat frequencies (Table 2):

When feeding, *Jakoba libera* attaches to a surface with a bent anterior flagellum and with the cell body approximately parallel to the surface (Fig. 2a). Often, the anterior flagellum will flex repeatedly and push the body backward and forwards or change its orientation (Video 1 & Animation 1). The feeding current is generated by the posterior flagellum that beats in a plane inside the groove. The beating wave propagates towards the posterior end of the groove, where the flagellum is loosely constricted by the cell body. The posterior flagellum extends a third of a body length outside of the cell and this portion is straight and rigid. When swimming, the anterior flagellum is mainly responsible for propulsion as it beats in a three-dimensional power-and-return stroke while the posterior flagellum remains beating inside the groove (Video 2).

At its feeding stage, *Reclinomonas americana* sits with the cell body inside a lorica that is permanently attached to the substrate, with the ventral groove facing up (Video 3 & Animation 2) (fig. 2b). It has a very tall and pronounced right wall, or 'sail'. The anterior flagellum, which is a little more than a body length long, is highly active and beats outside of the lorica in a three-dimensional pattern. It bends over the ventral groove and the distal end points posteriorly. The motion of the proximal portion of this flagellum is partially restricted by the lorica due to the

reclined position of the cell – hence the name of this species. The posterior flagellum remains inside the groove, beating in a plane parallel to the floor and between the two walls. A very short, straight portion of the posterior flagellum extends beyond the posterior end of the groove and moves rigidly while being loosely tethered to the cell.

Table 2. Beat frequencies of flagella in feeding (attached) and free-swimming flagellates and swimming speeds of *Jakoba libera*, *Reclinomonas americana*, *Kipferlia bialata*, *Carpediemonas membranifera*, and *Malawimonas californiensis*.

	Feeding Beat Frequency (Hz)				**Free-swimming Beat Frequency (Hz)**				**Free-swimming**	
	Posterior Flagellum		**Anterior Flagellum**		**Posterior Flagellum**		**Anterior Flagellum**		**Speed (μm s^{-1})**	
	Mean ± SD	**n**	**Mean ± SD**	**n**	**Mean ± SD**	**n**	**Mean ± SD**	**n**	**Mean ± SD**	**n**
J. libera	37 ± 3	6	-	-	32 ± 0.5	2	17 ± 2	2	15 ± 3	2
R. americana	49 ± 4	5	48 ± 4	5	60 ± 5	10	44 ± 3	11	105 ± 12	8
K. bialata	26 ± 3	4	6 ± 2	5	24 ± 19	2	10 ± 2	2	12 ± 5	2
C.membranifera	27 ± 2	5	6 ± 0	5	31 ± 4	2	7 ± 1	2	27 ± 13	2
M.californiensis	42 ± 6	5	7 ± 1	5	-	-	-	-	-	-

After cell division, one daughter cell remains in the parental lorica, while the other is free-swimming (Flavin & Nerad 1993; O'kelly 1997). This swarmer is slender and highly mobile (Table 1 and 2) (Video 4). The anterior flagellum of the aloricate swimmer performs broader power-and-return strokes in front of the cell with the distal tip always pointing posteriorly. The posterior flagellum is longer (approximately 2 body lengths) and trails freely, beating along the groove.

Kipferlia bialata attaches to a surface with the posterior end of the cell body, normally with the groove facing away from the surface and generating a feeding current with the two beating flagella (Video 5 & Animation 3) (fig. 2c). The anterior flagellum is about a body length long and performs three-dimensional power-and-return strokes. The motion of the posterior flagellum is three-dimensional, and the beating waves propagate to the distal tip spanning from outside to the floor of the ventral groove. When free-swimming, the flagellar kinematics are the same as

when attached. The anterior flagellum is responsible for the displacement and causes the cell body to rotate on its longitudinal axis. Meanwhile, the posterior flagellum beats slowly and with long pauses, possibly with a role in the steering (Video 6).

Carpediemonas membranifera and *Malawimonas californiensis* have similar predation behavior and flagellar kinematics (Video 7 and 8 & Animation 4 of *C. membranifera*) (fig. 2d and 2e). For feeding, the cell temporarily attaches to surfaces with a quarter of the distal end of the posterior flagellum, and the cell hovers or skids around while generating a feeding current with both flagella. The anterior flagellum is a body length long and executes the same power-and-return strokes as *K. bialata*. The posterior flagellum is three body lengths long and beats in a plane that slightly emerges outside of the groove. The flagellum often beats only the portion inside the groove. Thus, the posterior flagellum does not follow a central longitudinal axis of the body. *C. membranifera* does not fully rely on feeding currents to capture prey. The flagellate was recorded 'scooping' inside the groove a particle that was attached to the surface with the movement of the cell body (Video 9). Swimming cells use the posterior flagellum for propulsion (Video 10 of *C. membranifera*). The overall contribution of the anterior flagellum to motility is minor and possibly more dedicated steering.

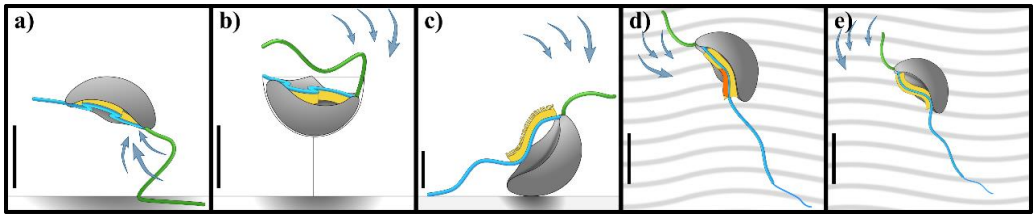

Figure 2. Schematic representations of the Excavata species: a) *Jakoba libera*, b) *Reclinomonas americana*, c) *Kipferlia bialata*, d) *Carpediemonas membranifera*, and e) *Malawimonas californiensis*. While foraging, *J. libera*, *R. americana*, and *K. bialata* are attached to the surface (bottom line); instead, *C. membranifera* and *M. californiensis* glide on the substrate (wavy background). Each species panel includes cell body (gray), anterior flagellum (blue), posterior flagellum (green), feeding current direction (arrows), and flagellar vane number and position (yellow). Note that *C. membranifera* has a third vane (orange) and the dimensions are not scaled. Reference scale bar = 5 µm.

7.3.2 The ventral groove and the flagellar vane

The portion of the posterior flagellum inside the groove is equipped with vanes. Each vane is supported by an intraflagellar paraxonemal lamella, making much of the flagellum itself paddle-shaped. These thin extensions of the flagellum double, at least, its surface area and are somewhat flexible. We observed the number of vanes, their orientation, and their spatial-temporal distribution at the mid-cross-section of the groove (Animation 5) (fig. 3). Three functional types

were observed: 1) single inward vane, moving parallel to the groove floor, 2) single outward vane, moving in a 3D motion, and 3) double vanes.

Single inward vane (Jakoba libera and Reclinomonas americana)

The posterior flagellum of *J. libera* and *R. americana* remains inside the groove throughout the beat cycle and is equipped with a single vane that extends inwards, towards the floor of the ventral cavity. It beats in an oblique plane between the two walls: from the top of the left-side wall towards the bottom of the right-side wall (Animation 5a & Video 11 and 12) (fig. 3a). The taller right wall curves over the groove; and because of the different wall heights, the floor of the groove follows a depression on the right side of the cell. Thus, the flagellar beating plane is parallel to the floor and the vane is observed sweeping across it, in proximity or in direct contact.

Single outward vane (Kipferlia bialata)

The flagellum has a single vane that extends outwards with a slight tilt to the left side and has a terminal row of tape-like hairs (Yubuki et al. 2013). The beating pattern is three-dimensional, spanning from the bottom to the outside of the groove (Animation 5b & Video 13) (fig. 3b). The initial left-side tilt of the vane becomes almost parallel to the groove floor when it collides with the base of the left wall, and it subsequently points outwards when it emerges outside of the groove again, at the end of the beat cycle.

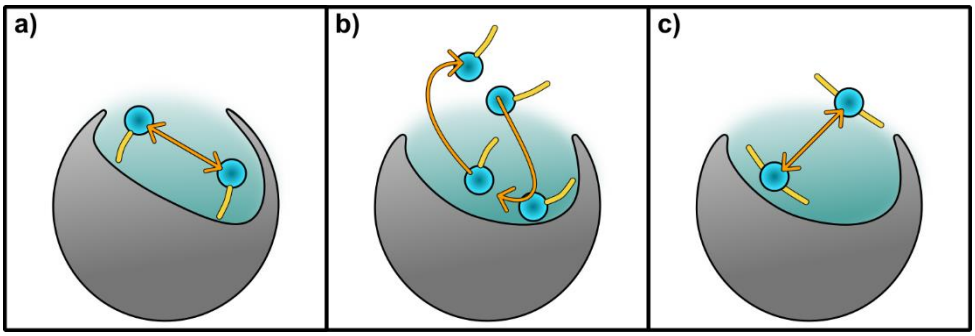

Figure 3. Posterior flagellum kinematics inside the ventral groove. Schematic representations of mid-transversal cross-section views of the ventral groove (teal shadow) and the position of the flagellum (blue circle) equipped with a vane/s (yellow) between the maximum beat wave amplitudes (arrows). The right-side wall of the cell is on the right side of the viewer. The three cross sections correspond to the observations of a) *Jakoba libera* and *Reclinomonas americana*; b) *Kipferlia bialata*; c) *Carpediemonas membranifera* and *Malawimonas californiensis*.

Double vanes (Carpediemonas membranifera and Malawimonas californiensis)

The posterior flagellum of *C. membranifera* and *M. californiensis* has two opposite vanes that are perpendicular to the beating plane. The outwards vane has a slight tilt to the left while, symmetrically, the inwards vane points to the right. The beat wave oscillates from just outside of the groove to the bottom-left corner of the cavity, executing an oblique trajectory between the walls (Animation 5c & Video 14 and 15) (fig. 3c). A third, much shorter vane, orthogonal to the two main vanes, has been reported for *C. membranifera* (Simpson & Patterson 1999).

7.3.3 Feeding current and clearance estimates

Example particle tracks for 4 species (Fig. 4) represent two-dimensional projections of three-dimensional flows and depend also on what angle the cell was observed. Thus, the particle tracks can be used only to qualitatively describe the feeding current. The feeding current flows are similar among all species, with an accelerating flow arriving at the mid-to-anterior end of the ventral groove and leaving again from the mid-to-posterior end of the groove. Far from the ventral groove, particle motion is dominated by Brownian diffusion, and the feeding current only dominates particle motion within 10-30 µm of the cell.

Flow velocities in the ventral groove varied between species by a factor of ca. 3, apparently unrelated to the beat frequency of the posterior flagellum (Table 2). The resulting estimates of cell-volume-specific clearance rates vary by an order of magnitude, between 0.2-3 x 10^6 per day (Table 3).

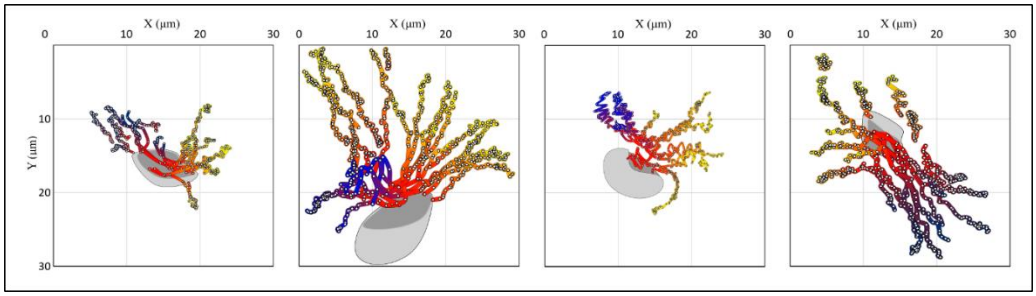

Figure 4. Example particle tracks for 4 species: a) *Jakoba libera*, b) *Reclinomonas americana*, c) *Kipferlia bialata*, and d) *Carpediemonas membranifera*. Tracer particles are positioned (dots) at a frequency of 60 Hz (Except *R. americana*: 50 Hz), and the distance between positions thus indicates flow speed. Far from the flagellate particle tracks are dominated by Brownian motion. The color indicates the direction of the flow, from yellow through red to blue.

Table 3. Estimated clearance rates. The specific clearance rate is the clearance rate normalized by cell volume.

Species	Tracer particle velocity inside the groove ($\mu m\ ms^{-1}$)	Clearance rate ($\mu m^3 s^{-1}$)	Specific clearance (d^{-1})
Jakoba libera	0.18 ± 0.05	918	3.3×10^6
Reclimonas americana	0.12 ± 0.03	1152	1.7×10^6
Kipferlia bialata	0.05 ± 0.03	280	0.24×10^6
Carpediemonas membranifera	0.13 ± 0.05	413	1.3×10^6

7.3.4 Computational fluid dynamics (CFD)

The main outcomes of the CFD modeling are first that the magnitude of the clearance rate depends mainly on the beating of the posterior flagellum inside/over the ventral groove and on the dimensions of the vane, and that all other morphological features have only limited effect (Fig. 5). The model flagellates have clearance rates of 250 - 450 $\mu m^3 s^{-1}$, of similar order to that estimated experimentally for the examined species (Fig. 5). Whether the posterior flagellum beats parallel or perpendicular to the bottom of the groove has limited effect, so both orientations observed are equally well suited for feeding. Broader vanes lead to higher power consumption, but also to higher clearance rates.

Second, the presence of the anterior flagellum and the 'free' part of the posterior flagellum extending outside the groove improves the architecture of the feeding current by extending the region around the cell within which the advective feeding current is strong enough to overcome the diffusive Brownian motion of passive prey particles. This is illustrated by longer streamlines that are plotted only where the Peclet number (Pe) exceeds 1 (Fig. 5; The Peclet number indicates the relative significance of advection over diffusion, $Pe = au/D$, where a is prey radius (0.5 µm), D is Brownian diffusion computed from Einstein relation, and u is the feeding current velocity). This enhancement of the feeding current is also obvious in our observations (Fig. 4) and is particularly significant for flagellates attached to a surface (Fig. 5). The improvement, however, happens at the cost of higher power consumption.

Finally, the containment of the vaned flagellum in the ventral groove improves the magnitude of clearance rate. A vaned flagellum beating outside a groove creates a feeding current characterized by intense sideways oscillations that cancel out during a complete beat cycle, resulting in a lower (averaged) clearance rate. Conversely, the presence of a groove generates a smoother and more directional flow, leading to a higher clearance rate (Fig. 6). The advantage of beating inside a grove vanishes for a naked flagellum without a vane (Fig. 6c).

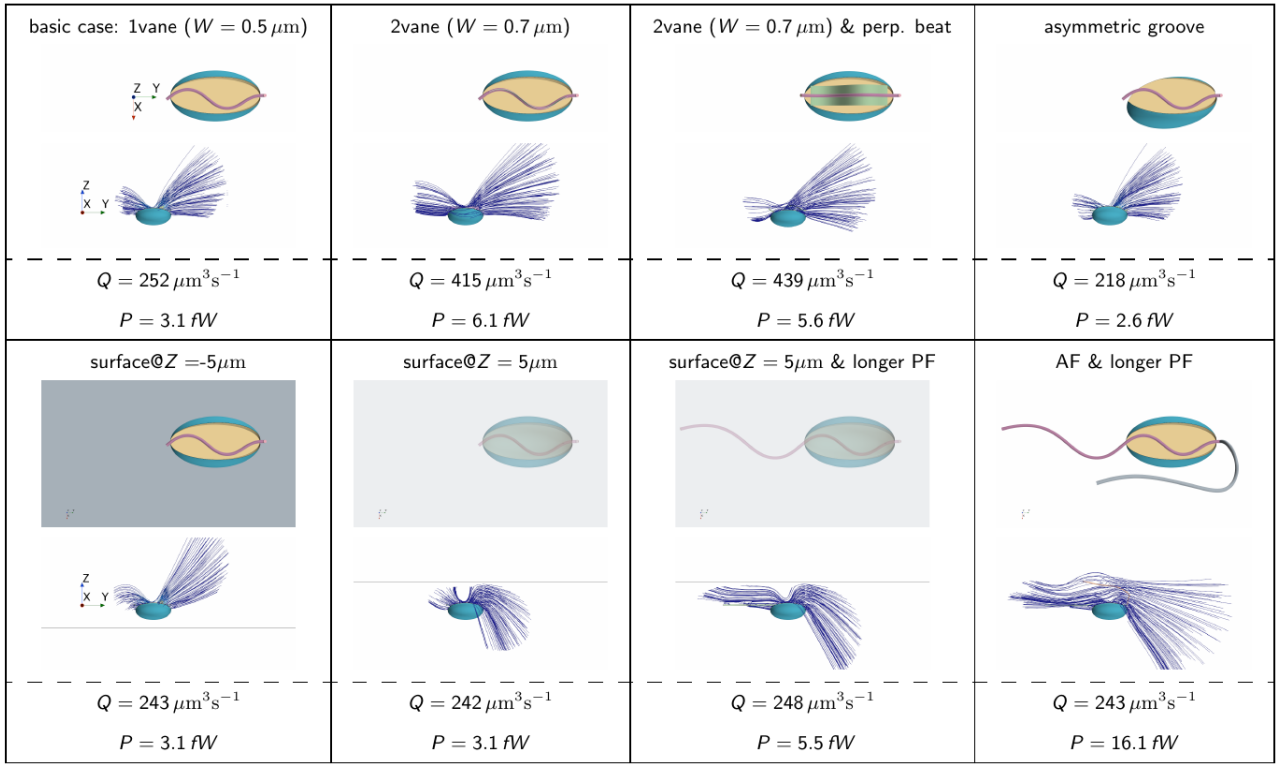

Figure 5. CFD cases demonstrating the influence of various morphological aspects and surface proximity. In each panel, the case is first described (number of vanes, width of vane, asymmetry of groove, the presence of a surface dorsally (-5 µm) or ventrally (+5 µm) to the cell, and the presence of an active anterior and extended posterior flagellum. The anterior end of the cell is to the right. Streamlines represent the averaged flow field, with sections omitted where the flow velocity is below 2 µm s^{-1} (corresponding to a Peclet number of ~1 for 0.5 µm passive prey particles). This threshold indicates where the advective feeding current overcomes the diffusive Brownian motion of passive prey particles. *Q* is the estimated clearance rate and P is the estimated power consumption.

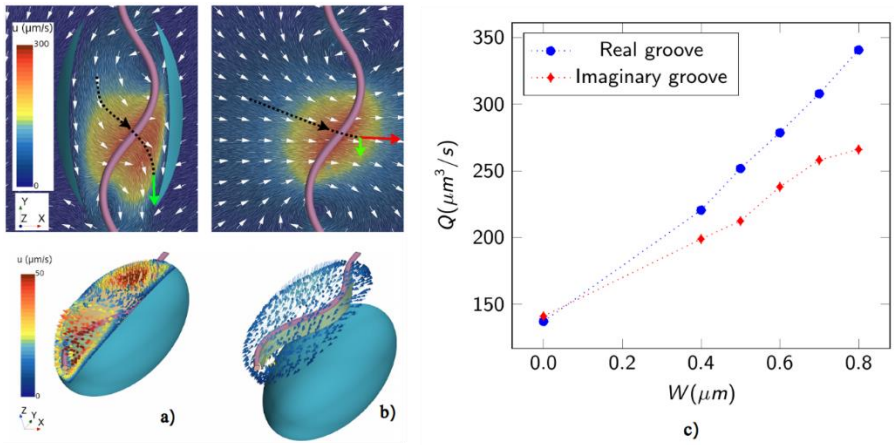

Figure 6. Effect of confinement on the feeding current generated by a (vaned) flagellum. A snapshot of the flow during the flagellum beating cycle (a, top), shows that the vaned flagellum pushes the flow against the wall of the groove, directing the flow posteriorly (green arrow). This interaction, during the complete beat cycle, results in a relatively strong averaged flow through the groove (a, bottom). In the absence of the groove (b, top), the vaned flagellum pushes the flow in free space where only a small component of such flow is directed downwards (green arrow), while most of the flow is directed sideways (red arrow). The oscillating sideways flows cancel out during the beat cycle, resulting in a weak average flow through an imaginary groove (b, bottom). The clearance rate increases with the width of the vane, but most so for a flagellum within a groove (c).

7.4 Discussion

We have here described the suspension feeding and swimming behavior of several species of typical excavates drawn from across the three main phylogenetic groups. While phylogenetically diverse, they are all characterized by a vaned flagellum beating in a ventral groove. Obviously, this flagellar arrangement is primarily an adaptation to feeding, not swimming. In fact, like many other phagotrophic flagellates, excavates seem to be mainly attached to a surface when feeding, and free-swimming excavate cells appear to be slow and inefficient swimmers (Table 2). One exception among our study species is the swarmer stage of *R. americana* which adopts a different morphology and flagellar beat pattern than the attached foraging stage, and it lacks the flagellar vane (O'Kelly 1997). Also, the swimming form of *Jakoba incarcerata* usually lack a ventral groove and have a longer anterior flagellum (Simpson & Patterson 2001). This contrasts with the less effective swimming behavior of the 'normal grooved' cells of *Jakoba libera* described here.

The clearance rates estimated here are of a similar order of magnitude as experimental estimates reported for *J. libera* by (Eccleston-Parry & Leadbeater 1994; Mohapatra & Fukami 2005), ~250-800 $\mu m^3\ s^{-1}$ (Table 3 and Fig. 5 for our experimental and computational estimates). These

estimates, in turn, are within the typical range for phagotrophic flagellates of similar sizes (Edwards et al. 2023b).

Key to the functioning of the flagellum in clearing prey from ambient water is the interaction between the groove and the vaned flagellum. A vaned flagellum beating in a depression on the cell surface may be particularly efficient in generating a feeding current. First, having the force near the cell brings the feeding current streamlines near the cell surface (Figs 4 and 5) where prey is captured, thus increasing prey encounter and retention rates. Second, adding a vane to a beating flagellum is an energy-efficient way of increasing the clearance rate, compared to increasing the beat frequency. The power consumption of a beating flagellum constrained in a groove increases linearly with its width, as does the resulting clearance rate, and the relation between power consumption and clearance rate is, therefore, near-linear (Fig. 7). In contrast, in the viscous environment in which flagellates operate the clearance rate scales with the beat frequency while the power consumption with the beat frequency squared, the clearance rate increases only with the square root of the power consumption (Fig.7), rendering this a much less energy-efficient way of increasing the clearance rate. One may question the significance of the energy efficiency argument because the operational cost of flagella typically constitutes only a tiny fraction of the total metabolism of rapidly growing cells (Schavemaker & Lynch 2022). However, flagellates may increase their activity but reduce their metabolism by orders of magnitude when resources are scarce (Fenchel 1989) a state in which they may be much of the time in nature – and in this situation, energy efficiency may become important.

Broadened (vaned) constrained flagella are widespread among phagotrophic flagellates. Choanoflagellates have a vaned flagellum beating inside a collar filter, and the equatorial flagellum of dinoflagellates drives a diaphragm-like ‘sock’ in the circumferential depression on the cell surface (cingulum), arrangements that both allow efficient feeding currents (Kiørboe 2024). These are not homologous structures, however. For example, the vanes in excavates are each supported by intraflagellar paraxonemal lamella, while the fibrillar vanes of choanoflagellates extend out of the flagellar membrane, and the cingulum-contained flagellum in dinoflagellates is equivalent to the anterior flagellum of excavates, rather than their posterior flagellum.

There are other poorly studied phagotrophic flagellates from other branches of the eukaryotic tree of life with a flagellar arrangement similar and potentially homologous to that found in the typical excavates, namely a posterior flagellum with a vane supported by an intraflagellar lamellum that beats in association with some form of a conspicuous ventral groove. The best examples are colponemids within the alveolates (Gigeroff et al. 2023; Janouškovec et al. 2013) and the Nebulidia within the newest proposed supergroup – Provora (Janouškovec et al. 2017; Tikhonenkov et al. 2022). The foraging mechanisms in these species are yet to be explored in detail, but the similarity of structures may suggest similar fluid dynamic behavior, albeit both

colponemids and nebulids are eukaryovores and ingest their prey at the anterior end of the cell, not the posterior (Gigeroff et al. 2023).

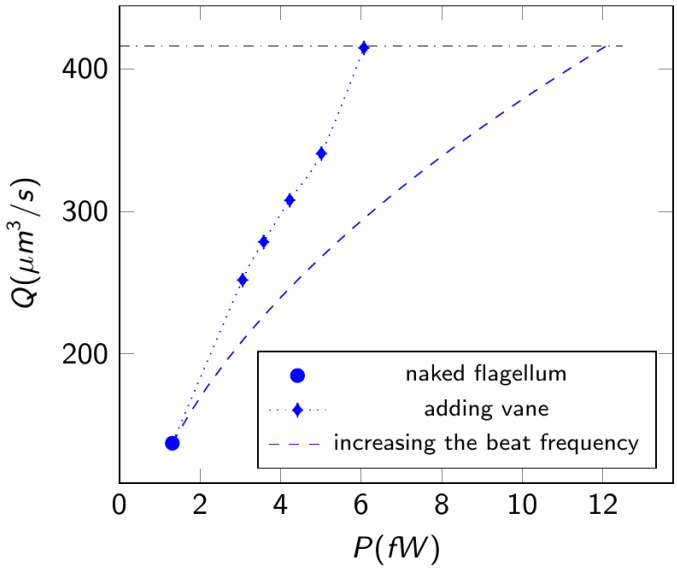

Figure 7. Clearance rate (Q) vs power consumption (P). Comparing clearance rates when adding vanes versus increasing the beat frequency. The data points represent simulation results for vane widths of 0.4µm, 0.5µm, 0.7µm, 0.8µm (1-vane configuration), and the last point 0.7µm (2-vane configuration). The dashed line illustrates the effect of increasing the beat frequency given by $Q = Q_{naked} * \sqrt{P/P_{naked}}$.

The anterior flagellum and the 'free' part of the posterior flagellum apparently do not directly contribute to driving water through the groove. However, they may mix the ambient water and increase the spatial extension where the feeding current is effective, thus constantly providing fresh, prey-containing water to the immediate vicinity of the cell. This effect shares similarities with the mechanism observed in the pumping of choanocyte chambers in sponges (Asadzadeh et al. 2020). Such mixing may be relevant for cells attached to a surface where the viscous boundary layer may rapidly be depleted of prey. Typical excavates attached to a marine snow particle may not only be feeding on the elevated concentration of bacteria swarming around a particle (Stocker & Seymour 2012) but may also be feeding on the high density of bacteria typically attached to the particle surface, as observed above for *C. membranifera* (Kiørboe et al. 2004). Here again, the interaction between the posterior flagellum and the groove appears important.

7.4.1 Phylogenetic implications of functional morphology

In this study, we examined species from all three principal clades of 'excavates' – Discoba, Metamonada, and Malawimonadida. The foraging mechanisms appear fundamentally similar across the examined species, in terms of posterior flagellum activity, feeding current magnitude, and engulfment behavior. Arguably the greatest differences, between *Kipferlia* and the other subjects, divide species within principal clades rather than between them, since *Kipferlia* and *Carpediemonas* are both metamonads. This functional similarity is broadly consonant with the hypothesis that the 'typical excavate' cell architecture is ultimately homologous across Discoba, Metamonada, and Malawimonadida (Heiss et al. 2018; O'Kelly 1993; Simpson 2003). The relationships among excavates are not well resolved, however, most recent phylogenomic analyses show the three main clades representing at least two very distantly related lineages (Heiss et al. 2018; Tikhonenkov et al. 2022). Reconciling the excavate homology hypothesis with these molecular phylogenetic results is possible if it is supposed that the Last Eukaryote Common Ancestor (LECA) was a 'typical excavate' in its morphology. Indeed, some form of excavate ancestry for all living eukaryotes has been advocated after some 'rooted' phylogenomic analyses of eukaryotes (Al Jewari & Baldauf 2023; Derelle et al. 2015). It is credible speculation, at least, that the typical excavate foraging system studied here may have been used by our distant ancestors more than 1 billion years ago (Porter 2020). This suggests an ancient history of bacterivory via relatively elaborate suspension feeding (rather than feeding solely by creeping on surfaces, for example), and permits reasonable estimates of the effectiveness of that feeding within ancient microbial ecosystems. Given these biological and earth ecosystem evolution stakes, more research into the details of typical excavate cell architecture, their extant diversity, and their phylogenetic relationships, is warranted.

Acknowledgments

We received funding from The Independent Research Fund Denmark (7014-00033B), the Carlsberg Foundation (CF17-0495), the Simons Foundation (931976), and the European Union's Horizon 2020 research and innovation program under Marie Skłodowska-Curie grant agreement no. 955910. The Centre for Ocean Life is supported by the Villum Foundation.

References

Al Jewari C, Baldauf SL. 2023. An excavate root for the eukaryote tree of life. Sci Adv. 9(17):

Asadzadeh SS, Walther JH, Andersen A, Kiørboe T, Asadzadeh SS. 2022. Hydrodynamic interactions are key in thrust-generation of hairy flagella. Phys Rev Fluids. 7(7):

Berdach JT. 1977. In situ preservation of the transverse flagellum of Peridinium cinctum (Dinophyceae) for scanning electron microscopy. J Phycol. 13(3):243–51

Derelle R, Torruella G, Klimeš V, Brinkmann H, Kim E, et al. 2015. Bacterial proteins pinpoint a single eukaryotic root. Proc Natl Acad Sci U S A. 112(7):E693–99

Eccleston-Parry JD, Leadbeater BSC. 1994. A comparison of the growth kinetics of six marine heterotrophic nanoflagellates fed with one bacterial species. Mar Ecol Prog Ser. 105(1):167–77

Edwards KF, Li Q, McBeain KA, Schvarcz CR, Steward GF. 2023a. Trophic strategies explain the ocean niches of small eukaryotic phytoplankton. Proceedings of the Royal Society B: Biological Sciences. 290(1991):

Edwards KF, Li Q, Steward GF. 2023b. Ingestion kinetics of mixotrophic and heterotrophic flagellates. Limnol Oceanogr

Flavin M, Nerad TA. 1993. Reclinomonas americana N. G., N. Sp., a New Freshwater Heterotrophic Flagellate. Journal of Eukaryotic Microbiology. 40(2):172–79

Gigeroff AS, Eglit Y, Simpson AGB. 2023. Characterisation and Cultivation of New Lineages of Colponemids, a Critical Assemblage for Inferring Alveolate Evolution. Protist. 125949

Heiss AA, Kolisko M, Ekelund F, Brown MW, Roger AJ, Simpson AGB. 2018. Combined morphological and phylogenomic re-examination of malawimonads, a critical taxon for inferring the evolutionary history of eukaryotes. R Soc Open Sci. 5(4):

Janouškovec J, Tikhonenkov D V., Burki F, Howe AT, Rohwer FL, et al. 2017. A New Lineage of Eukaryotes Illuminates Early Mitochondrial Genome Reduction. Current Biology. 27(23):3717-3724.e5

Janouškovec J, Tikhonenkov D V., Mikhailov K V., Simdyanov TG, Aleoshin V V., et al. 2013. Colponemids represent multiple ancient alveolate lineages. Current Biology. 23(24):2546–52

Kiørboe T. 2016. Fluid dynamic constraints on resource acquisition in small pelagic organisms. Eur Phys J Spec Top. 225(4):669–83

Kiørboe, T. (2023). Predation in a Microbial World: Mechanisms and Trade-Offs of Flagellate Foraging. Annual Review of Marine Science, 16(1), null. https://doi.org/10.1146/annurev-marine-020123-102001

Kiørboe T, Grossart HP, Ploug H, Tang K, Auer B. 2004. Particle-associated flagellates: Swimming patterns, colonization rates, and grazing on attached bacteria. Aquatic Microbial Ecology. 35(2):141–52

Kolisko M, Silberman JD, Cepicka I, Yubuki N, Takishita K, et al. 2010. A wide diversity of previously undetected free-living relatives of diplomonads isolated from marine/saline habitats. Environ Microbiol. 12(10):2700–2710

Lara E, Chatzinotas A, Simpson AGB. 2006. Andalucia (n. gen.) - The deepest branch within Jakobids (Jakobida; Excavata), based on morphological and molecular study of a new flagellate from soil. Journal of Eukaryotic Microbiology. 53(2):112–20

Mohapatra BR, Fukami K. 2005. Effect of different bacterial species on the growth kinetics of the heterotrophic nanoflagellate Jakoba libera. Basic Appl Ecol. 6(1):67–73

Nielsen LT, Asadzadeh SS, Dölger J, Walther JH, Kiørboe T, Andersen A. 2017. Hydrodynamics of microbial filter feeding. Proc Natl Acad Sci U S A. 114(35):

Nielsen LT, Kiørboe T. 2021. Foraging trade-offs, flagellar arrangements, and flow architecture of planktonic protists. Proceedings of the National Academy of Sciences. 118(3):e2009930118

O'Kelly CharlesJ. 1993. The Jakobid Flagellates: Structural Features of Jakoba, Reclinomonas and Histiona and Implications for the Early Diversification of Eukaryotes. Journal of Eukaryotic Microbiology. 40(5):627–36

O'kelly CJ. 1997. Ultrastructure of Trophozoites, Zoospores and Cysts of Reclinomonas americana Flavin & Nerad, 1993 {Protista incertae sedis: Histionidae}

Pánek T, Táborský P, Pachiadaki MG, Hroudová M, Vlček Č, et al. 2015. Combined culture-based and culture-independent approaches provide insights into diversity of jakobids, an extremely plesiomorphic eukaryotic lineage. Front Microbiol. 6(NOV):

Patterson DJ. 1990. Jakoba Libera (Ruinen, 1938), A Heterotrophic Flagellate From Deep Oceanic Sediments. Journal of the Marine Biological Association of the United Kingdom. 70(2):381–93

Pinskey JM, Lagisetty A, Gui L, Phan N, Reetz E, et al. 2022. Three-dimensional flagella structures from animals' closest unicellular relatives, the Choanoflagellates. Elife. 11:

Porter SM. 2020. Insights into eukaryogenesis from the fossil record. Interface Focus. 10(4):

Schavemaker PE, Lynch M. 2022. Flagellar energy costs across the tree of life. Elife. 11:

Simpson AGB. 2003. Cytoskeletal organization, phylogenetic affinities and systematics in the contentious taxon Excavata (Eukaryota)

Simpson AGB, Patterson DJ. 1999. The Ultrastructure of Carpediemonas membranifera (Eukaryota) with Reference to the "Excavate Hypothesis." Europ. J. Protistol. 35:353–70

Simpson AGB, Pattersonj DJ. 2001. On Core Jakobids and Excavate Taxa: The Ultrastructure of Jakoba incarcerata. J. Eukaryotic Microbiology. 48(4):480–92

Stock A, Jurgens K, Bunge J, Stoeck T. 2009. Protistan diversity in suboxic and anoxic waters of the Gotland Deep (Baltic Sea) as revealed by 18SrRNA clone libraries. Aquatic Microbial Ecology. 55(3):267–84

Stocker R, Seymour JR. 2012. Ecology and Physics of Bacterial Chemotaxis in the Ocean. Microbiology and Molecular Biology Reviews. 76(4):792–812

Suzuki-Tellier S, Andersen A, Kiørboe T. 2022. Mechanisms and fluid dynamics of foraging in heterotrophic nanoflagellates. Limnol Oceanogr. 67(6):1287–98

Tikhonenkov D V., Mikhailov K V., Gawryluk RMR, Belyaev AO, Mathur V, et al. 2022. Microbial predators form a new supergroup of eukaryotes. Nature. 612(7941):714–19

Yubuki N, Simpson AGB, Leander BS. 2013. Comprehensive Ultrastructure of Kipferlia bialata Provides Evidence for Character Evolution within the Fornicata (Excavata). Protist. 164(3):423–39

7.5 Appendix Paper II

7.5.1 Model morphology of symmetric and asymmetric groove

The versatile model morphology can accommodate both symmetric and asymmetric groove walls. In the symmetric case, the original spheroid has a major axis orientation of [0.00, 1.0, 0.00]. This configuration represents a groove where both sides of the groove walls are identical in shape and dimensions. However, in the asymmetric case, the major axis is oriented differently, such as [0.15, 1.0, 0.00], resulting in an uneven or asymmetrical groove as shown in Fig S1.

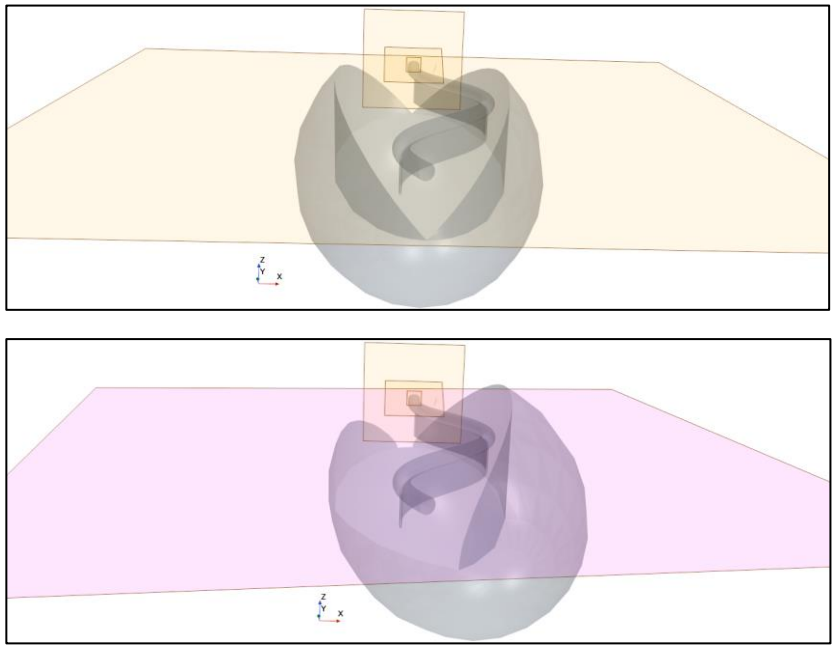

Figure S1. The modeling of symmetric and asymmetric groove walls. Top: The original spheroid with a major axis orientation of [0.00, 1.0, 0.00]. Bottom: The major axis is oriented in [0.15, 1.0, 0.00].

7.5.2 Computational fluid dynamics (CFD)

We utilized the commercial CFD program STAR-CCM+ (version 18.02.008-R8) to numerically solve the Navier-Stokes equation and the equation of continuity for incompressible Newtonian flow. The finite-volume approach was employed for the simulation. The flow conditions were characterized by both a small frequency parameter and a low Reynolds number, resulting in a quasi-steady Stokes flow regime. Our computational model adopted the morphology of the organism, and a spherical domain with a diameter of 200 µm was chosen which is ensured as large enough to not impact the results. The model cell was held stationary at the center of the domain. The no-slip boundary condition was applied to both the cell surfaces and the groove. The posterior and anterior flagella were modeled with a diameter of 0.25 µm, while the vane had a thickness of 20 nm. All these components were subjected to the no-slip boundary condition. The flagellar beat was modeled as a planar wave for the posterior flagellum, and a 3-dimensional wave for the anterior flagellum. The waveform model for both posterior and anterior flagella in a general form is as follows:

$$\phi(s,t) = A_{\phi}\left(1 - exp(-s/\delta)\right)sin\left(2\pi ft - 2\pi\, s/\lambda_{\phi}\right) + CL_{fl}\ ,$$

where $\varphi(s,t)$ represents the orientation angle of the flagellum tangent relative to the flagellar axis. The parameter s denotes the distance along the flagellum from its attachment point on the cell body, which is normalized by the length of the flagellum (L_{fl}). The variable t represents time. $A\varphi$ corresponds to the amplitude of the angle, $\lambda\varphi$ represents the wavelength, f indicates the beat frequency, and δ is an amplitude modulation factor that decreases the amplitude at the flagellum's attachment point to the cell body. The term C represents the turning angle of the flagellum, measured in radians (Geyer et al., 2016).

The beat pattern in the (x, y, z) domain presented here is derived from an expanded version of the planar waveform originally suggested by Geyer et al. (2016). This extended waveform incorporates a more comprehensive three-dimensional pattern for the anterior flagellum. As a result, the (X(s), Y(s), Z(s)) coordinates of the flagellum are generated as follows:

$X(s) = \int_0^s dx$, $(s) = \int_0^s dY$, and $Z(s) = \int_0^s dZ$

where

$dx = \left(1/\sqrt{1 + C_z^2}\right)cos(\phi)ds$, $dy = \left(1/\sqrt{1 + C_z^2}\right)sin(\phi)ds$, and $dz = \left(C_z/\sqrt{1 + C_z^2}\right)ds$

which ensures that $ds^2 = dx^2 + dy^2 + dz^2$.

In the case of a planar waveform of the posterior flagellum, the relevant parameters are

$A_\phi = 0.7, \delta = 0.1, \lambda_\phi = L_{fl}/3.2 + 2.0tan(\pi\, s/3\, L_{fl}), C_z = 0$;

And in the case of 3-dimensional waveform of the anterior flagellum,

$A_\phi = 1.25, \delta = 0.1, \lambda_\phi = 12.5, C_z = 5cos\left(\pi\left(s/L_{fl} + 0.3\right)\right).sin\left(0.5\pi\left(s/L_{fl}\right)\right)$.

We employ a combination of mesh morphing and the overset method to facilitate the movement of the computational mesh corresponding to the flagellar motion. The overset method deforms the mesh around the flagella, referred to as the overset region, rather than moving the entire mesh. This approach significantly reduces computational costs. Additionally, we generate a stationary background mesh that includes the cell, which overlaps with the deforming overset mesh. The two mesh regions are implicitly coupled, and field data are interpolated between them (i.e., the overset and background meshes) to generate a smooth solution at each iteration. By utilizing mesh morphing, we avoid the need to reconstruct the mesh geometry for different flagellum positions during the flagellar beat. The morphing motion redistributes mesh vertices in response to the flagellum's movement at each time step. As a result, the mesh undergoes morphing between two time steps, aligning with the flagellar motion. At each time step, the discretized forms of the governing equations are solved within the entire computational domain. To accommodate the complex geometry of the model organism, we employ polyhedral cells for the discretization (Fig.S2), as they offer flexibility and enable mesh morphing.

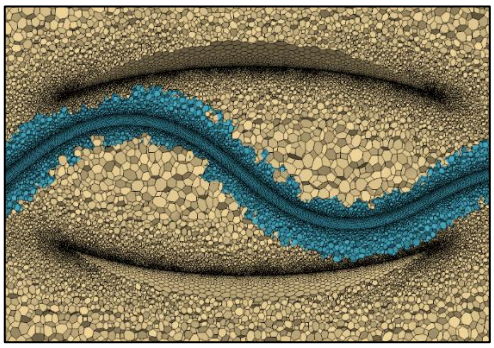

Figure S2. Visualization of the computational polyhedral cells in the beat plane. The computational domain consists of two separate regions, one including the (vaned) posterior and anterior flagella (overset mesh), and the other one stationary (background mesh) and includes the cell.

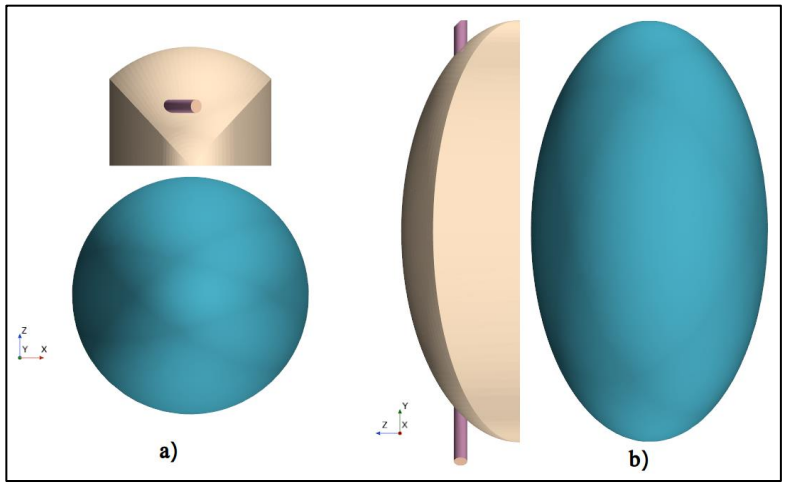

Figure S3. Two different views (a,b) depict the case with an imaginary groove (gold). The spheroid of the cell body (green) is displaced 2.3µm in the -Z direction, resulting in a groove-less spheroid cell. The shape of the imaginary groove mirrors the real groove in the base case before the displacement. The clearance rate into this imaginary groove is calculated for the 'imaginary groove' scenario.

Reference

Geyer, V. F., Sartori, P., Friedrich, B. M., Jülicher, F., & Howard, J. (2016). Independent Control of the Static and Dynamic Components of the Chlamydomonas Flagellar Beat. *Current Biology*, *26*(8), 1098–1103. https://doi.org/10.1016/j.cub.2016.02.053

CHAPTER 8

Paper III

New Insights in Flagellate Predation: the Significance and Function of the Feeding Groove of 'Typical Excavates'

Sei Suzuki-Tellier[1], Thomas Kiørboe[1], Alastair G.B. Simpson[2]

[1]Centre for Ocean Life, National Institute of Aquatic Resources, Technical University of Denmark, Kgs Lyngby, Denmark;

[2] Department of Biology, and Centre for Comparative Genomics and Evolutionary Bioinformatics, Dalhousie University, Halifax, NS, Canada.

This paper has not yet been submitted to any journal.

Abstract

Phagotrophic flagellates are the main consumers of bacteria and picophytoplankton. Despite their ecological significance in the ‘microbial loop’, many of their predation mechanisms remain unclear. ‘Typical excavates’ bear a ventral groove, where prey is captured for ingestion. The consequences of feeding through a ‘semi-rigid’ furrow on the prey-size range have not been explored. An unidentified moving element called "the wave" that sweeps across the groove toward the phagocytosis site has been observed in a few species; its function is unclear. We investigated the presence, behavior, and function of the wave in four species from the three Excavata clades (Discoba, Metamonada, and Malawimonadida) and found it present in all studied cases, suggesting the potential homology of this feature across the deep-branching supergroup. The wave displayed a species-specific behavior and was crucial for phagocytosis. The morphology of the feeding groove had an upper-prey-size limit for successful prey captures, but smaller particles were not constrained. Additionally, the ingestion efficiencies were species-dependent. By jointly studying these feeding traits, we speculate on adaptations to differences in food availability to better understand their ecological functions.

8.1 Introduction

Phagotrophic flagellates are the main consumers of bacteria and picophytoplankton in aquatic systems and thus play a key role by regulating the microbial communities and, hence, biogeochemical cycles (Azam et al., 1983; Fenchel, 1982; Jürgens & Matz, 2002; Worden et al., 2015). Most phagotrophic flagellates are well-adapted to the nutritionally dilute conditions and the physical constraints of their microscale environments, with the ability to daily clear volumes of water for prey corresponding to ~10^6 times their own volume (Edwards et al., 2023; Hansen et al., 1997; Kiørboe & Hirst, 2014). Following Boenigk and Arndt (2000a, 2002), modes of predation generally span from swimming interception-feeding (i.e. suspended prey encountered by a swimming consumer), attached filter- or interception-feeding (i.e. suspended prey harvested from a feeding current), to substrate-associated raptorial-feeding (i.e. a consumer moving on the substrate that actively searches for surface-bounded food particles). These foraging strategies can be carried out with different number of flagella and flagellar arrangements and kinematics and may involve complementary structures such as prey-capturing tentacles, a haptonema, or a ventral groove (Kiørboe, 2023). Consequently, differences in predation efficiency, prey size spectrum, and predation risk emerge. Thus, phagotrophic flagellates are functionally diverse. However, their assorted ecological roles in aquatic microbial systems remain mostly understudied and are often simplified to a single function in general aquatic assessments. Moreover, phagotrophic flagellates are not a consolidated taxonomical group. Instead, they spread across the Eukaryotic tree of Life and are present in all the major phylogenetic branches (Patterson & Larsen, 1991; Tikhonenkov et al., 2020).

The ‘excavates’ assemblage encompasses three monophyletic taxa, Discoba, Metamonada, and Malawimonadida, each of which includes free-living phagotrophic flagellates called ‘typical excavates’. Examples include *Jakoba, Reclinomonas,* and other jakobids (in Discoba), *Carpediemonas* and other ‘Carpediemonas-like organisms’ (CLOs) (in Metamonada), and *Malawimonas*. The phylogenetic relationships amongst the three excavate groups are unclear (see below), however, ‘typical excavates’ in each group share a ventral feeding groove that is supported by a specific, complex arrangement of the flagellar apparatus cytoskeleton and is associated with a posterior flagellum that is equipped with one or more vanes (Simpson, 2003) (Fig. 1a). Thus, the major feeding structures of these organisms are rather similar. The foraging behavior amongst groove-bearing excavates is also similar: the posterior flagellum beats within the boundaries of the groove (or into the groove) and generates a flow to capture prey, which is ingested at the posterior end (Suzuki-Tellier et al. in prep). Species-specific differences can be found, for instance, in the orientation and number of flagellar vanes (e.g. Heiss et al., 2018; Simpson & Patterson, 1999; Yubuki et al., 2013). Although predation by typical excavates is very briefly reported in some descriptive studies (e.g. Patterson, 1990) and recently examined in more detail (Suzuki-Tellier et al. in prep), some groove-feeding processes and their ecological implications have not yet been explored.

The confinement of the beating flagellum inside the ventral groove increases the force that generates the feeding current and results in a greater clearance rate, i.e., the volume of water screened for prey per unit time (Suzuki-Tellier et al. in prep). However, the increase in force might trade off with an unknown limit on prey size imposed by the semi-rigid structure of the feeding pocket. Some phagotrophic flagellates with different, more flexible feeding apparatuses, such as the stramenopile *Paraphysomonas* sp., can engulf eukaryotic cells of their own size, as well as small bacteria (Arndt et al., 2000). The width of the prey-size spectrum in typical excavate flagellates has not been determined; consequently, it is unclear whether the groove architecture imposes a sacrifice in the ability to capture and ingest large prey.

Live imaging of some typical excavate species shows the presence of a bulge in the bottom of the groove that moves periodically from the anterior to the posterior end. This phenomenon is known to several researchers and microscopists who study typical excavates, especially CLOs (AGBS, unpublished. obs.), but to our knowledge has been mentioned only in passing in the literature (e.g. Suzuki-Telllier et al. in prep). The nature and purpose of this structure remain unknown, and it is unclear whether this morphological trait is found in all major groups of excavates, in other words, is a potential homology.

Here, we study the foraging function of the ventral groove in four 'typical excavates' belonging to the three different major clades: the jakobid *Reclinomonas americana* (Discoba), the 'CLO' *Kipferlia bialata* (Metamonada), and the malawimonads *Malawimonas californiensis* and *Gefionella okellyi*. First, we investigate the presence or absence of the moving ventral groove bulge (hereafter 'wave') to document the phyletic distribution of this trait. Then, we analyze the behavior of the moving wave and its role during phagocytosis. Lastly, we examine the prey size range of the groove-bearing flagellates (except *Gefionella okellyi*).

8.2 Materials and methods

8.2.1 Culturing

The flagellate cultures were maintained at 18°C in the dark, feeding on bacteria that grew on Miller's LB broth media. The aerobic species *R. americana* isolate ATCC50394, *G. okellyi* isolate 249, and '*M. californiensis*' isolate ATCC50740 (kindly provided by Franz Lang, Université de Montréal) grew with 0.3% LB in Milli-Q® water, or in sterilized North Sea water (salinity 30‰) for '*M. californiensis*'. *Kipferlia bialata* isolate WC1A (kindly provided by Julie Boisard and Courtney Stairs, University of Lund) grew under near-anoxia conditions on 3% LB in the sterilized North Sea water.

8.2.2 Microscope imaging

Imaging was carried out using an inverted microscope Olympus IX71 with a phase contrast Olympus UPLanFL N oil immersion x100 / 1.30 objective. The microscope was equipped with a high-speed *Phantom Camera* (Miro LAB 320) and videos were recorded at 50 or 100 frames per second (fps) with 512 x 512 pixels of resolution. Recordings required short light exposure intervals (10–15 minutes) at moderate intensities, to mitigate the effects of heating and irradiation. Videos of the ventral groove activity and of prey captures were analyzed using the Phantom Camera Control software, and images for morphometric data were analyzed with ImageJ (Fiji) (Schneider et al., 2012).

The observation chamber consisted of a plastic ring (16 mm inner diameter and 3 mm height) fixed with Vaseline® on a coverslip (40x40 mm) that was filled with 600 µL of culture. For the anaerobic species, the ring was also sealed on top with a second coverslip by surface tension.

8.2.3 Observations of ventral groove wave

We recorded up to 11 sweeps of the ventral groove wave per individual in 6 – 18 individuals of each species. The sweep interval, i.e., the period between the start of consecutive sweeps was recorded, and the sweep speed was calculated.

8.2.4 Prey-size range experiments

Three species (*K. bialata*, *R. americana*, and *M. californiensis*) were offered latex beads of 4, 2, 1, or 0.5 µm in diameter in four separate experimental treatments. We recorded a maximum of 10 predator-bead encounters per individual in 6 – 12 individuals of each species and per bead size, resulting in 70 – 100 bead encounters per treatment, except for *R. americana* with 2-µm beads and *M. californiensis* with 1-µm beads that had 33 and 32 encounters, respectively. Once a flagellate inside an opened observation chamber was in focus under the microscope, the bead solution treated with surfactant (Bovine Serum Albumin, 1 mg/mL) was gently added at an approximate final concentration of 10^5 – 10^7 beads · mL^{-1}. Predator-bead encounters were recorded with the high-speed camera. Interactions were classified as 1) 'capture' when the bead entered the groove or was retained by the flagellate outside the groove, and 2) 'no capture' when the bead followed the feeding flow and approached the groove but did not enter. The fate of captured beads was recorded as ingestion or 'no ingestion'. The dimensions of the major and minor axis of each flagellate were also recorded.

8.3 Results

8.3.1 The ventral groove wave

We named the moving bulge at the bottom of the feeding groove 'the wave', due to its steady movement. We found that all four species in this study presented an active transverse wave that repeatedly swept longitudinally along the ventral groove, from the anterior to the posterior (Fig. 1; Videos 1 – 4; Animations 1 – 2). The passing of the wave did not disrupt the flagellar activity. Captured prey was phagocytized only as the traveling wave physically pushed the particle against the internal wall of the rear end of the groove, toward the cytopharyngeal region. Some prey was lost while 'waiting' for the arrival of the wave. Thus, the arrival of the wave was essential for phagocytosis, and it promoted vacuole formation. During vacuole formation, the posterior end of the groove and cell could slightly deform due to the morphology of the prey (especially for large prey). This was clearly observed when *R. americana* ingested a bacterium that was as long as the ventral groove (Fig. 2 and Video 5). To phagocytize the long prey, the wave was seen sweeping across a few times, which deformed and extended the posterior end of the predator's body a little more with each sweep, until the whole bacterium was contained in a sack-like extension of the cell (with the same shape as the food). Subsequently, the extended 'sack' was slowly 'reabsorbed' into the main body for digestion.

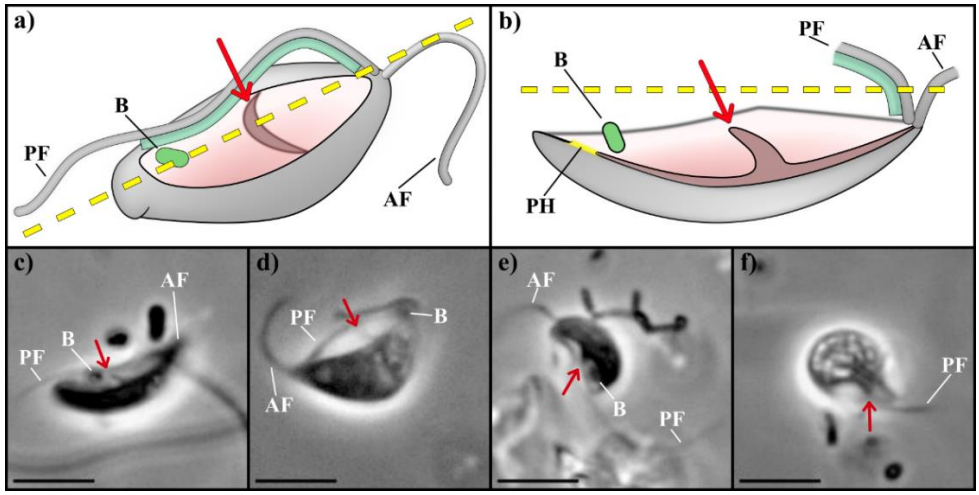

Figure 1. 'Typical excavate' features and the moving 'wave' (red arrow) in the feeding groove. Top panels: a) schematic representation of the ventral view of an excavate, b) longitudinal cross-section view of image a). Bottom panels: phase contrast microscope images of *Kipferlia bialata* (c), *Reclinomonas americana* (d), *Malawimonas californiensis* (e), and *Gefionella okellyi* (f). Abbreviations: AF = anterior flagellum; PF = posterior flagellum with a vane; B = bacterium; PH = phagocytosis region. Scale bar = 5 μm.

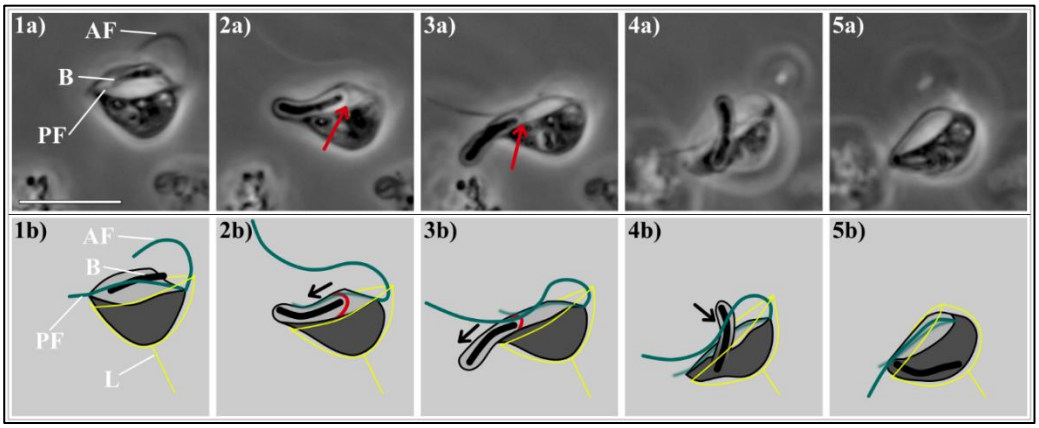

Figure 2. The elastic ingestion of a long bacterium by *Reclinomonas americana*. Top row panels: sequence of phase-contrast microscope images of the ingestion process. Bottom row panels: schematic drawings representing the respective microscope images above. Image sequence: 1a and 1b) the long bacterium is captured inside the groove and retained by the immobile posterior flagellum; 2a and 2b) the wave sweeps across, pushing the prey (black arrow direction) and the posterior end of the groove and cell begins to extend; 3a and 3b) the wave sweeps across more frequently (black arrow direction) and the cell extension grows longer, containing the prey; 4a and 4b) after 4 wave-sweeps, a sack-like cell-extension containing a vacuole with the bacterium inside has been formed, and the 'sack' is slowly 'reabsorbed' into the main cell body; 5a and 5b) the food is incorporated in the main cell body for digestion. Abbreviations: AF = anterior flagellum (green); PF = posterior flagellum (green); B = bacterium (black); L = lorica (yellow). Scale bar = 10 μm.

The sweep interval and speed of the wave in the ventral groove varied between species (Table 1, without prey). *Kipferlia bialata* had the most active wave with fast translations at short and regular intervals. In contrast, the waves of *R. americana*, *M. californiensis*, and *G. okellyi* were slower and had a less uniform behavior. *Reclinomonas americana* and *G. okellyi* had wave sweep intervals that were an order of magnitude longer than *K. bialata*. We obtained only a single observation of the sweep interval in *M. californiensis*, which resulted in a period of more than 6 minutes between two sweeps.

The sweep behavior of *K. bialata* and *R. americana* was studied during active interactions with captured particles (Table 1, with prey). Overall, *K. bialata* had no significant change in behavior. In contrast, *R. americana* reduced the sweep interval by 50 % when handling captured prey while the sweep speed remained approximately the same.

Table 1. Wave activity of the feeding groove of *K. bialata, R. americana, M. californiensis, G. okelyii*. Values correspond to the weighted averages ($\bar{x}_w$) and weighted standard deviations (SD_w) of the observed sweep recurrences, durations, and speeds. Four species were studied without prey interactions (w/o prey), of which two species were also observed during active prey capture events. * = single observation.

		Sweep interval (min)		**Wave speed (µm/s)**	
		$\bar{x}_w$	SD_w	$\bar{x}_w$	SD_w
w/o prey	*Kipferlia bialata*	0.2	0.1	2.0	0.6
	Reclinomonas americana	2.0	1.2	1.0	0.3
	Malawimonas californiensis	6.3*	NA	0.6	0.1
	Gefionella okellyi	1.8	0.6	0.9	0.2
w/ prey	*Kipferlia bialata*	0.3	0.1	1.7	0.5
	Reclinomonas americana	1.0	0.7	1.0	0.4

8.3.2 Prey-size range

The three excavates examined in this section (*Kipferlia bialata*, *R. americana*, and *M. californiensis)* all use the beating flagella to generate a feeding current that directs particles toward the ventral groove. *Kipferlia bialata* and *R. americana* forage for food while attached to a surface and with the ventral groove facing the opposite way, whilst *M. californiensis* cells 'skip' along the surface, frequently changing the orientation of the ventral groove. When a particle entered the groove, we considered the event as a capture of two possible types: 1) an 'active capture', when the anterior or posterior flagellum of the excavate physically retained the prey (see examples in Video 1 and Video 6a); and 2) a 'passive capture', when the flagella played no direct role, and the local flow kept the prey inside the groove (Video 7a). An active capture in all three studied species typically involves the posterior flagellum keeping prey inside the groove by holding the particle against the interior wall. The prey can then be ingested once the ventral wave sweeps across. *R. americana* can change the position of the beating anterior flagellum, at times completely stopping, to retain the captured particle and to ensure its entry into the ventral groove. In contrast, the anterior flagellum of *K. bialata* and *M. californiensis* never changes during feeding. To reject unwanted captures, the excavates resume the original flagellar kinematics and the particle is eventually removed from the ventral groove. Occasionally, the moving wave pushes stuck particles out of the groove.

Reclinomonas americana was the only species capable of temporarily retaining the 4-µm beads, using the anterior flagellum beating changes described above. However, the big spheres never entered the groove and they were all evidently rejected (Fig. 3) (Video 5b). *Kipferlia bialata* and *R. americana* actively captured the 2-µm beads (Video 6a and Video 6b, respectively), while *M. californiensis* was unable to capture beads larger than 1 µm (Video 5c and Video 6c). Nonetheless, the 2-µm beads got stuck around halfway down the groove of *K. bialata* and they were all consequently rejected, while the 2-µm beads often reached the posterior end of the groove of *R. americana* and were ingested. However, after phagocytizing three 2-µm beads, *R. americana* rejected all subsequent incoming particles. All three excavates were capable of capturing and ingesting 0.5 and 1-µm beads, sometimes phagocytizing multiple beads at the same time (Videos 7 a, b, c; and Videos 8 a, b, c). Although some 1-µm beads were 'actively captured', all the 0.5-µm beads and most of the 1-µm beads were 'passively captured'.

We measured the efficiencies in capture and ingestion by each species for each bead-size treatment (Fig. 3). The capture efficiency can be calculated as the proportion of captured particles over the number of encounters, and the ingestion efficiency as the ratio of ingested particles out of the total captures. Lastly, the excavates formed vacuoles containing the beads that stayed close to the posterior end of the cell, and a high proportion was eventually egested.

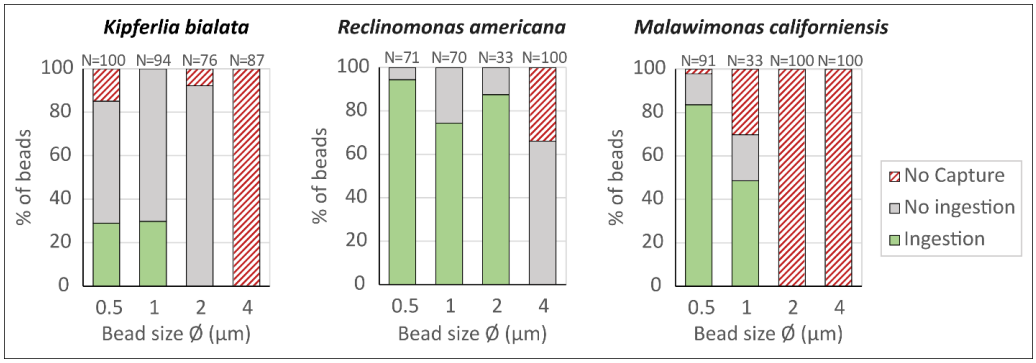

Figure 3. Bead-size dependency on capture and ingestion efficiencies of three excavates. *Reclinomonas americana* has the broadest prey-size range (0.5 – 4µm), as opposed to *M. californiensis* which is restricted to the smaller spectrum (0.5 – 1µm). However, both *R. americana* and *M. californiensis* have a high ingestion efficiency, as opposed to the low ingestion rates of *K. bialata*. 'N' is the total number of beads offered of a specific size. 'No Capture' events (red stripes) were beads that never entered the ventral groove. 'No Ingestion' events (light gray) were beads that entered and subsequently exited the groove. 'Ingestion' events (green) were captured beads that were eventually phagocytized.

8.4 Discussion

8.4.1 The wave in the feeding groove

Despite anecdotal observations of a transversal slender element moving posteriorly along the feeding groove of some excavates (personal observations), no previous study has identified its nature or precise function. Ultrastructure studies of typical excavates (Heiss et al., 2018; O'Kelly, 1997; O'Kelly & Nerad, 1999; Yubuki et al., 2013) show a rather smooth floor of the groove, which is lined internally by a complex system of microtubules and fibers that run more or less longitudinally. Therefore, we termed the moving form as 'the wave', envisioning it as a deformation or undulation of the floor of the groove. We investigated the presence of the wave in four groove-bearing species in the three main clades, with the attempt of representing the phyletic diversity of 'excavates'.

Excavates spark interest because of the hypothesis that living typical excavates may resemble the Last Common Eukaryotic Ancestor (LECA) from at least a billion years ago (Derelle et al., 2015). Gaining knowledge on the feeding mechanisms of excavates may therefore shed light on the primitive predation mechanisms of LECA. 'Typical excavates' bear a ventral groove that is associated with a beating flagellum equipped with a vane or vanes (Simpson, 2003). Our results confirm that the four species of this study (representing the groups Discoba, Metamonada, and Malawimonada) possess the ventral wave; thus, we can argue that this feature is widespread in 'typical excavates'. Yet, it may not extend to all; for example, *Paratrimastix elaionoma* (Preaxostyla; Metamonada) has a trap-door-like 'tongue' attached to the right wall of the groove, which sits over the posterior end of the groove, and which has an overlapping function with that of the wave (ensuring that particles end up positioned in the region where phagocytosis occurs) (Simpson et al., 2000). *Paratrimastix* is much larger than the species studied here, and capable of phagocytizing several bacteria at once, thus a different particle handling system is not surprising. No ventral wave is recorded to our knowledge in groove-bearing flagellates outside the excavate clade such as nebulids (e.g. *Ancoracysta*) or colponemids. It would be useful to study such taxa, specifically for the presence of a wave; though it seems unlikely for colponemids, at least, since prey capture and ingestion is documented to be at the anterior end of the cell and not the posterior (Gigeroff et al., 2023). Likewise, it would be interesting to examine flagellates that fall phylogenetically within excavate clades but have differently organized grooves and flagellar arrangements, such as percolomonads and *Pharygomonas* flagellates (Heterolobosea; Discoba) and *Trepomona*s (Diplomonadida; Metamonada).

The sweeping wave pushes captured particles into the (equivalent of the) cytopharynx and is crucial for phagocytosis. The wave is also active in the absence of prey and occasionally removed misplaced particles. For this reason, we speculate that it also has a 'clearing' role to help reduce fouling of the groove. Transportation of prey along the surface of the body towards the ingestion region of the cell, i.e., surface motility, is common amongst protists and occurs in many forms

(Bloodgood, 2020). Better studied examples include the haptonema of haptophyte algae (Kawachi et al., 1991; Kawachi & Inouye, 1995), the actinopodia of *Actinomonas* sp. (Ishigaki & Terazaki, 1998), and the microvilli collar of choanoflagellates (Boenigk & Arndt, 2000a). These examples share the same general feeding pattern with typical excavates: a flagellum or flagella generates a feeding current to draw particles toward the cell body, and the captured particles are transported to the phagocytic region of the cell along the surface membrane of some specialized structure. However, in these other examples, captured particles move slowly along the surface without it noticeably deforming, suggesting a mechanism like gliding motility in apicomplexan parasites (Frénal et al., 2017) or surface-attached *Chlamydomonas* (Shih et al., 2013) (for example) but with the prey taking the place of the substrate; in other words, due to an intracellular motor gaining traction against the prey particle. In the excavate wave, by contrast, the motion of the prey appears to be due to the external force applied by the wave, rather than by traction against the particle directly. Mechanically speaking, this may be more similar to a pseudopodial activity than to the 'gliding-like' particle movements described above. Thus, we can consider the function of the wave as a distinct form of surface motility, typical of excavates.

8.4.2 Morphological constraints with larger prey

The ventral groove of a typical excavate is a semi-rigid pocket-like apparatus that must collect the food for phagocytosis. We found that the three species experience an upper prey-size limit for ingestion due, presumably, to the morphology of the groove. The observed size-dependent captures of each species correlate with their cell and groove dimensions (Suzuki-Telllier et al. in prep and Table S1). The largest excavate, *R. americana*, has the broadest cross-sectional area of the ventral groove (M = 9.6 μm^2, SD = 1.7 μm^2), followed by *K. bialata* (M = 5.6 μm^2, SD = 1.1 μm^2), and *M. californiensis* (2.3 μm^2). This matches the order of the optimal bead-size range for captures and ingestions of these species. Furthermore, the observation of *R. americana* ingesting 2 μm- beads (Video 7b) and a long bacterium (Fig. 2 and Video 5) highlights the increased chances of recording 'surprisingly' big-prey ingestions through direct observations of predator-prey interactions. Such results could be lost during incubation experiments, if say the big prey were egested.

8.4.3 Prey handling by excavates

Predation in flagellates comprises two phases: 1) the food searching, and 2) the prey processing. From the moment a food particle is captured, it is manipulated for subsequent ingestion or rejection. The handling time is the period when the predator exclusively processes the prey and cannot search for more food and in many stramenopiles defines the maximum ingestion rate when food is abundant (as defined in Suzuki-Tellier et al., 2022). The three excavate species actively handled captured large prey inside the groove by holding the food against the interior wall with

the posterior flagellum. *Reclinomonas americana* also employed the anterior flagellum for prey capture and handling. Consequently, the feeding flow was interrupted, and prey search did not resume until the flagellar activity was restored. Alternatively, some phagotrophic flagellates can process captured prey while searching (like filter-feeding choanoflagellates (Boenigk & Arndt, 2000a) and the stramenopile *Pteridomonas* sp. (Suzuki-Tellier et al., 2022). In this case, the upper limit of the ingestion rate is defined by the digestion rate or vacuole capacity. When encountering smaller particles (≤ 1 µm), the excavates changed their feeding behavior and continuously generated a current while one or multiple beads were captured and ingested inside the groove. Hence, prey handling is prey-size dependent. This suggests that the groove-feeding mechanism of a 'typical excavate' favors capture efficiency when handling smaller prey sizes. In contrast to phagotrophic flagellates that stop food-searching to exclusively handle the captured prey (e.g. *Ochromonas moestrupii* or *Cafeteria roenbergensis*), the 'typical excavate' feeding structure can switch to an 'automated' prey handling mode with small prey: the wave moves the food, one or more particles at the same time, into the cytopharyngeal region without interrupting the flagellar activity that is continuously generating a feeding current.

8.4.4 Prey selection

Prey selection can occur passively (due to predator-prey contact probabilities or limits in feeding structure morphology), actively pre-ingestion (by prey-avoidance or prey-rejection behaviors), or actively post-ingestion (also known as digestive selection by egestion) (Boenigk & Arndt, 2002; Jürgens & DeMott, 1995). Furthermore, critical cues for prey selection can be physical (size or shape of the food) or chemical (surface properties of prey). The three excavates had high capture efficiencies on the bead sizes they were capable of capturing (Fig. 3). Moreover, the ingestion efficiencies of *R. americana* and *M. californiensis* were also high on the bead sizes they were capable of ingesting. Thus, the capture and ingestion efficiencies of *R. americana* and *M. californiensis* size-dependent traits that further demonstrate the upper spatial restrictions imposed by the morphology of the feeding groove (i.e., passive prey selection). However, the high capture efficiencies of the 0.5 and 1-µm beads of *K. bialata* resulted in low ingestion efficiencies: most of the particles entering the groove, easily exited it following the feeding current. There are two possible explanations for this behavior: 1) the predator passively selects against the smaller particles due to morphological limitations, that is, the ventral groove of *K. bialata* is 'leaky'; 2) the predator actively selects against the smaller beads by not retaining them with the posterior flagellum. Yet, further investigation was beyond the scope of this study.

8.4.5 Conclusions

Overall, the excavates actively controlled the feeding activity inside the ventral groove with the associated posterior flagellum and the moving wave. Capture efficiencies of smaller particles (0.5

and 1-µm beads) were high, whilst the bigger beads (4 and/or 2-µm beads) were spatially restricted from entering inside the groove. For the smaller particles, the excavates had no handling times and acted like filter-feeding flagellates. The prey-size range, the ingestion efficiency, and the ventral wave behavior were species-specific, illustrating different feeding behaviors. These different predation modes are likely adaptations to the food availability in the environments that the species inhabit. *Kipferlia bialata* is found in sediments in near anoxic conditions (Kolisko et al., 2010), where bacteria and inert particles are presumably abundant. Furthermore, the higher frequency of wave sweeps of *K. bialata* results in shorter handling times, which maximize the capture rate. Thus, the food conditions and the feeding behavior of *K. bialata* would allow this species to be more selective with its prey (Boenigk & Arndt, 2000b). On the other hand, we suggest that the distinct high capture efficiency and broader prey-size range of *R. americana* is an adaptation to permanently attached foraging in a lower food concentration habitat, i.e., aerobic freshwater (Flavin & Nerad, 1993). This study focused on the feeding functions of the ventral groove and the floor wave in excavates, and prey selection arguments are hypothetical. Further experiments using both digestible food, like bacteria, and inert particles would fully assess prey selection in excavates. Although the investigated excavate species are of similar size (Table S1), they hold a species-specific ecological function in prey size and a feeding behavior likely adapted to their habitats.

In this study we confirmed that the 'wave' is present in typical excavates from across the three main excavate clades, but, as far as we know, is restricted to them. Previous ultrastructural studies of typical excavates show a strong similarity of the groove architecture across these three groups, including several non-microtubular structures that have no clear homologs known outside the excavate clades (Heiss et al., 2018; Simpson, 2003). This is the best evidence to date that the typical excavate feeding system is homologous across the three main excavate clades. Despite being an intermittent element without a known ultrastructural presence, the wave represents an additional 'characteristic and potentially unique' morphological feature of the typical excavate feeding system, and thus additional evidence for homology. Further studies examining the ultrastructure and cell biology of the wave would be valuable to determine the mechanistic basis of this motility phenomenon. This research would also represent a further test of the homology of the wave across typical excavates if conducted comparatively across multiple taxa. Pending such future studies, however, any eukaryote evolution scenario that imagines LECA having a typical excavate morphology should assume that it also had a 'wave' system linking prey capture in the groove with phagocytosis, similar to that seen in extant typical excavates.

Acknowledgments

We received funding from The Independent Research Fund Denmark (7014-00033B), the Carlsberg Foundation (CF17-0495), the Simons Foundation (931976), and the European Union's Horizon 2020 research and innovation program under Marie Skłodowska-Curie grant agreement no. 955910. The Centre for Ocean Life is supported by the Villum Foundation.

References

Arndt, H., Dietrich, D., Auer, B., Cleven, E.-J., Gräfenhan, T., Weitere, M., & Mylnikov, A. P. (2000). Functional diversity of heterotrophic flagellates in aquatic ecosystems. In B. S. C. Leadbeater & J. C. Green (Eds.), *Flagellates* (0 ed., pp. 252–280). CRC Press. https://doi.org/10.1201/9781482268225-18

Azam, F., Fenchel, T., Field, J. G., Gray, J. S., Meyer-Reil, L. A., & Thingstad, F. (1983). The Ecological Role of Water-Column Microbes in the Sea. *Marine Ecology Progress Series*. https://doi.org/10.3354/meps010257

Bloodgood, R. A. (2020). Prey capture in protists utilizing microtubule filled processes and surface motility. *Cytoskeleton*, *77*(11), 500–514. https://doi.org/10.1002/cm.21644

Boenigk, J., & Arndt, H. (2000a). Comparative studies on the feeding behavior of two heterotrophic nanoflagellates: The filter-feeding choanoflagellate Monosiga ovata and the raptorial-feeding kinetoplastid Rhynchomonas nasuta. *Aquatic Microbial Ecology*, *22*(3), 243–249. https://doi.org/10.3354/ame022243

Boenigk, J., & Arndt, H. (2000b). Particle Handling during Interception Feeding by Four Species of Heterotrophic Nanoflagellates. *Journal of Eukaryotic Microbiology*, *47*(4), 350–358. https://doi.org/10.1111/j.1550-7408.2000.tb00060.x

Boenigk, J., & Arndt, H. (2002). Bacterivory by heterotrophic flagellates: Community structure and feeding strategies. *Antonie van Leeuwenhoek*, *81*(1), 465–480. https://doi.org/10.1023/A:1020509305868

Boenigk, J., Matz, C., Jürgens, K., & Arndt, H. (2001). Confusing Selective Feeding with Differential Digestion in Bacterivorous Nanoflagellates. *Journal of Eukaryotic Microbiology*, *48*(4), 425–432. https://doi.org/10.1111/j.1550-7408.2001.tb00175.x

Derelle, R., Torruella, G., Klimeš, V., Brinkmann, H., Kim, E., Vlček, Č., Lang, B. F., & Eliáš, M. (2015). Bacterial proteins pinpoint a single eukaryotic root. *Proceedings of the National Academy of Sciences*, *112*(7), E693–E699. https://doi.org/10.1073/pnas.1420657112

Edwards, K. F., Li, Q., & Steward, G. F. (2023). Ingestion kinetics of mixotrophic and heterotrophic flagellates. *Limnology and Oceanography*, *68*(4), 917–927. https://doi.org/10.1002/lno.12320

Fenchel, T. (1982). Ecology of Heterotrophic Microflagellates. IV. Quantitative Occurrence and Importance as Bacterial Consumers. *Marine Ecology Progress Series*, *9*(1), 35–42.

Flavin, M., & Nerad, T. A. (1993). Reclinomonas americana N. G., N. Sp., a New Freshwater Heterotrophic Flagellate. *Journal of Eukaryotic Microbiology*, *40*(2), 172–179. https://doi.org/10.1111/j.1550-7408.1993.tb04900.x

Frénal, K., Dubremetz, J.-F., Lebrun, M., & Soldati-Favre, D. (2017). Gliding motility powers invasion and egress in Apicomplexa. *Nature Reviews Microbiology*, *15*(11), Article 11. https://doi.org/10.1038/nrmicro.2017.86

Gigeroff, A. S., Eglit, Y., & Simpson, A. G. B. (2023). Characterisation and Cultivation of New Lineages of Colponemids, a Critical Assemblage for Inferring Alveolate Evolution. *Protist*, *174*(2), 125949. https://doi.org/10.1016/j.protis.2023.125949

Hansen, P. J., Bjørnsen, P. K., & Hansen, B. W. (1997). Zooplankton grazing and growth: Scaling within the 2-2,-µm body size range. *Limnology and Oceanography*, *42*(4), 687–704. https://doi.org/10.4319/lo.1997.42.4.0687

Heiss, A. A., Kolisko, M., Ekelund, F., Brown, M. W., Roger, A. J., & Simpson, A. G. B. (2018). Combined morphological and phylogenomic re-examination of malawimonads, a critical taxon for inferring the evolutionary history of eukaryotes. *Royal Society Open Science*, *5*(4), 171707. https://doi.org/10.1098/rsos.171707

Ishigaki, T., & Terazaki, M. (1998). Grazing Behavior of Heterotrophic NanoFlagellates Observed with a High Speed VTR System. *Journal of Eukaryotic Microbiology*, *45*(5), 484–487. https://doi.org/10.1111/j.1550-7408.1998.tb05104.x

Jürgens, K., & DeMott, W. R. (1995). Behavioral flexibility in prey selection by bacterivorous nanoflagellates. *Limnology and Oceanography*, *40*(8), 1503–1507. https://doi.org/10.4319/lo.1995.40.8.1503

Jürgens, K., & Matz, C. (2002). Predation as a shaping force for the phenotypic and genotypic composition of planktonic bacteria. *Antonie van Leeuwenhoek*, *81*(1), 413–434. https://doi.org/10.1023/A:1020505204959

Kawachi, M., & Inouye, I. (1995). Functional roles of the haptonema and the spine scales in the feeding process of Chrysochromulina spinifera (Fournier) Pienaar et Norris (Haptophyta = Prymnesiophyta). *Phycologia*, *34*(3), 193–200. https://doi.org/10.2216/i0031-8884-34-3-193.1

Kawachi, M., Inouye, I., Maeda, O., & Chihara, M. (1991). The haptonema as a food-capturing device: Observations on Chrysochromulina hirta (Prymnesiophyceae). *Phycologia*, *30*(6), 563–573. https://doi.org/10.2216/i0031-8884-30-6-563.1

Kiørboe, T. (2023). Predation in a Microbial World: Mechanisms and Trade-Offs of Flagellate Foraging. *Annual Review of Marine Science*, *16*(1), null. https://doi.org/10.1146/annurev-marine-020123-102001

Kiørboe, T., & Hirst, A. G. (2014). Shifts in Mass Scaling of Respiration, Feeding, and Growth Rates across Life-Form Transitions in Marine Pelagic Organisms. *The American Naturalist*, *183*(4), E118–E130. https://doi.org/10.1086/675241

Kolisko, M., Silberman, J. D., Cepicka, I., Yubuki, N., Takishita, K., Yabuki, A., Leander, B. S., Inouye, I., Inagaki, Y., Roger, A. J., & Simpson, A. G. B. (2010). A wide diversity of previously undetected free-living relatives of diplomonads isolated from marine/saline habitats. *Environmental Microbiology*, *12*(10), 2700–2710. https://doi.org/10.1111/j.1462-2920.2010.02239.x

O'Kelly, C. J. (1997). Ultrastructure of trophozoites, zoospores and cysts of Reclinomonas americana Flavin & Nerad, 1993 (Protista incertae sedis: Histionidae). *European Journal of Protistology*, *33*(4), 337–348. https://doi.org/10.1016/S0932-4739(97)80045-4

O'Kelly, C. J., & Nerad, T. A. (1999). Malawimonas jakobiformis n. gen., n. sp. (Malawimonadidae n. fam.): A Jakoba-like Heterotrophic Nanoflagellate with Discoidal Mitochondrial Cristae. *Journal of Eukaryotic Microbiology*, *46*(5), 522–531. https://doi.org/10.1111/j.1550-7408.1999.tb06070.x

Patterson, D. J. (1990). Jakoba libera (Ruinen, 1938), a heterotrophic flagellate from deep oceanic sediments. *Journal of the Marine Biological Association of the United Kingdom*, *70*(2), 381–393. https://doi.org/10.1017/S0025315400035487

Patterson, D. J., & Larsen, J. (1991). *The Biology of free-living heterotrophic flagellates*. Published for the Systematics Association by Clarendon Press ; Oxford University Press. http://catdir.loc.gov/catdir/enhancements/fy0635/91019780-d.html

Schneider, C. A., Rasband, W. S., & Eliceiri, K. W. (2012). NIH Image to ImageJ: 25 years of image analysis. *Nature Methods*, *9*(7), Article 7. https://doi.org/10.1038/nmeth.2089

Shih, S. M., Engel, B. D., Kocabas, F., Bilyard, T., Gennerich, A., Marshall, W. F., & Yildiz, A. (2013). Intraflagellar transport drives flagellar surface motility. *ELife*, *2*, e00744. https://doi.org/10.7554/eLife.00744

Simpson, A. G. B. (2003). Cytoskeletal organization, phylogenetic affinities and systematics in the contentious taxon Excavata (Eukaryota). *International Journal of Systematic and Evolutionary Microbiology*, *53*(6), 1759–1777. https://doi.org/10.1099/ijs.0.02578-0

Simpson, A. G. B., Bernard, C., & Patterson, D. J. (2000). The ultrastructure of Trimastix marina Kent 1880 (Eukaryota), an excavate flagellate. *European Journal of Protistology*, *36*(3), 229–251. https://doi.org/10.1016/S0932-4739(00)80001-2

Simpson, A. G. B., & Patterson, D. J. (1999). The ultrastructure of Carpediemonas membranifera (Eukaryota) with reference to the "excavate hypothesis." *European*

Journal of Protistology, *35*(4), 353–370. https://doi.org/10.1016/S0932-4739(99)80044-3

Suzuki-Tellier, S., Andersen, A., & Kiørboe, T. (2022). Mechanisms and fluid dynamics of foraging in heterotrophic nanoflagellates. *Limnology and Oceanography*, *67*(6), 1287–1298. https://doi.org/10.1002/lno.12077

Suzuki-Tellier, S., Miano, F., Asadzadeh, S.S., Simpson, A.G.B., Kiørboe, T. Functional Morphology and Fluid Dynamics of Foraging in 'Typical Excavates'; a Key Assemblage for Understanding Deep Eukaryote Evolution (in preparation).

Tikhonenkov, D. V., Mikhailov, K. V., Hehenberger, E., Karpov, S. A., Prokina, K. I., Esaulov, A. S., Belyakova, O. I., Mazei, Y. A., Mylnikov, A. P., Aleoshin, V. V., & Keeling, P. J. (2020). New Lineage of Microbial Predators Adds Complexity to Reconstructing the Evolutionary Origin of Animals. *Current Biology*, *30*(22), 4500-4509.e5. https://doi.org/10.1016/j.cub.2020.08.061

Worden, A. Z., Follows, M. J., Giovannoni, S. J., Wilken, S., Zimmerman, A. E., & Keeling, P. J. (2015). Rethinking the marine carbon cycle: Factoring in the multifarious lifestyles of microbes. *Science*, *347*(6223), 1257594. https://doi.org/10.1126/science.1257594

Yubuki, N., Simpson, A. G. B., & Leander, B. S. (2013). Comprehensive Ultrastructure of Kipferlia bialata Provides Evidence for Character Evolution within the Fornicata (Excavata). *Protist*, *164*(3), 423–439. https://doi.org/10.1016/j.protis.2013.02.002

8.5 Appendix Paper III

8.5.1 Supplementary table

Table S1. Cell dimensions of the flagellates observed during the prey-size range experiment with beads of different diameters. Note that it was not always possible to measure the cell height and length for all individuals studied due to perspective.

			Cell morphometrics			
Species	**Bead size (µm) treatment**	**N**	Average length (µm)	SD	Average height (µm)	SD
Kipferlia bialata	4	10	9.2	0.8	2.6	0.3
	2	8	9.8	1.3	3.0	0.4
	1	10	8.6	1.0	2.5	0.4
	0.5	10	9.2	1.1	2.6	0.3
Reclinomonas americana	4	7	8.8	0.3	6.0	1.0
	2	8	8.6	1.0	5.9	0.6
	1	4	8.3	1.0	5.9	0.9
	0.5	6	7.9	1.2	5.8	0.8
Malawimonas californiensis	4	10	5.5	0.5	2.9	0.6
	2	10	5.5	0.3	2.7	0.4
	1	6	5.3	0.3	3.1	0.3
	0.5	12	5.1	0.4	2.5	0.2

CHAPTER 9

Discussion

This section expands on some concepts discussed in the papers, putting some results into a broader perspective and reflecting on potential proceeding work that would further improve our fundamental knowledge of flagellate predation.

9.1 Dispersal and pelagic feeding

Most phagotrophic nanoflagellates feed while attached to a substrate. Although swimming predators experience higher clearance rates, the preference for attachment is likely due to higher concentrations of prey near organic surfaces, e.g., marine snow (Andersen & Kiørboe, 2020). Tethered phagotrophic nanoflagellates dominate in rich food conditions, whilst the number of swimming individuals increases when food is scarce (Christensen-Dalsgaard & Fenchel, 2003; Pfandl et al., 2004). Therefore, for surface-associated flagellates, the purpose of swimming is probably to colonize new hotspots of prey (Andersen & Kiørboe, 2020).

Some species have specialized forms for dispersal that likely exclude the feeding function. For instance, *Jakoba libera* and *Reclinomonas americana* change their cell shape and flagellum length (O'Kelly, 1997; Simpson & Patterson, 2001), and *Pseudobodo* sp. extends its spiraled flagellum (Chapter 6). By elongating or extending the beating flagellum, the predators position the propelling force further away from the body, reducing the drag and optimizing swimming efficiency (Langlois et al., 2009). Conversely, a shorter flagellum promotes feeding because it positions the force closer to the cell, increasing the clearance rate. This may explain why *Pseudobodo* sp. spirals the flagellum (making it 'shorter') when it attaches to a surface to feed.

Other phagotrophic nanoflagellates can forage while swimming to a new food-rich region. Filter-feeding predators, such as the heterokont *Pteridomonas danica*, can search, capture, and handle more than one food particle at a time (Chapter 6). This feeding mode follows a type I functional response (Holling, 1959) (Fig 9.1), that is, the ingestion rate is positively correlated with the density of available prey. On the other hand, many phagotrophic flagellates stop generating the feeding current when they capture prey, to exclusively handle it. Here, handling times limit the maximum ingestion rate, following a type II functional response (Holling, 1959) (Fig 9.1). Hence, filter feeders increase capture efficiency by maximizing searching time, which is an optimal strategy

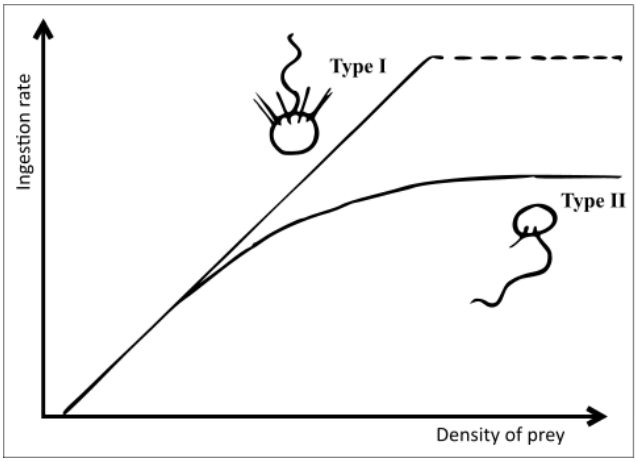

Figure 9.1. Holling's (1959) functional responses type I and type II. The filtering flagellate *Pteridomonas* sp. can handle prey while searching for more; thus, it follows a type I functional response and the ingestion rate will be limited by its vacuole capacity (dashed line). *Paraphysomonas* sp. stops searching for prey while handling prey, therefore it follows a type II functional response, as its ingestion rate will be limited by the time dedicated to manipulating its food before resuming prey search again.

in nutrient-poor pelagic waters where prey encounters are low; instead, feeding modes with handling times are likely more suited for food-rich localities (Boenigk & Arndt, 2000, 2002), such as on organic surfaces. Moreover, handling food with the flagella often implies subtle to drastic kinematic changes. For example, *Paraphysomonas foraminifera* shifts the flagellar position and increases the beat frequency (Christensen-Dalsgaard & Fenchel, 2004; Chapter 6), and *Cafeteria roenbergensis* stops beating completely (Boenigk & Arndt, 2000; Chapter 6). Very few studies have observed nanoflagellates that handle prey with the flagella (flagellar prey-handling) feeding while free-swimming (Boenigk & Arndt, 2000; Pfandl et al., 2004), and the involved mechanisms and fluid dynamics remain undescribed. The variation in flagellar kinematics can result in differences in flow architecture and predation risk (Nielsen & Kiørboe, 2021). Thus, we can speculate that flagellar prey handling in the water column can lead to an increased risk of becoming food for larger rheotactic predators. However, this argument is held with the assumption that the flagellates perform the same feeding behavior when foraging on a surface and in the water column. Thus, more experimental observations are required. Nonetheless, flagellar prey handling can be twenty-five times faster than handling prey captured on a filtering structure (Ishigaki & Terazaki, 1998). Faster handling times result in dynamic prey selections, which again are more practical in higher prey-concentration regions.

Overall, the filter-feeding mode seems to be more favorable for swimming predators that navigate in typically low food conditions, like the choanoflagellate *Diaphanoeca grandis* (Nielsen et al., 2017), or for surface-associated predators that forage in the water column until finding a new nutrient hotspot to colonize. Filter feeders optimize searching time over prey handling time, and the flow fields during propulsion and feeding are the same, thus, they will trade off equally with predation risk. On the other hand, substrate-associated suspension feeders that handle prey with the flagella dominate pelagic systems (Boenigk & Arndt, 2002). Therefore, these species must be

efficient in colonizing new microhabitats, by swimming fast or by effectively locating and steering toward new food sources (i.e., chemotaxis). Hence, fast colonization might account for the potential higher predation risk and the lower ingestion rates that potentially come at a cost when handling prey with flagella while swimming. Although the chemotactic response has been explored in a few nanoflagellate species (Sibbald et al., 1987; Fenchel & Blackburn, 1999; Kiørboe et al., 2004), the trade-offs between predation risk and feeding efficiency with different predation strategies (of varied flagellar arrangement and kinematics) during dispersal are largely unexplored. By studying the dispersal stages of phagotrophic nanoflagellates, we can gain insight into the population dynamics in shifting microhabitats, the non-surface-bounded predator-prey interactions, and the temporal-spatial composition of microbial communities.

9.2 Hairy and vaned flagella

9.2.1 Mastigonemes and vanes in other clades

Amongst the microbial predators examined in this work, we found two types of feeding structures that effectively increase the force produced by a beating flagellum, resulting in higher clearance rates. Namely, the hispid flagellum of the stramenopile species and the vaned flagellum beating inside a groove of excavates. Our results show that a hispid or vaned flagellum will generate clearance rates of around 10^6 specific cell volumes per day (Chapters 6 and 7), regardless of the vane configuration, flagellar position, or beating behavior. Thus, the diverse predation forms of stramenopiles and excavates perform efficiently for survival (Kiørboe & Hirst, 2014), and differences have most likely evolved from foraging trade-offs with predation risk, food availability, predation competition, etc. Other phylogenetically non-related species have similar specialized feeding structures. For instance, colponemids (Alveolata) (Gigeroff et al., 2023; Janouškovec et al., 2013) and Nebulidia (Provora) (Janouškovec et al., 2017; Tikhonenkov, Mikhailov, et al., 2022) have a posterior flagellum with a vane that is associated with a form of a conspicuous ventral groove like ‘typical excavates’. However, colponemids and Nebulidia prey on large (small eukaryotes) rather than on small prey (bacteria) and they phagocytize food at the anterior rather than at the posterior end of the cell. Thus, the similar morphologies appear to function differently, although this has not been examined in any detail. The deep-branching stramenopile *Platysulcus tardus* (Shiratori et al., 2015) also has a shallow ventral groove and two flagella that emerge apically: the posterior flagellum trails behind and close to the ventral furrow, while the anterior flagellum actively beats in front of the cell. Unlike excavates, the short anterior flagellum of *P. tardus* is equipped with mastigonemes and the posterior flagellum lacks a vane. *Platysulcus tardus* has been described as ‘gliding’ on surfaces and likely feeds on bacteria. Lastly, *Arpakorses versatilis* (Telonemia) (Tikhonenkov, Jamy, et al., 2022) lacks a ventral groove and has one flagellum equipped with complex tripartite mastigonemes. To feed on bacteria, the hispid flagellum supposedly beats to generate a flow and the second flagellum attaches to the substrate.

Interestingly, *A. versatilis* behaves differently to forage eukaryotic prey: the attached cell makes circular movements and captures food that is intercepted within the radius. These phylogenetically distant species share some of the well-adapted feeding morphologies (homologous or not) of stramenopiles and 'typical excavates'. However, it is unclear if they serve the same purpose, thus, their functional morphology and feeding behaviors are avenues yet to be explored.

9.2.2 Other functions of hispid flagella

Mastigonemes, i.e., rows of stiff hair-like protrusions on a flagellum, are responsible for reversing the flow towards the body of the flagellate. A micro-swimmer that is pulled by a leading flagellum will be faster and stealthier than a flagellate swimming with a 'pushing' naked flagellum (Nielsen & Kiørboe, 2021). When tethered, the flow-producing force converges adjacent streamlines closer to the predator, increasing the probability of prey encounter (Langlois et al., 2009). Hence, a flagellum with mastigonemes promotes propulsion and feeding. Here, I propose two additional roles. Firstly, a mechano-sensory function. *P. foraminifera* and *Pseudobodo* sp., which intercept prey with the hispid flagellum, react to the presence of an approaching particle before it visibly makes physical contact. We speculated that the first contact is established with the mastigonemes. The flagella of many organisms are involved in sensory perception (Moran et al., 2014). Thus, the hairs on the flagellum must aid the reception of mechanical stresses and expand the sensitive outreach, acting similarly to the mechanoreceptory setae of copepods (Kiørboe et al., 1999). Moreover, a mechanosensory transmembrane protein has recently been found interacting with mastigonemes (Liu et al., 2023). Lastly, prey intercepted by a hispid flagellum is retained without apparent physical contact: between the two handling flagella of *P. foraminifera*, and between the flagellum and the body of *Pseudobodo* sp. When the flagellates intercept a food particle, they shift the position of the flagellum, increasing the beat frequency and reducing the wave amplitude. The changes in the beating behavior of the hispid flagellum locally generate a zero net flow that immobilizes the food particle until the flagellate proceeds to ingest or reject it. Despite the highly active beating flagellum, the waters within a radius of approximately 1 – 2 body lengths away from the predator are motionless (personal observations). The precise fluid dynamics and the role of mastigonemes during these events are unknown. However, this form of 'contactless prey handlings' may be a strategy to optimize decision-making time during prey selection.

9.3 A flat-screen vs. reality

Methods using two-dimensional (2D) analysis present limitations when it comes to studying the real three-dimensional (3D) world. In this thesis, high-speed video microscopy has allowed us to describe in detail the many feeding stages of phagotrophic nanoflagellates. Although 3D events

were easily perceived through the lens when objects distanced away from the focus plane, the interpretation of these observations was at times complicated or inconclusive. For instance, many flagellar beat patterns are complex and rarely follow a plane; hence, they have been described in general terms throughout this thesis. Particle tracking rendered 2D architectures of the feeding flows, which were used to estimate clearance rates and forces with the assumption of radial symmetry. Lastly, the computational fluid dynamics (CFD) simulations delivered very useful 3D scenarios, yet, using the limited parameters obtained from microscopic imaging. Thus, many models were simplified interpretations of reality. Even though these methods have been good tools to carry out our research, further detailed studies of flagellar beat patterns and flow architecture close to the predator were challenging and, therefore, not attempted.

50 years ago, Berg and Brown pioneered 3D imaging by tracking the swimming path of the bacteria *Escherichia coli* (Berg & Anderson, 1973). Since then, a variety of 3D methods have emerged. For example, the coupling of two cameras positioned orthogonally derived tracks of *Chlamydomonas* and *Volvox* (Drescher et al., 2009), multifocal imaging (MFI) was used to obtain the fluid flow and flagellar kinematics of human and sea urchin sperm (Hansen et al., 2021), and high-speed multifocal plane fluorescence microscopy showed the flagellar beats of *Trypanosoma brucei* and *Leishmania mexicana*. In the last couple of decades, promising advances in holographic imaging systems have provided accessible instruments that are increasingly being used by the scientific community of aquatic sciences (see review Nayak et al., 2021). In a nutshell, holography records the interference pattern (the phase and intensity) of light diffracted from particles in a volume illuminated by two sources: a coherent light and a reference beam (Katz & Sheng, 2010). Since recorded holograms, i.e., the interference patterns, are not informative *per se*, optical or numerical reconstructions are necessary to yield the 3D information about the particles in the sample volume. In aquatic research, digital holographic microscopy has been used to identify plankton and particles and to measure biological and biophysical interactions. Scientists have been able to study the shifts in the swimming behavior of predatory dinoflagellates in dense suspensions (Sheng et al., 2007), measure growth rates and predation events of individual microorganisms (Bachimanchi et al., 2022), and describe the flagellar temporal-spatial waveform beat sequences of *Chlamydomonas reinhardtii* (Wilson & Bees, 2022). Moreover, the combination of digital holography with particle image velocimetry (PIV) allowed Malkiel et al. (2003) to study the 3D flow field produced by a feeding copepod. However, the lack of resolution seems to have hindered the application of this latter technique to micron-scaled biophysical processes. Most 3D microscopy methods can present challenges that may not be suitable to study specific biological events: required fluorescent labeling of the sample, computational intensive processing, sensitivity to inherent noise of the sample, low depth of focus, low time resolution, etc. Despite the extant limitations, future technological improvements will secure the presence of 3D imaging instruments on the benchtop of many marine labs.

Finally, certain measurements are hard to acquire from a moving organism (swimming). Current-feeding copepods were tethered to a human hair to study their grazing behavior (Xu et al., 2017; Ryderheim et al., 2022), and the flagellar kinematics of *C. reinhardtii* were observed while the organism was gently fixed by micropipette aspiration (Rüffer & Nultsch, 1990; Wan et al., 2014). Less intrusive is the observation of freely swimming flagellates tethered to a mid-plane of focus by acoustic tweezers (Rode et al., 2022). All the phagotrophic nanoflagellates species in this thesis fed while attached to a substrate; therefore, the feeding processes and flagellar behaviors were easily observed. However, future work on swimming micro predators might require a tethering method.

Figure 9.2. A copepod tethered to human hair (approx. 100 μm thick). The image is courtesy of Fredrik Ryderheim.

9.4 Final remarks

The benchmark studies by Fenchel (Fenchel, 1982a, 1982b, 1982c, 1982d) have fueled our understanding of the functional ecology of phagotrophic nanoflagellates. Following research has shed more light on the diverse feeding processes and prey selection behaviors of these small predators through direct observations (e.g., Ishigaki & Terazaki, 1998; Boenigk & Arndt, 2000; Boenigk et al., 2001; Christensen-Dalsgaard & Fenchel, 2004), opening the 'black box' in which traditional ecological assessments had placed them. However, the truth remains that phagotrophic nanoflagellates are still significantly understudied. With the advent of newly isolated species, new feeding modes will arise, and the study of predation behavior should go hand-in-hand with the phylogenetic and morphological descriptions of new specimens, boosting reports with information on functional morphology and ecology.

In this thesis, I have endeavored to expand our knowledge of predation by nanoflagellates with a biophysical, ecological, and taxonomical approach. Our results provide mechanistic support to previously observed functional responses, a first detailed insight to excavate feeding, a better understanding of the functional morphology of hispid and vaned flagella, and plausible evidence for the homology and eukaryotic ancestry of 'typical excavate' feeding structures. We conclude that further research on the fluid dynamics and flow architecture by hispid and vaned flagella will aid the understanding of foraging trade-offs between clearance rates of different flagellar configurations with predation risk. Although out of the scope of this thesis, prey selection has been evident during my observations of feeding behaviors. Food selectivity has been extensively studied, however, mostly for stramenopile species (Jürgens & DeMott, 1995; Boenigk et al., 2001; Matz & Jürgens, 2001; Pfandl et al., 2004). Hence, prey selection studies should expand across different taxonomical groups and predation modes. For instance, in excavates.

Many open questions on phagotrophic nanoflagellate predation will require a cross-disciplinary scientific approach. Direct observations of feeding behaviors through classic and novel microscopy combined with theoretical modeling and computational fluid dynamics simulations promise in-depth examinations of the governing biophysical processes. In addition, functional studies of feeding structures can constitute supporting evidence for phylogenetic relations and, in turn, phylogeny can depict the ecological evolution of observed predatory traits. Future interdisciplinary work on microbial feeding mechanisms will warrant an integral comprehension of the biological interactions that structure the marine food webs, and that ultimately support life on this blue planet.

References

Andersen, A., & Kiørboe, T. (2020). The effect of tethering on the clearance rate of suspension-feeding plankton. *Proceedings of the National Academy of Sciences*, *117*(48), 30101–30103. https://doi.org/10.1073/pnas.2017441117

Bachimanchi, H., Midtvedt, B., Midtvedt, D., Selander, E., & Volpe, G. (2022). Microplankton life histories revealed by holographic microscopy and deep learning. *ELife*, *11*, e79760. https://doi.org/10.7554/eLife.79760

Berg, H. C., & Anderson, R. A. (1973). Bacteria Swim by Rotating their Flagellar Filaments. *Nature*, *245*(5425), Article 5425. https://doi.org/10.1038/245380a0

Boenigk, J., & Arndt, H. (2000). Particle Handling during Interception Feeding by Four Species of Heterotrophic Nanoflagellates. *Journal of Eukaryotic Microbiology*, *47*(4), 350–358. https://doi.org/10.1111/j.1550-7408.2000.tb00060.x

Boenigk, J., & Arndt, H. (2002). Bacterivory by heterotrophic flagellates: Community structure and feeding strategies. *Antonie van Leeuwenhoek*, *81*(1), 465–480. https://doi.org/10.1023/A:1020509305868

Boenigk, J., Matz, C., Jürgens, K., & Arndt, H. (2001). Confusing Selective Feeding with Differential Digestion in Bacterivorous Nanoflagellates. *Journal of Eukaryotic Microbiology*, *48*(4), 425–432. https://doi.org/10.1111/j.1550-7408.2001.tb00175.x

Christensen-Dalsgaard, K. K., & Fenchel, T. o. m. (2004). Complex Flagellar Motions and Swimming Patterns of the Flagellates Paraphysomonas vestita and Pteridomonas danica. *Protist*, *155*(1), 79–87. https://doi.org/10.1078/1434461000166

Christensen-Dalsgaard, K. K., & Fenchel, T. (2003). Increased filtration efficiency of attached compared to free-swimming flagellates. *Aquatic Microbial Ecology*, *33*(1), 77–86. https://doi.org/10.3354/ame033077

Drescher, K., Leptos, K. C., & Goldstein, R. E. (2009). How to track protists in three dimensions. *Review of Scientific Instruments*, *80*(1), 014301. https://doi.org/10.1063/1.3053242

Fenchel, T. (1982a). Ecology of Heterotrophic Microflagellates. I. Some Important Forms and Their Functional Morphology. *Marine Ecology Progress Series*, *8*(3), 211–223.

Fenchel, T. (1982b). Ecology of Heterotrophic Microflagellates. II. Bioenergetics and Growth. *Marine Ecology Progress Series*, *8*(3), 225–231.

Fenchel, T. (1982c). Ecology of Heterotrophic Microflagellates. III. Adaptations to Heterogeneous Environments. *Marine Ecology Progress Series*, *9*(1), 25–33.

Fenchel, T. (1982d). Ecology of Heterotrophic Microflagellates. IV. Quantitative Occurrence and Importance as Bacterial Consumers. *Marine Ecology Progress Series*, *9*(1), 35–42.

Fenchel, T., & Blackburn, N. (1999). Motile Chemosensory Behaviour of Phagotrophic Protists: Mechanisms for and Efficiency in Congregating at Food Patches. *Protist*, *150*(3), 325–336. https://doi.org/10.1016/S1434-4610(99)70033-7

Gigeroff, A. S., Eglit, Y., & Simpson, A. G. B. (2023). Characterisation and Cultivation of New Lineages of Colponemids, a Critical Assemblage for Inferring Alveolate Evolution. *Protist*, *174*(2), 125949. https://doi.org/10.1016/j.protis.2023.125949

Hansen, J. N., Gong, A., Wachten, D., Pascal, R., Turpin, A., Jikeli, J. F., Kaupp, U. B., & Alvarez, L. (2021). Multifocal imaging for precise, label-free tracking of fast biological processes in 3D. *Nature Communications*, *12*(1), Article 1. https://doi.org/10.1038/s41467-021-24768-4

Holling, C. S. (1959). Some Characteristics of Simple Types of Predation and Parasitism. *The Canadian Entomologist*, *91*(7), 385–398. https://doi.org/10.4039/Ent91385-7

Ishigaki, T., & Terazaki, M. (1998). Grazing Behavior of Heterotrophic NanoFlagellates Observed with a High Speed VTR System. *Journal of Eukaryotic Microbiology*, *45*(5), 484–487. https://doi.org/10.1111/j.1550-7408.1998.tb05104.x

Janouškovec, J., Tikhonenkov, D. V., Burki, F., Howe, A. T., Rohwer, F. L., Mylnikov, A. P., & Keeling, P. J. (2017). A New Lineage of Eukaryotes Illuminates Early Mitochondrial Genome Reduction. *Current Biology*, *27*(23), 3717-3724.e5. https://doi.org/10.1016/j.cub.2017.10.051

Janouškovec, J., Tikhonenkov, D. V., Mikhailov, K. V., Simdyanov, T. G., Aleoshin, V. V., Mylnikov, A. P., & Keeling, P. J. (2013). Colponemids Represent Multiple Ancient Alveolate Lineages. *Current Biology*, *23*(24), 2546–2552. https://doi.org/10.1016/j.cub.2013.10.062

Jürgens, K., & DeMott, W. R. (1995). Behavioral flexibility in prey selection by bacterivorous nanoflagellates. *Limnology and Oceanography*, *40*(8), 1503–1507. https://doi.org/10.4319/lo.1995.40.8.1503

Katz, J., & Sheng, J. (2010). Applications of Holography in Fluid Mechanics and Particle Dynamics. *Annual Review of Fluid Mechanics*, *42*(1), 531–555. https://doi.org/10.1146/annurev-fluid-121108-145508

Kiørboe, T., Grossart, H.-P., Ploug, H., Tang, K., & Auer, B. (2004). Particle-associated flagellates: Swimming patterns, colonization rates, and grazing on attached bacteria. *Aquatic Microbial Ecology*, *35*(2), 141–152. https://doi.org/10.3354/ame035141

Kiørboe, T., & Hirst, A. G. (2014). Shifts in Mass Scaling of Respiration, Feeding, and Growth Rates across Life-Form Transitions in Marine Pelagic Organisms. *The American Naturalist*, *183*(4), E118–E130. https://doi.org/10.1086/675241

Kiørboe, T., Saiz, E., & Visser, A. (1999). Hydrodynamic signal perception in the copepod Acartia tonsa. *Marine Ecology Progress Series*, *179*, 97–111. https://doi.org/10.3354/meps179097

Langlois, V. J., Andersen, A., Bohr, T., Visser, A. W., & Kiørboe, T. (2009). Significance of swimming and feeding currents for nutrient uptake in osmotrophic and interception-feeding flagellates. *Aquatic Microbial Ecology*, *54*(1), 35–44. https://doi.org/10.3354/ame01253

Liu, P., Liu, Y., & Zhou, J. (2023). Ciliary mechanosensation – roles of polycystins and mastigonemes. *Journal of Cell Science*, *136*(3), jcs260565. https://doi.org/10.1242/jcs.260565

Malkiel, E., Sheng, J., Katz, J., & Strickler, J. R. (2003). The three-dimensional flow field generated by a feeding calanoid copepod measured using digital holography. *Journal of Experimental Biology*, *206*(20), 3657–3666. https://doi.org/10.1242/jeb.00586

Matz, C., & Jürgens, K. (2001). Effects of Hydrophobic and Electrostatic Cell Surface Properties of Bacteria on Feeding Rates of Heterotrophic Nanoflagellates. *Applied and Environmental Microbiology*, *67*(2), 814–820. https://doi.org/10.1128/AEM.67.2.814-820.2001

Moran, J., McKean, P. G., & Ginger, M. L. (2014). Eukaryotic Flagella: Variations in Form, Function, and Composition during Evolution. *BioScience*, *64*(12), 1103–1114. https://doi.org/10.1093/biosci/biu175

Nayak, A. R., Malkiel, E., McFarland, M. N., Twardowski, M. S., & Sullivan, J. M. (2021). A Review of Holography in the Aquatic Sciences: In situ Characterization of Particles, Plankton, and Small Scale Biophysical Interactions. *Frontiers in Marine Science*, *7*. https://www.frontiersin.org/articles/10.3389/fmars.2020.572147

Nielsen, L. T., Asadzadeh, S. S., Dölger, J., Walther, J. H., Kiørboe, T., & Andersen, A. (2017). Hydrodynamics of microbial filter feeding. *Proceedings of the National Academy of Sciences*, *114*(35), 9373–9378. https://doi.org/10.1073/pnas.1708873114

Nielsen, L. T., & Kiørboe, T. (2021). Foraging trade-offs, flagellar arrangements, and flow architecture of planktonic protists. *Proceedings of the National Academy of Sciences*, *118*(3), e2009930118. https://doi.org/10.1073/pnas.2009930118

O'Kelly, C. J. (1997). Ultrastructure of trophozoites, zoospores and cysts of Reclinomonas americana Flavin & Nerad, 1993 (Protista incertae sedis: Histionidae). *European Journal of Protistology*, *33*(4), 337–348. https://doi.org/10.1016/S0932-4739(97)80045-4

Pfandl, K., Posch, T., & Boenigk, J. (2004). Unexpected Effects of Prey Dimensions and Morphologies on the Size Selective Feeding by Two Bacterivorous Flagellates (Ochromonas sp. And Spumella sp.). *Journal of Eukaryotic Microbiology*, *51*(6), 626–633. https://doi.org/10.1111/j.1550-7408.2004.tb00596.x

Rode, M., Bioue, A., Miano, F., Bruus, H., Kiørboe, T., & Andersen, A. (2022). Acoustic tethering of microorganisms. *Journal of Experimental Biology*, *225*(20), jeb244089. https://doi.org/10.1242/jeb.244089

Rüffer, U., & Nultsch, W. (1990). Flagellar photoresponses of Chlamydomonas cells held on micropipettes: I. Change in flagellar beat frequency. *Cell Motility*, *15*(3), 162–167. https://doi.org/10.1002/cm.970150305

Ryderheim, F., Olesen, A. J., Krock, B., Lundholm, N., & Kiørboe, T. (2022). Costs and benefits of predator-induced defence in a toxic diatom. *Proceedings of the Royal Society B: Biological Sciences*, *289*(1972), 20212735. https://doi.org/10.1098/rspb.2021.2735

Sheng, J., Malkiel, E., Katz, J., Adolf, J., Belas, R., & Place, A. R. (2007). Digital holographic microscopy reveals prey-induced changes in swimming behavior of predatory dinoflagellates. *Proceedings of the National Academy of Sciences*, *104*(44), 17512–17517. https://doi.org/10.1073/pnas.0704658104

Shiratori, T., Nakayama, T., & Ishida, K. (2015). A New Deep-branching Stramenopile, Platysulcus tardus gen. Nov., sp. Nov. *Protist*, *166*(3), 337–348. https://doi.org/10.1016/j.protis.2015.05.001

Sibbald, M. J., Albright, L. J., & Sibbald, P. R. (1987). Chemosensory responses of a heterotrophic microflagellate to bacteria and several nitrogen compounds. *Marine Ecology Progress Series*, *36*(2), 201–204.

Simpson, A. G. B., & Patterson, D. J. (2001). On Core Jakobids and Excavate Taxa: The Ultrastructure of Jakoba incarcerata. *Journal of Eukaryotic Microbiology*, *48*(4), 480–492. https://doi.org/10.1111/j.1550-7408.2001.tb00183.x

Tikhonenkov, D. V., Jamy, M., Borodina, A. S., Belyaev, A. O., Zagumyonnyi, D. G., Prokina, K. I., Mylnikov, A. P., Burki, F., & Karpov, S. A. (2022). On the origin of TSAR: Morphology, diversity and phylogeny of Telonemia. *Open Biology*, *12*(3), 210325. https://doi.org/10.1098/rsob.210325

Tikhonenkov, D. V., Mikhailov, K. V., Gawryluk, R. M. R., Belyaev, A. O., Mathur, V., Karpov, S. A., Zagumyonnyi, D. G., Borodina, A. S., Prokina, K. I., Mylnikov, A. P., Aleoshin, V. V., & Keeling, P. J. (2022). Microbial predators form a new supergroup of eukaryotes. *Nature*, *612*(7941), Article 7941. https://doi.org/10.1038/s41586-022-05511-5

Wan, K. Y., Leptos, K. C., & Goldstein, R. E. (2014). Lag, lock, sync, slip: The many 'phases' of coupled flagella. *Journal of The Royal Society Interface*, *11*(94), 20131160. https://doi.org/10.1098/rsif.2013.1160

Wilson, L. G., & Bees, M. A. (2022). *The chiral beat of algal flagella: Force and torque via imaging* (arXiv:2210.08669). arXiv. https://doi.org/10.48550/arXiv.2210.08669

Xu, J., Hansen, P. J., Nielsen, L. T., Krock, B., Tillmann, U., & Kiørboe, T. (2017). Distinctly different behavioral responses of a copepod, Temora longicornis, to different strains of toxic dinoflagellates, Alexandrium spp. *Harmful Algae*, *62*, 1–9. https://doi.org/10.1016/j.hal.2016.11.020